NYO-9661
MITNE-15

A STUDY OF THE FAST FISSION EFFECT IN LATTICES OF URANIUM RODS IN HEAVY WATER

by

J.R. WOLBERG
T. J. THOMPSON
I. KAPLAN

February 21, 1962

Contract at (30-1) 2344
U.S. Atomic Energy Commission

Department of Nuclear Engineering
Massachusetts Institute of Technology
Cambridge, Massachusetts

MASSACHUSETTS INSTITUTE OF TECHNOLOGY
DEPARTMENT OF NUCLEAR ENGINEERING
Cambridge 39, Massachusetts

A STUDY OF THE FAST FISSION EFFECT IN LATTICES OF URANIUM RODS IN HEAVY WATER

by

J. R. WOLBERG, T. J. THOMPSON, and I. KAPLAN

February 21, 1962

NYO-9661
AEC Research and Development Report
UC-34 Physics
(TID-4500, 17th Edition)

Contract AT(30-1)2344
U.S. Atomic Energy Commission

DISTRIBUTION

NYO-9661
AEC Research and Development Report
UC-34 Physics
(TID-4500, 17th Edition)

1. USAEC, New York Operations Office (D. Richtmann)
2. USAEC, Division of Reactor Development (P. Hemmig)
3. USAEC, New York Patents Office (H. Potter)
4. USAEC, New York Operations Office (S. Strauch)
5. USAEC, Division of Reactor Development, Reports and Statistics Branch
6. USAEC, Maritime Reactors Branch
7. USAEC, Civilian Reactors Branch
8. USAEC, Army Reactors Branch
9. USAEC, Naval Reactors Branch
10. Advisory Committee on Reactor Physics (E. R. Cohen)
11. ACRP (G. Dessauer)
12. ACRP (D. de Bloisblanc)
13. ACRP (M. Edlund)
14. ACRP (R. Ehrlich)
15. ACRP (I. Kaplan)
16. ACRP (H. Kouts)
17. ACRP (F. C. Maienschein)
18. ACRP (J. W. Morfitt)
19. ACRP (B. I. Spinrad)
20. ACRP (P. F. Zweifel)

21. ACRP (P. Gast)

22. ACRP (G. Hansen)

23. ACRP (S. Krasik)

24. ACRP (T. Merkle)

25. ACRP (T. M. Snyder)

26. ACRP (J. J. Taylor)

27. - 29. O.T.I.E., Oak Ridge, for Standard Distribution, UC-34, TID-4500 (17th Edition)

30. - 49. J. R. Wolberg

50. - 100. Internal Distribution

ABSTRACT

The fast fission factor, ϵ, in uranium cannot be measured directly. It is related to a quantity, δ_{28}, defined as the ratio of the fission rate in U^{238} to the fission rate in U^{235}. This ratio can be measured, and ϵ and δ_{28} may be related by a formula of the type $\epsilon = 1 + C\delta_{28}$, where C is a constant involving nuclear properties of U^{235} and U^{238}. The relation between δ_{28} and ϵ is not unique and depends on the particular form of the theory used for ϵ. Hence, it is now customary to quote experimental values of δ_{28} rather than of ϵ.

The research to be reported on the fast fission effect has been concerned mainly with the measurement of δ_{28} and with certain related problems. The areas of research may be grouped as follows:

1) development of a new method for measuring δ_{28}, which involves the ratio of the 1.60 Mev La^{140} activity in uranium foils of different U^{235} concentration;

2) measurement of δ_{28} in natural uranium rods 1.01 inches in diameter in three lattices moderated by heavy water, in a single 1.01-inch natural uranium rod immersed in heavy water, and in a single 0.25-inch diameter rod with a U^{235} concentration of 1.14 weight per cent immersed in heavy water;

3) studies of the effect of changes in the experimental conditions on the measurement of δ_{28};

4) measurements of the flux of neutrons with energies greater than the U^{238} fission threshold, as a function of position within a fuel rod and in the moderator;

5) measurements of δ_{25}, the ratio of epicadmium to subcadmium fissions in U^{235};

6) studies of the fission product gamma ray spectrum as a function of time after irradiation, for gamma rays with energies up to 2.7 Mev.

The new method for measuring δ_{28} involves an irradiation within a fuel rod, without requiring a supplementary fission chamber experiment. The uncertainty associated with this technique is smaller than that of the earlier methods, the major uncertainty being in the ratio (β^{25}/β^{28}) for La^{140}, where the β's represent fission product yields. The values of δ_{28} reported in this thesis are in reasonable agreement with previously measured and calculated values, and the results can be corrected as better fission product yield data become available. The method can also be used to replace the fission chamber experiment required in integral gamma counting methods. This procedure was followed, and the La^{140} technique was used only to determine the value of δ_{28} in one lattice.

The value of δ_{28} measured in the tightest lattice was only 6.8 per cent greater than the value of 0.0559 determined for a single rod, indicating that the fast interaction effects in the lattices studied were small.

The measurements of the fast neutron flux showed a rapid decrease in the moderator, confirming the low values of the interaction effect.

The perturbations in the fission product yields associated with changing the neutron energy spectrum were shown not to have a significant effect on the values of δ_{28} determined by using integral gamma counting. Under certain conditions, the results were affected by pulse pileup at a lower count rate than was expected.

The values of δ_{25} measured in the lattices agreed with values determined from gold cadmium ratios. Values of δ_{25} were also measured in a 1.01-inch single rod and for foils positioned in the moderator.

The fission product gamma-ray spectra observed in the study confirmed the existence of the La^{140} peak at 1.60 Mev. It was shown that this was the only important high energy gamma ray for the time interval from about a week to several months after an irradiation.

ACKNOWLEDGMENTS

The combined work of a number of individuals and groups is important to the success of an effort as complex as the MIT Heavy Water Lattice Project. The results of this particular report are primarily due to the work of the principal author, John R. Wolberg, who has submitted substantially this same report in partial fulfillment for the requirements of the Ph.D. degree at M.I.T. The assistance of other students working on the project was most helpful, as was the assistance of those mentioned specifically below.

Mr. A. E. Profio has been responsible for much of the work of the project as a whole and has contributed many ideas and given direction in the design of the facility, methods of carrying out the experiments, and the over-all program. Over-all direction of the project is shared by A. E. Profio and two of the authors, I. Kaplan and T. J. Thompson. The advice of Dr. Norman C. Rasmussen was sought on many occasions and has proved to be of extreme usefulness. Mr. Joseph Barch has been of invaluable assistance in setting up experiments and in the construction and operation of the facility. Maintenance of the electronic equipment was the responsibility of Mr. David Gwinn, and his many helpful suggestions are appreciated.

Staffs of the MIT Reactor and the Reactor Machine Shop have provided daily assistance to the project and advice during the experimental portion of the work. The development of the computer code utilized in this work was made possible by the efficient cooperation of the M.I.T. Computation Center.

The authors acknowledge that these individuals and groups were essential to the completion of this work.

TABLE OF CONTENTS

LIST OF FIGURES

LIST OF FIGURES (continued)

LIST OF TABLES

INTRODUCTION

The United States Atomic Energy Commission is sponsoring a research program on the physics of heavy water-moderated, sub-critical lattices at the Massachusetts Institute of Technology, in Cambridge, Massachusetts. The program includes experimental and theoretical research in several areas of reactor physics; a summary of the activities of the project is included in NYO-9658, "Heavy Water Lattice Project Annual Report," September 30, 1961.[H.3] Although an objective of the program is to study slightly enriched uranium lattices, the emphasis of the initial measurements was on methods, and experiments were made with natural uranium lattices. The purposes of making the initial measurements in these lattices were two-fold:

1) to compare the M.I.T. results with previous measurements from similar studies made at other laboratories;

2) to add some useful data to those already in existence for natural uranium.

This study, done as part of the M.I.T. lattice project, includes the research on the fast fission effect. A list of the areas of research considered in the study is included in the Abstract. Topics of general interest, including a discussion of the parameters affecting the values of δ_{28} and a discussion of previous measurements, are considered in Chapters I and II. Discussions of the experimental methods and the results and conclusions of this study are included in Chapters III and IV. Additional topics related to the study are included in the Appendices.

CHAPTER I.
DISCUSSION OF FAST FISSION

1.1 DEFINITION OF FAST FISSION

The term "fast fission" is generally applied to fissions that occur in U^{238}; it is used because only a fast neutron can cause fission in this isotope of uranium. Fast fission can also occur in U^{235}, but most fissions of this isotope are caused by neutrons of thermal energy. An examination of the U^{238} fission cross-section[H.6] shows that the reaction has a threshold which is not well defined: σ_f increases from 0.001b at 0.6 Mev to 0.018b at 1 Mev and reaches a constant value of 0.57b at about 2 Mev. Although the energy of the neutrons emitted in fission varies from 0.1 to more than 10 Mev, the average energy is close to 2 Mev.[G.2] A fission neutron can therefore cause fast fission if it makes its first collision in the fuel, and in natural or slightly enriched uranium reactors, a significant number of such fissions occur.

Two important quantities are used as measures of the amount of fast fission: δ_{28} and ϵ. The quantity δ_{28} is the ratio of the number of fissions in U^{238} to the number of fissions in U^{235} within a given fuel rod. This ratio is an experimentally measurable quantity and is therefore used in discussions of experimental work on fast fission. As part of the work associated with this thesis, δ_{28} has been measured in several lattices in the MIT subcritical facility. The fast fission factor, ϵ, is the term used to include the contribution of fast fission in the four-factor formula for the multiplication factor, k_∞. Epsilon can be calculated theoretically but cannot be measured. It is not a uniquely defined quantity, and several definitions have been used. These include:

1) The number of neutrons making their first collision with the moderator per neutron produced by thermal fission. (Spinrad[S.3])

2) The number of neutrons slowing down below the U^{238} fission threshold per neutron produced by thermal fission. (Castle, Ibser, Sacher, and Weinberg[C.3])

3) The number of neutrons slowing down below 0.1 Mev per neutron produced by thermal fission. (Carlvik and Pershagen[C.1])

A discussion of the fast fission factor, ϵ, as used in the four-factor formula is included in Appendix A. In this thesis, the experimental aspects of fast fission and related topics are emphasized and the quantity δ_{28} will, therefore, be used extensively.

1.2 PHENOMENA CAUSING FAST FISSION

The nuclide, U^{238}, has even numbers of neutrons and protons. Quantum mechanical calculations and experiments have shown that even-even nuclei are more stable than even-odd or odd-even nuclei. Thus, the binding energy of an unpaired neutron or proton is smaller than the binding energy of a paired neutron or proton. The even-even structure of the U^{238} nucleus and the difference in binding energy for paired and unpaired neutrons help explain the threshold nature of the U^{238} fission reaction. The addition of a neutron to a nucleus of U^{238} results in the formation of the compound nucleus, U^{239}. The energy of the compound nucleus in excess of that of the ground state of U^{239} is equal to the kinetic energy of the captured nucleus plus the binding energy of the neutron, minus the recoil energy of the compound nucleus. If this excess energy is greater than the energy required to separate two possible nuclear fragments, fission can occur. Because U^{238} is an even N nuclide, the additional neutron is an unpaired neutron and its binding energy is less than the separation energy required to cause fission in U^{238}. To cause fission in U^{238}, it is therefore necessary to supply additional energy in the form of kinetic energy of the incident neutron. The amount of additional energy required has been calculated to be about one Mev, and the dependence of the fission cross-section of U^{238} on energy has been found experimentally to agree with theory.[E.2]

In contrast, U^{235} can undergo fission with thermal neutrons;

U^{235} is an even Z-odd N nuclide, and the additional neutron can be paired with the unpaired neutron in its nucleus. The liquid drop model predicts that the binding energy of this neutron is about 1.3 Mev greater than the binding energy of the neutron added to the U^{238} nucleus.[G.2] This additional energy is enough to make the binding energy of the additional neutron greater than the separation energy required to cause fission. Thermal neutrons can, therefore, cause fissions in U^{235} and, when the compound U^{236} nucleus has been formed, the probability of fission is more than 80 per cent.

1.3 IMPORTANCE OF FAST FISSION

Although the microscopic cross-section for fast fission of U^{238} is much smaller than the microscopic cross-section for thermal fission of U^{235}, a significant number of fissions occur in the U^{238} in natural and slightly enriched uranium systems, mainly because of the large ratio of the number of atoms of U^{238} to the number of atoms of U^{235}. This ratio is 138 in natural uranium. The ratio δ_{28} is a function of many parameters and, in most reactors, has values in the range from 0.01 to 0.10. These fast fissions affect the design and operation of reactors by their influence on neutron multiplication, conversion ratio, and power output.

1.3.1 Neutron Multiplication

The effect of fast fission on neutron multiplication is to increase k_∞ by an amount approximately equal to $\eta p f \frac{(\nu_{28}-1)}{\nu_{25}} \delta_{28}$ which usually amounts to several per cent. In the early graphite-moderated, natural uranium reactors, a serious problem was to provide enough excess reactivity to meet operating requirements. The contribution of fast fission to the neutron multiplication was an important source of excess reactivity in these reactors. Today the problem has changed from providing enough excess reactivity to permit operation, to providing enough to permit desirable core lifetimes, and the fast fission contribution to the multiplication factor is still a factor in affecting the lifetime and, thus, the economics of some reactors.

1.3.2 Conversion Ratio

By increasing the number of neutrons slowing down per thermal fission, fast fission increases resonance absorption in U^{238} and tends to increase the conversion ratio of the reactor. The effect on conversion ratio can be significant in breeder reactors where a conversion ratio of at least 1.0 is required.*

1.3.3 Power Output

In a reactor fueled with natural or slightly enriched uranium, the fraction of the total power contributed by fast fissions is nearly equal to δ_{28}. This fraction is about 8 per cent in the Dresden Power Reactor, which is approximately the value of δ_{28} in this reactor. The difference between the energy released per fission in U^{238} and that in U^{235} is negligible; however, during the lifetime of the reactor, the Pu^{239} concentration increases, and there is therefore a third source of power. The presence of Pu^{239} complicates the calculation of the fast power fraction, but is only important at high burnup.

1.4 PARAMETERS AFFECTING FAST FISSION

This section provides a qualitative discussion of the ways in which various reactor parameters affect δ_{28}. This quantity can, in turn, be related to the fast fission factor, ϵ, by an equation of the form $\epsilon = 1 + C\delta_{28}$. Experimental data are included in section 2.3.

1.4.1 Rod Diameter

The probability of a fast neutron causing a fast fission before it leaves the rod increases with increasing rod diameter and δ_{28} would have its maximum value in an infinitely large block of uranium. The probability approaches zero as the rod diameter approaches zero. In the MIT lattices, the 1-inch diameter, natural uranium rods were

---

*Weinberg and Wigner[W.1] point out that the effect of fast fission on breeding was first considered by T. Snyder.

large enough so that the fast fission effect was significant. An example given by Weinberg and Wigner[W.1] illustrates the importance of the effect of rod diameter on the fast fission effect. Consider a uranium-graphite lattice with a ratio of moderator volume to fuel volume such that k_∞ is in the neighborhood of its maximum value. Changing the rod diameter from 0.4 inches to 2.0 inches changes k_∞ from 1.09 to 1.11. Although the product, ηpf, decreases from 1.075 to 1.05, the increase in ϵ from 1.012 to 1.055 is large enough to account for the increase in k_∞. In general, however, other problems such as heat transfer and thermal stresses must also be considered in the selection of the optimum rod diameter.

For tightly packed lattices, the probability of a fast neutron leaving one rod and causing a fission in another rod becomes important. This increase in the number of fast fissions is called the "interaction fast effect." When the interaction fast effect predominates over single-rod fast fission, the importance of rod diameter decreases. Lattices exhibiting this type of behavior are H_2O lattices or lattices of clustered fuel rods. In the MIT lattices studied with natural uranium rods of 1.01 inches in diameter, this effect was small.

1.4.2 Rod Spacing

Rod spacing has an important effect on δ_{28} in systems in which the interaction fast effect is significant. Such systems include tight-packed, water-moderated lattices and lattices of clustered fuel rods. In these lattices, the distance between rods is approximately equal to or smaller than the mean free path of fast neutrons in the moderator.

1.4.3 Moderator to Fuel Ratio

A small value of the ratio of moderator volume to fuel volume implies a small value of the rod spacing; hence, as the interaction fast effect becomes important, δ_{28} increases with decreasing moderator to fuel ratio. One must, however, differentiate between the moderator to fuel ratio of uniform lattices, and lattices of fuel rod clusters.

1.4.4 Moderator

The moderator can have a significant effect on δ_{28} because the mean free path of fast neutrons varies with the moderator. For lattices in which the interaction fast effect is important, a decrease in fast neutron, mean free path decreases δ_{28}. In general, the moderator with the lowest value of $\xi\sigma_s$ will permit the largest interaction fast effect for a given lattice configuration. The functional dependence of δ^{28} on the moderator is complicated, however, by the fact that fast fission is a threshold reaction.

For lattices in which the interaction fast effect is unimportant, the only effect that the moderator has on δ_{28} is in the "backscattering effect." A fast neutron leaving a fuel rod can be scattered back into the rod and still have enough energy to cause a fast fission. This effect would be smallest for hydrogenous moderators because of the large energy loss associated with a collision with hydrogen. The backscattering effect is small, but workers at Harwell claim to have measured it;[B.1] there are, however, conflicting data from Sweden.[N.3] This effect is discussed in section 2.3.

1.4.5 U^{238} Atom Density

For a given lattice configuration, decreasing the U^{238} atom density decreases the value of δ_{28}. A change of this type can be brought about by increasing the U^{235} concentration, by alloying the uranium, or by using another form of uranium such as uranium oxide. For natural or slightly enriched uranium metal lattices, the variation in U^{238} density is small. For uranium oxide rods, the U^{238} density is approximately half that in uranium metal rods of the same enrichment, and the effect on δ_{28} is approximately the same as the density change.

1.4.6 U^{235} Concentration

For slightly enriched uranium lattices, the effect on δ_{28} of changes in U^{238} atom density caused by changes in U^{235} concentration

is small. For example, a change in the concentration of U^{235} from 1 per cent to 2 per cent only changes the U^{238} atom fraction from 99 per cent to 98 per cent, which is the fractional change in the U^{238} atom density. The U^{235} concentration also affects δ_{28} by changing the thermal fission source shape. This effect is small and, in most cases, is negligible. Values of δ_{28} measured in H_2O lattices at BNL for different enrichments are tabulated by Erdik.[E.1] The differences in the values of δ_{28} are small.

1.4.7 Fuel Element Shape

The shape of the fuel element has an effect on the value of δ_{28}. A change in shape which decreases the average distance a fast neutron must travel in the fuel before reaching the moderator, will decrease δ_{28}. Measurements have been made in non-cylindrical fuel elements: Futch measured δ_{28} in platelike and tubular fuel elements;[F.4] Hill measured δ_{28} in spheres as well as cylinders.[H.4] The work to date at MIT has been limited to measurements in cylindrical fuel rods.

1.4.8 Lattice Configuration

For a given rod diameter and moderator to fuel volume ratio, the value of δ_{28} can be changed by changing the lattice configuration if the interaction fast effect is significant. Clustered fuel arrangements are types of configurations which increase δ_{28} above the value for uniformly spaced lattices of the same moderator to fuel ratio. In such lattices, groups of rods are usually spaced closely enough to permit an interaction effect. There is no longer a unique value of δ_{28} in these lattices; δ_{28} becomes a function of position within the cluster, the highest values of δ_{28} being found in the innermost rods.

1.4.9 Rod Position Within a Lattice

For lattices in which the interaction effect is negligible, δ_{28} is not a function of rod position. For uniform lattices in which there is an interaction effect, the effect is smaller for the outer rods.

1.4.10 Position Within a Rod

Although δ_{28} has been defined as an average quantity within a fuel rod, the ratio of fissions in U^{238} to fissions in U^{235} is actually a function of position within the rod. It has been shown experimentally that the U^{238} fission density is almost constant in the radial direction.[P.4] Since there is a dip in the U^{235} fission density, $\delta_{28}(r)$ has its maximum value at $r = 0$ and its minimum value at the rod surface. The effect of axial position on δ_{28} is negligible. The mean free path of fast neutrons in fuel is only a few centimeters, and end effects become unimportant only a few centimeters away from the upper and lower ends of the fuel rod.

CHAPTER II.
BACKGROUND MATERIAL

2.1 EARLY RESEARCH

2.1.1 Observation of Fast Fission

The phenomenon of fast fission (fission of U^{238}) was first observed by Marshall and Szilard[M.2], who reported a value of $\nu_{28}\sigma_f$ equal to 1.3b in November, 1941. The following month, Szilard and Feld considered the effect of a natural uranium shell on the critical mass of a U^{235} core. By including the effect of U^{238} fission in the calculation, they were able to predict a value of the critical mass which was about one-third smaller than previously calculated values.[F.1]

2.1.2 First Theoretical Treatment of the Fast Effect in Heterogeneous Lattices

Heterogeneous reactors were first proposed by Fermi and Szilard[K.1], who thought that an optimum heterogeneous lattice would have a higher value of k_∞ than an equivalent homogeneous system, owing to the change in the resonance escape probability. The first reactor, CP-1, was fueled with uranium metal and uranium oxide slugs in a heterogeneous graphite lattice; but at that time, the increase in the fast fission effect due to a heterogeneous fuel arrangement was not included in the design calculations.

The first reported treatment of the problem of the fast effect in heterogeneous lattices was published in May, 1943 by Castle, Ibser, Sacher, and Weinberg.[C.3] These authors acknowledged that similar treatments had been made by Szilard, Feld, Ashkin, Wheeler, and others. The mean free path of fast neutrons in uranium is about 1.2 inches. Since this value was of the same order of magnitude as

the fuel slug dimensions in CP-1, the authors did not use diffusion theory. They defined and calculated suitable collision probabilities and then applied these to the determination of a fast fission factor. Their method is considered in section 2.4.

2.1.3 Measurements of δ_{28} in a Large Mass of Uranium

Measurements of δ_{28} were included in a series of experiments in which an attempt was made to determine if a large mass of natural uranium could support a chain reaction.[S.2] The experiment was made in Chicago in 1943 by Snell, Brolley, Levinger, and Wilkensen, with a five-ton mass of uranium. They reported a value of 0.8 for δ_{28}. The experiment was repeated at Oak Ridge by Brolley, Byerley, Feld, Olds, Scallettar, Slotkin and Stewart, with a 35-ton mass of uranium.[B.2] Using the catcher foil technique (which will be discussed in section 2.2), a value of δ_{28} equal to 0.42 was measured and was corrected to 0.37 for zero buckling. Chezem has recently measured a value of 0.582 ± 0.017[C.9] which was corrected to 0.425 for zero buckling.[C.11] Experiments at Saclay[C.10] are in agreement with Chezem's result and can be compared to a Russian value of 0.42.[C.11]

2.1.4 Measurement of δ_{28} in Fuel Elements

The first measurements of δ_{28} in fuel elements were made at Los Alamos in 1944 and reported by Hill.[H.4] The measurements were made in natural uranium spheres and cylinders irradiated in a graphite-moderated reactor. The results are considered in section 2.3.

2.2 EARLIER METHODS OF MEASURING δ_{28}

In all methods of measuring δ_{28} used so far, at least two uranium foils are irradiated within a fuel element, or within adjacent fuel elements. One foil is made of uranium depleted in U^{235} and the second foil is made either of natural uranium or of uranium of the same U^{235} concentration as the fuel. Two quantities, $\gamma(t)$ and $P(t)$, are defined as functions of time: $\gamma(t)$ is the ratio of the activity of the depleted foil to the activity of the second uranium foil, both activities

being determined at a time, t, after irradiation; P(t) is the ratio of the number of counts per fission of U^{235} to the number of counts per fission of U^{238}, with both count rates determined at time, t. It will be shown in section 3.2 below that

$$\delta_{28} = P(t) \frac{a\gamma(t) - S}{1 - a\gamma(t)}, \qquad (2.2.1)$$

where a and S are certain constants. The methods used to determine δ_{28} experimentally differ, depending on the techniques used for measuring $\gamma(t)$ and P(t).

2.2.1 Westinghouse Gamma Counting Method[K.8, K.9]

As explained in section 3.2 below, the photons of highest energy resulting from the U^{238} (n, γ) reaction are 1.20 Mev bremsstrahlung photons from the 1.20 Mev beta ray emitted in the decay of 23-minute U^{239}. To avoid counting bremsstrahlung from this beta ray, the Westinghouse method considers only the gamma activity of the foils above 1.20 Mev in energy.

In this method, the function $\gamma(t)$ is the ratio of the count rate of the depleted foil above 1.20 Mev at time t to the count rate above 1.20 Mev from the second foil at time t. The measurements of the count rates of the foils are made by using a scintillation crystal detector protected by a beta shield. The count rates are corrected for background, dead time, and differences in foil weights before the function $\gamma(t)$ is calculated.

The function P(t) is defined as the count rate above 1.20 Mev at time t per U^{235} fission, divided by the count rate above 1.20 Mev at time t per U^{238} fission. This function is measured by irradiating two foils in a double-chamber fission counter, and then measuring the function $\gamma(t)$ for the foils. If R is the ratio of the number of fissions in the depleted foil to the number of fissions in the natural foil as measured in the fission counter, δ_{28} can be calculated from the equation

$$\delta_{28} = \frac{aR - S}{1 - aR}. \qquad (2.2.2)$$

With $\gamma(t)$ and the value of δ_{28} calculated from Eq. 2.2.2, P(t) can be determined from Eq. 2.2.1. The function P(t) need only be determined once; measurements of δ_{28} are then made by determining values of $\gamma(t)$ and substituting these values and values of P(t) into Eq. 2.2.1.

2.2.2 Savannah River Laboratory Method[B.1]

In this method, during an irradiation of the depleted and natural uranium foils (test foils) at a position at which δ_{28} is unknown, two monitor foils are irradiated at a standard position. Gamma counting is used, and the value of δ_{28} is determined by comparing the ratio of the activities of the test foils with the ratio of the monitor-foil activities.

The advantage of this method is that the counting can be done at any convenient time after the irradiation and at any convenient bias setting. If counting below 1.20 Mev is used, sufficient time is allowed for the 23m U^{239} activity to become negligible.

The accuracy of this method is limited by the uncertainty in the value of δ_{28} at the standard position. The measurement of this value must be made by using another technique; the accuracy of this method is therefore limited to the accuracy of the method used to measure the standard value of δ_{28}. A disadvantage of the method is the need to irradiate and count two additional foils, and a prerequisite of the method is the availability of a convenient standard position.

2.2.3 Brookhaven Catcher Foil Method[K.6, K.7]

The catcher foil method was the earliest technique developed for the measurement of δ_{28} and has been refined by workers at Brookhaven. High-purity aluminum foils are placed adjacent to the uranium foils and, after the irradiation, the beta activity of the fission products which have impinged on the surface of the Al foils is counted. Additional foils are required to protect the back surfaces of the Al foils, and to determine the background due to Al foil activation. The measurement of P(t) is similar to the P(t) measurement of the Westinghouse technique. A

fission chamber is used to determine R, but $\gamma(t)$ is determined by counting the fission product beta activity of Al catcher foils placed adjacent to uranium foils irradiated within the fission chamber.

Several disadvantages of this method are discussed in section 3.2. Summarizing the conclusions:

1) The results are sensitive to the uranium foil surface conditions so that care must be taken to remove the oxide from the surfaces.

2) The use of many thin Al foils requires great care in seeing that the foils are positioned correctly and are not wrinkled in the loading procedure.

3) The number of foils required in this method is greater than the number required in the gamma-ray counting methods.

The main advantage of the method is that it permits repeated use of the uranium foils. It is unnecessary to wait for the decay of residual fission product activity, which is convenient when only a small supply of foil material is available. A shortage of depleted uranium resulted in the adoption of this method by Swedish workers.[N.3]

2.3 PREVIOUS MEASUREMENTS OF δ_{28}

This section summarizes previous measurements of δ_{28} in single rods, rod clusters, and uniform lattices. The MIT results are included in section 4.1.

2.3.1 Measurements of δ_{28} in Single Rods

Single rod measurements of δ_{28} are useful for comparison with theoretical treatments of the fast effect, and provide the limiting value of δ_{28} for lattices in which the rod spacing is large compared to the mean free path of fast neutrons in the moderator. Previous single rod measurements are summarized in Table 2.1 and Fig. 2.1. Comments concerning the effects of various parameters on single rod values of δ_{28} are included in section 4.1. In general, the data in Table 2.1 are compatible with the conclusions of section 1.4, but several additional comments should be made.

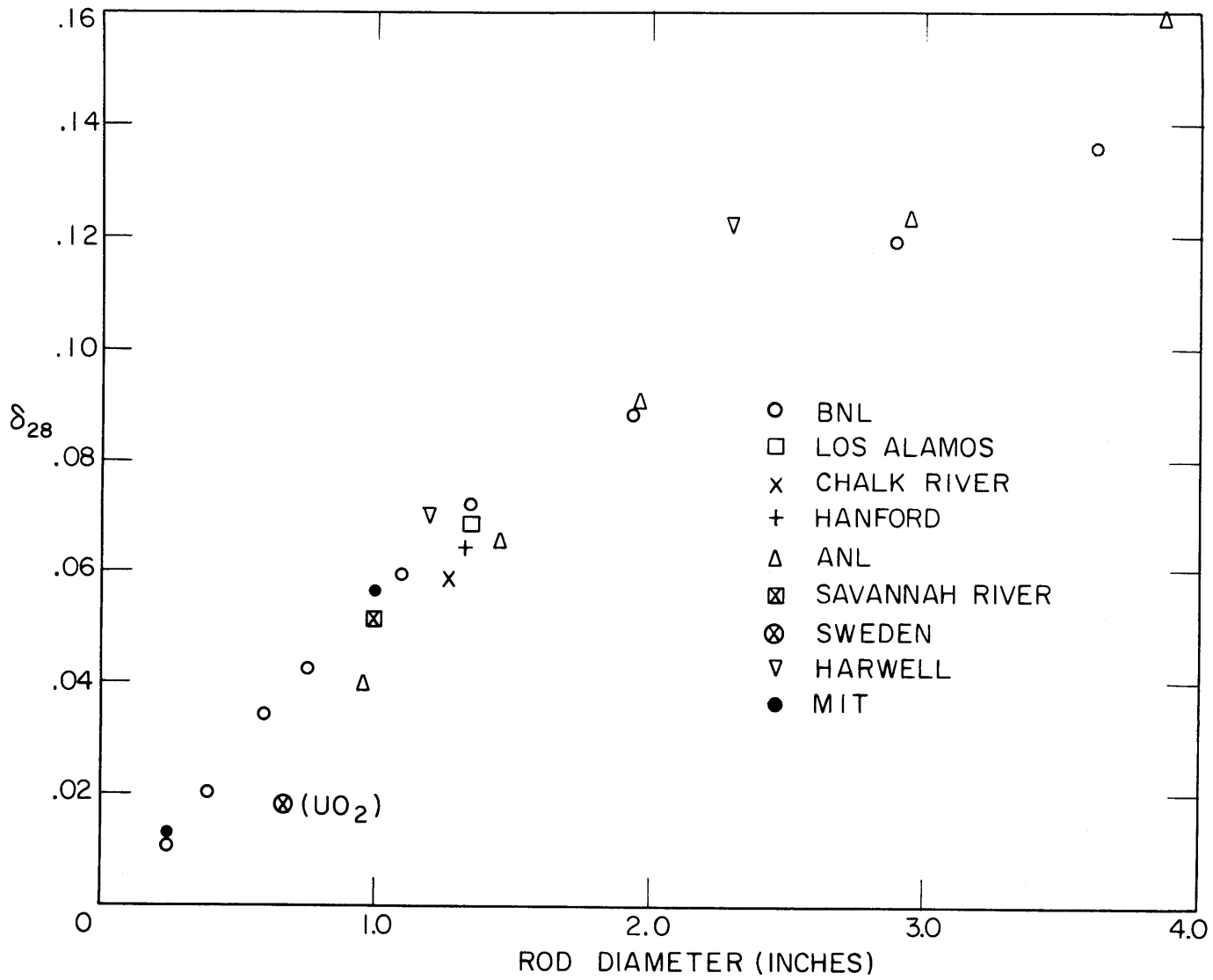

FIG. 2-1 SINGLE ROD VALUES OF δ_{28}

Table 2.1. Previous Single Rod Measurements of δ_{28}

Rod Diameter	U^{235} Concentration	Moderator	δ_{28}	Per Cent Uncertainty	Facility	Reference
0.25"	1.0%	Graphite	0.0113	4	BNL	(P.4), (W.4), (K.2) per modification of E.1
0.387	1.0		0.0200	4		
0.600	1.0		0.034	4		
0.750	1.0		0.042	4		
1.1	0.7(a)		0.059	4		
1.345	0.7		0.072	4		
1.938	0.7		0.088	4		
2.898	0.7		0.118	8		
3.636	0.7		0.135	8		
1.00	0.7	D_2O	0.051	6	SRL	(B.1)
0.57	0.7 (UO_2)	D_2O	0.0181	4.2	R3/Adam-Sweden	(N.3)
0.67	0.7 (UO_2)	Air	0.0186	4.2		
1.33	0.7	Graphite	0.0834		Hanford	(F.2)(b)
0.96	0.7	Graphite	0.039		Argonne	(F.2), (U.1)
1.46	0.7		0.065			
1.96	0.7		0.090			
2.96	0.7		0.123			
3.88	0.7		0.158			
1.346	0.7	Graphite	0.064		Los Alamos	(W.1), (W.4), (H.4)
1.28	0.7	D_2O	0.058		Chalk River	(C.1)(c)
1.2			0.070		Harwell	(C.11)(d)
2.25			0.122			

(a) Natural uranium. (b) Refers to a classified paper by W. E. Neimuth, HW-38738. (c) Refers to a private communication from E. Critoph. (d) Refers to AERE reports (C.7, C.8).

1) The neutron backscattering effect was considered in the discussion of the effect of the moderator on δ_{28}. It was mentioned that workers at Harwell had observed such an effect, but Swedish results disagreed with this conclusion. The Swedish R3/Adam data included in Table 2.1, show a higher value of δ_{28} for a uranium oxide rod in air as compared to a rod in D_2O. The difference is less than 3 per cent, but the backscattering effect should tend to make the value of δ_{28} higher for the rod in D_2O. Two possible explanations for the difference observed are: (a) statistics -- the difference is less than the experimental uncertainty in the measurements; (b) the presence of an interaction effect between the single rod in air in the central channel of the reactor and fuel rods in the reactor. The first ring of rods surrounding the channel in which the single rods were irradiated was removed before the experiment, but some interaction may have remained.

A fast fission, Monte Carlo program written by Rief[R.5] has been applied to the problem of the neutron backscattering effect. Calculations were made for a single uranium metal rod without cladding, surrounded by a void, and, for a single rod surrounded by graphite. The difference calculated for a rod 0.473 inches in diameter was small, but the values for a rod 1.27 inches in diameter showed a 9 per cent difference, the higher value being calculated for the rod in graphite. The effect is smaller for oxide rods than for metal rods of the same diameter because the U^{238} atom density of UO_2 is smaller than the density of uranium metal. The effect is also smaller for a rod in D_2O as compared to a rod in graphite because the energy loss associated with a neutron scattered by a deuterium nucleus is greater than the energy loss sustained by a neutron scattered by a carbon nucleus. A further decrease in the effect results from the presence of aluminum cladding on the fuel rods. Using the Monte Carlo calculations as a basis, one would therefore estimate a backscattering effect of less than 2 per cent for the rods used in the Swedish experiments. Since this is within the uncertainty of the measurements, it is not surprising that the effect was not observed. It would be interesting, however, to repeat the experiment with rods of larger diameter and to compare the results with the backscattering effect calculated

with the Monte Carlo code.

2) The BNL results seem to indicate that the measurements made in natural uranium rods lie along a smooth curve which includes measurements made in rods with a U^{235} concentration of about one per cent. In section 1.4 it was mentioned that the effect of U^{235} concentration on the value of δ_{28} should be small for natural and slightly enriched uranium rods. The effect of change in isotopic concentration should increase with increasing rod diameter, because the changes in fast neutron collision probabilities would be more evident. To observe changes in δ_{28} due to changes in U^{235} concentration, the best procedure would therefore be to compare values measured in large rods of equal diameter and different enrichments.

3) Large discrepancies can be observed among values of δ_{28} measured at different facilities. For this reason, it is difficult to test fine differences among the methods used to calculate δ_{28}.

2.3.2 Measurements of δ_{28} in Fuel Rod Clusters

Fuel rod clusters are used in certain lattices to improve reactor performance by improving the neutron economy, and to facilitate heat removal. The rod spacing within a cluster is usually small enough to permit a fast interaction effect; the value of δ_{28} then varies from rod to rod within the cluster, the largest values of δ_{28} being observed for the innermost rods. Several experimental studies of fuel rod clusters have included measurements of δ_{28}. The results of three studies are summarized in Table 2.2. Several conclusions can be made from an examination of these results.

1) The average value of δ_{28} is increased by increasing the number of rods in the cluster. The SRL and Swedish results illustrate this property, which can be explained on the basis of an increased interaction fast effect. As more rods are added, the average value of δ_{28} approaches a constant value which is that for an infinite lattice of the same spacing.

2) Increasing the spacing between rods decreases the values of δ_{28}. This effect is evident from the SRL and Chalk River results and can again be explained on the basis of the interaction fast effect.

Table 2.2. Measurements of δ_{28} in Fuel Rod Clusters

Rod Diameter	Fuel Material	Number of Rods	Rod Position[c]	Distance Between Closest Rods	Moderator	δ_{28}[a]	Facility	Reference
1.00"	U	1	E		D_2O	0.051 E	SRL	(F.4) Modified according to (B.1).
		2	E,H	1.34"		0.058 E		
		3	D,E,H	1.34		0.068 E		
		4	D,E,G,H	1.34		0.077 E		
		4	D,B,F,H	1.895		0.064 F		
		4	A,C,I,G	2.68		0.058 G		
		5	D,B,E,F,H	1.34		0.097 E		
		5	Same	1.34		0.071 F		
		5	Same	1.34		0.076		
		9	All	1.34		0.100 G		
		9	All	1.34		0.150 E		
		9	All	1.34		0.105		
1.04"	UO_2	19		0.705	Air	0.038	Chalk River[b]	(P.3) Refers to work at Chalk River
		19		0.705	D_2O	0.035		
		19		0.785	D_2O	0.038		
1.03"	U	19		0.785	D_2O	0.062		
		19		0.705	D_2O	0.071		
		19		0.705	Air	0.073		
0.67"	UO_2	19		0.83	Air	0.052	R3/Adam-Sweden[b]	(N.3)
		19		0.83	D_2O	0.052		
		19		0.83	H_2O	0.051		
		7		0.83	Air	0.039		
		7		0.83	D_2O	0.037		
		7		0.83	H_2O	0.038		
		1			Air	0.0186		
		1			D_2O	0.0181		

(a) Weighted average value unless otherwise specified.
(b) Hexagonal cluster configurations.
(c) Rod position according to the following diagram for the SRL results:

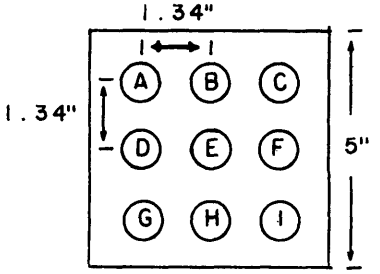

3) A decrease in the uranium atom density causes a decrease in the value of δ_{28}. The values of δ_{28} measured at Chalk River in UO_2 and uranium metal clusters, are lowest in the rods of uranium oxide.

4) The values of δ_{28} measured in fuel rod clusters depend on the moderator. Measurements of δ_{28} were made in clusters surrounded by air and by D_2O at Chalk River and in Sweden. In both cases, an increase in δ_{28} was observed when air was the surrounding medium. This result is reasonable because air is not a good moderator and the interaction fast effect should be greatest when the surrounding medium is air. The Swedish workers also measured δ_{28} in a cluster surrounded by H_2O. They could not detect a significant difference between the results in H_2O and in D_2O.

5) An increase in rod diameter increases δ_{28} in rod clusters by increasing the single rod contribution to the value of δ_{28}. A comparison of the Swedish and Chalk River results for clusters of 19 UO_2 rods can be misleading because the Swedish workers used 0.67-inch diameter rods and obtained higher values of δ_{28} than the Canadians who used 1.04-inch diameter rods. The Swedish results were for a tighter cluster with a higher interaction fast effect, which accounts for the difference.

6) The values of δ_{28} for the rods located at the centers of the clusters are greater than for rods at the edge of the cluster. The SRL results are included to illustrate the magnitude of this effect. Similar measurements made in the Swedish study also confirm this conclusion.

2.3.3 Measurements of δ_{28} in Uniform Lattices

The values of δ_{28} measured in uniform graphite- and D_2O-moderated lattices are only slightly greater than the values measured in single rods of the same diameter because rod spacings of interest in these lattices are usually too large to permit a significant interaction effect. In lattices moderated by H_2O or other hydrogeneous materials, rod spacings are usually small enough to permit an interaction fast effect. A summary of measurements of δ_{28} in H_2O lattices is included in the 1958 Geneva papers[K.5] and is reproduced in Table 2.3. Additional results are tabulated by Erdik[E.1].

Table 2.3. Measurements of δ_{28} in Water-Moderated, Uniformly Spaced Lattices.[K.5]

Rod Diameter	Fuel	Enrichment	W/U[(a)]	δ_{28}	Error in (δ_{28})[(b)]	Facility
0.387	Metal	1.0%	1.0	0.183	0.010	BNL
			1.5	0.129	0.006	
			2.0	0.114	0.003	
			3.0	0.086	0.004	
			4.0	0.079	0.005	
		1.15	1.0	0.177	0.005	
			1.5	0.127	0.004	
			2.0	0.108	0.002	
			3.0	0.077	0.001	
			4.0	0.066	0.001	
		1.3	1.0	0.173	0.004	
			1.5	0.134	0.001	
			2.0	0.109	0.001	
			3.0	0.086	0.001	
			4.0	0.073	0.001	
0.250	Metal	1.0	1.5	0.129	0.003	
			2.0	0.105	0.003	
			3.0	0.086	0.003	
			4.0	0.063	0.002	
		1.15	1.5	0.136	0.002	
			2.0	0.106	0.002	
			3.0	0.080	0.007	
			4.0	0.063	0.002	
0.600	Metal	1.15	2.0	0.104	0.015	Bettis
			3.0	0.081	0.012	
0.387	Metal	1.3	2.0	0.099	0.015	
			2.4	0.103	0.005	
			3.0	0.078	0.012	
0.600	UO_2	1.3	3.0	0.071	0.010	
	(7.53 g/cm^2)		4.0	0.059	0.009	
			5.0	0.051	0.004	
0.388			4.0	0.063	0.003	
			5.0	0.054	0.003	
	UO_2		2.9	0.078	0.004	
	(10.53 g/cm^2)		3.6	0.070	0.004	
			4.9	0.059	0.003	

(a) Water to uranium volume ratio.
(b) Errors listed for BNL measurements do not include the errors in P(t).

Several conclusions can be made from an examination of the data.

1) In H_2O moderated lattices, the values of δ_{28} are larger than values measured in single rods of the same diameter as the rods in the lattice. The increase in δ_{28} is caused by the large interaction effect. A measurement of the degree of interaction was made at Bettis.[K.4] A uranium oxide rod in an H_2O-moderated lattice, was replaced by a lead rod containing the foils used to measure δ_{28}. A decrease of only 10 per cent in the U^{238} fission product activity of the foils was observed, indicating that only 10 per cent of the fast fissions in a rod in the lattice under consideration came from fast neutrons born within the rod.

2) In water-moderated lattices, δ_{28} is highly dependent on the ratio of the moderator to the fuel volumes for tight lattices, owing to the changes in the interaction fast effect.

3) The existence of a large interaction effect in water-moderated lattices suggests the applicability of a homogeneous treatment, in which δ_{28} is calculated for an equivalent homogeneous system.[R.1] This method is not applicable for calculations of δ_{28} in the MIT D_2O lattices containing one-inch diameter rods, because the interaction effect in these lattices was small.

2.3.4 Measurements of δ_{28} in Non-Cylindrical Fuel Elements

Measurements of δ_{28} have been made in plate type, tubular, and concentric tubular fuel elements at the Savannah River Laboratory.[F.4] Hill has measured δ_{28} in spheres.[H.4] Since the emphasis of the present work is on cylindrical fuel elements, the measurements in non-cylindrical fuel elements will not receive further mention.

2.4 METHODS OF CALCULATING THE FAST FISSION EFFECT

The quantities used as measures of the fast effect are δ_{28} and ϵ. The parameter, δ_{28}, the ratio of fission in U^{238} to fission in U^{235}, is a measurable quantity. The definition of ϵ, the fast fission factor, varies with the theory used to describe the neutron economy. A brief discussion of several methods for calculating these quantities follows.

2.4.1 Method of Castle, Ibser, Sacher, and Weinberg

This method was the first published treatment of the fast effect. It is included in most texts on reactor theory (i.e., Glasstone and Edland;[G.2] Weinberg and Wigner;[W.1] Meghreblian and Holmes[M.3]) and yields satisfactory results for uranium metal lattices in which the interaction fast effect is small. Graphite lattices and many D_2O lattices are included in this category. It can be modified for use in hydrogen-moderated assemblies or assemblies of clustered fuel rods, but in these systems other methods are generally used.

The authors defined ϵ as the number of neutrons slowing down below the U^{238} fission threshold per neutron born in thermal fission. They assumed that all fast neutrons were born above this threshold and suggested that this assumption leads to an error of only 3 per cent in the calculated value of $\epsilon - 1$. The assumption is invalid, but the method yields good results because the cross-sections used in the calculation were chosen to fit the results of measurements.

The expression for ϵ is derived in the texts cited; it is:

$$\epsilon = 1 + \frac{\left(\nu_{28} - 1 - \frac{\sigma_c}{\sigma_f}\right)\frac{\sigma_f}{\sigma_{tr}} P}{1 - \frac{\nu_{28}\sigma_f + \sigma_e}{\sigma_{tr}} P'}, \qquad (2.4.1)$$

where P is the average probability of a collision within the fuel rod of a fast neutron on its first flight, and P′ is the collision probability on the second or subsequent flights; each subsequent collision probability is assumed to be equal to P′. Collision probabilities for cylindrical, spherical and slab type fuel elements can be found in a report by Case, DeHoffmann, and Placzek.[C.2]

The following set of constants was chosen to agree with experimental results:

$\nu_{28} = 2.5$ (neutrons per fissions)

$\sigma_f = 0.29$b (fission cross-section)

σ_c = 0.04b (radiative capture cross-section)

σ_e = 1.5b (elastic scattering cross-section)

σ_{tr} = 4.3b (transport cross-section)

It is assumed that $\sigma_{tr} = \sigma_f + \sigma_c + \sigma_i$; and σ_i, the inelastic scattering cross-section, is 2.47b. A fast neutron which is inelastically scattered is assumed to be scattered below the U^{238} fission threshold.

2.4.2 Method of Spinrad

Spinrad defined ϵ as the number of neutrons escaping into the moderator per neutron produced in thermal fission. In assemblies of rod clusters, the definition was extended to neutrons escaping the cluster per neutron produced in thermal fission. To calculate this quantity, he defined three neutron groups:

Group 1. Neutrons with energies above the U^{238} fission threshold. They can be removed from the group by absorption, leakage or inelastic scattering. They can also undergo elastic scattering and remain within the group.

Group 2. Neutrons born in fission with energies below the U^{238} fission threshold. These neutrons can be removed from the group by leakage or absorption. They can also undergo elastic scattering and remain within the group.

Group 3. Neutrons that have been scattered out of group 1. These neutrons can be lost from the group only by leakage or absorption and can undergo elastic scattering. They have energies within the same range as the neutrons of group 2, but are considered to have a different energy spectrum.

A formulation of this method is included in the March, 1960 issue of Nuclear Science and Engineering.[F.2] By defining suitable cross-sections and using the concept of collision probabilities, an expression for ϵ is derived. Cross-sections calculated by Fleishman and Soodak who used BNL-325,[H.6] Cranberg's expression for the fission spectrum for groups 1 and 2,[C.5] and an Ee^{-E} spectrum for group 3 are included in Table F.1.

Fleishman and Soodak also derived an equation for δ_{28}. This equation, and a comparison of calculated and measured values of δ_{28}, are given in Appendix F.

The application of this method to fuel rod clusters has been considered by Dessauer.[D.1] The clusters were homogenized and the variation of δ_{28} and ϵ as functions of rod radius, and uranium, D_2O and Al fractions was studied.

The method was also used for comparison with experimental results in D_2O-U lattices at Chalk River.[C.6, H.5] In these papers, Critoph includes a set of cross-sections which lead to agreement with the Chalk River experimental results.

Girard gives an equation used by the French workers for calculations of ϵ.[G.1] This equation uses a different set of cross-section values, but the formulation is basically the same as that of Spinrad. The Spinrad method is considered in ANL 5800,[R.1] and still another set of cross-sections is given.

2.4.3 Method of Carlvik and Pershagen[C.1]

Carlvik and Pershagen define ϵ as the number of neutrons that either slow down below 0.1 Mev in the fuel or leave the fuel, per primary neutron produced by thermal fission. They derive a two-group equation for ϵ which they consider to be closer to physical reality than the earlier formulation of Castle et al. They state that the earlier formulation gives reasonable results only for uranium metal rods because the cross-sections have been chosen to agree with experiments. For fuel elements or uranium metal assemblies in which a homogenization process is used, the question of which average cross-section to choose for the other elements becomes critical. This argument is similar to one used by Spinrad. The two methods differ, however, in the choice of the model to be used for the calculation.

The two groups used by Carlvik and Pershagen are:

Group 1. Neutrons with energies above fission threshold for U^{238}.

Group 2. Neutrons between 0.1 Mev and the fission threshold for U^{238}. The level 0.1 Mev is chosen because most neutrons are born with energies above this value.

A discussion of this method can be found in the 1958 Geneva series.[P.3] A comparison of measured values and values of δ_{28} calculated with this method is given in section 4.1.5 below.

The problem of using this method when there is a significant interaction fast effect is considered by the authors. They suggest a method of calculating the increased collision probability due to the presence of nearby rods. They also suggest a simple method for calculating the difference between first and subsequent collision probabilities.

2.4.4 Methods of Calculating δ_{28} in Lattices with Large Interaction Fast Effects

The simplest approach for this type of lattice is to calculate δ_{28} for a homogeneous lattice of the same composition. As Chernick points out, this value will yield a lower limit for δ_{28} or ϵ.[C.4] A homogeneous treatment is most applicable for very tight lattices and a discussion of this method is included in ANL 5800.[R.1]

The use of collision probabilities in tight lattices results in very complicated expressions, and approximate solutions can be found only with the aid of many simplifying assumptions. This problem has been considered by Radkowsky, Chernick and Mozer and others.[C.4] In his master's thesis at MIT, Weitzberg reviews several of the methods which have been proposed.[W.2]

Monte Carlo methods have been applied to the problem. An IBM 704 code (FF-MOCCA) written by Rief is being used at BNL.[R.4] Values of ϵ have been calculated for uranium-beryllium systems, and uranium and uranium oxide-water systems. A Monte Carlo fast fission code is being written in the IBM Fortran language by E. Allard at MIT.[A.1]

CHAPTER III.
EXPERIMENTAL METHODS

The main purpose of this study has been the development of improved methods for measuring δ_{28}, the ratio of fissions in U^{238} to fissions in U^{235}. In addition, other parameters and effects have been studied experimentally. After a brief discussion of the available facilities, the methods used in the experimental work will be discussed.

3.1 FACILITIES

Most of the irradiations needed for the measurements were made in a subcritical assembly driven by neutrons from the MITR thermal column. Figures 3.1 and 3.2 are cross-section drawings of the system. A detailed description of the assembly is included in Report NYO-9658, the "Heavy Water Lattice Research Project Annual Report," September 30, 1961.[H.3] Neutrons from the 5 × 5-foot face of the MITR thermal column are reflected through 90 degrees into a tank containing the moderator and the vertical fuel rods. The use of a "holhraum" (graphite-lined cavity) rather than solid graphite in the space adjacent to the thermal column face was necessary because the attenuation through solid graphite would result in an intolerably low flux at the base of the tank. The selected configuration of the cavity and the "pedestal" (the graphite region immediately below the tank) was the result of a compromise between two criteria:

1) Maximizing the flux entering the tank.
2) Shaping the entering flux to a J_o radial distribution.

The experimental and theoretical work on the cavity assembly was done mainly by Mr. John T. Madell and is described in detail in Report NYO-9657.[M.1] The selected pedestal configuration was the result of work done by Mr. Philip F. Palmedo and is described in Report NYO-9660.[P.1] The main emphasis in the pedestal work was on the shaping of the flux entering the tank.

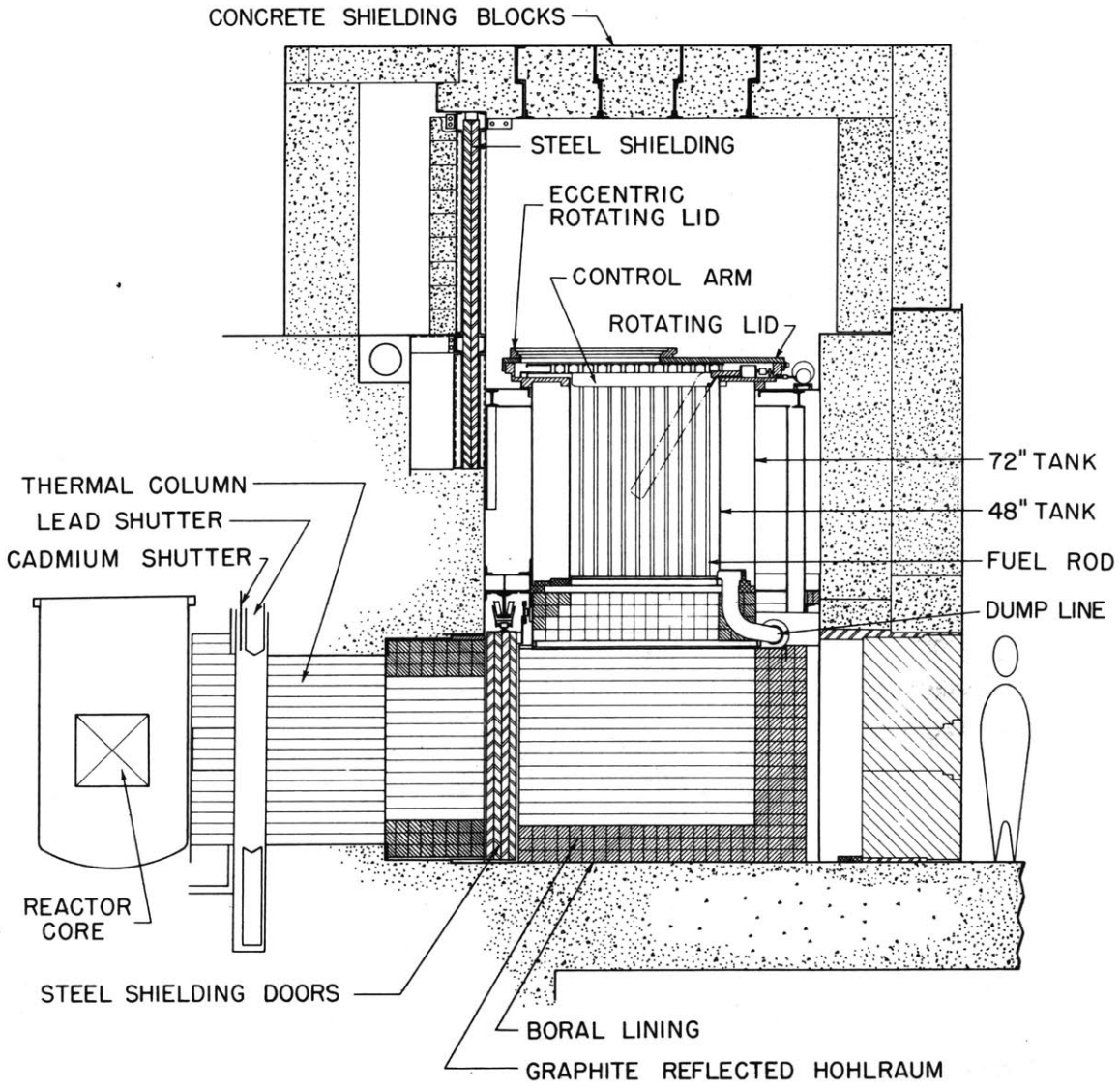

FIG. 3-1 VERTICAL SECTION OF THE SUBCRITICAL ASSEMBLY

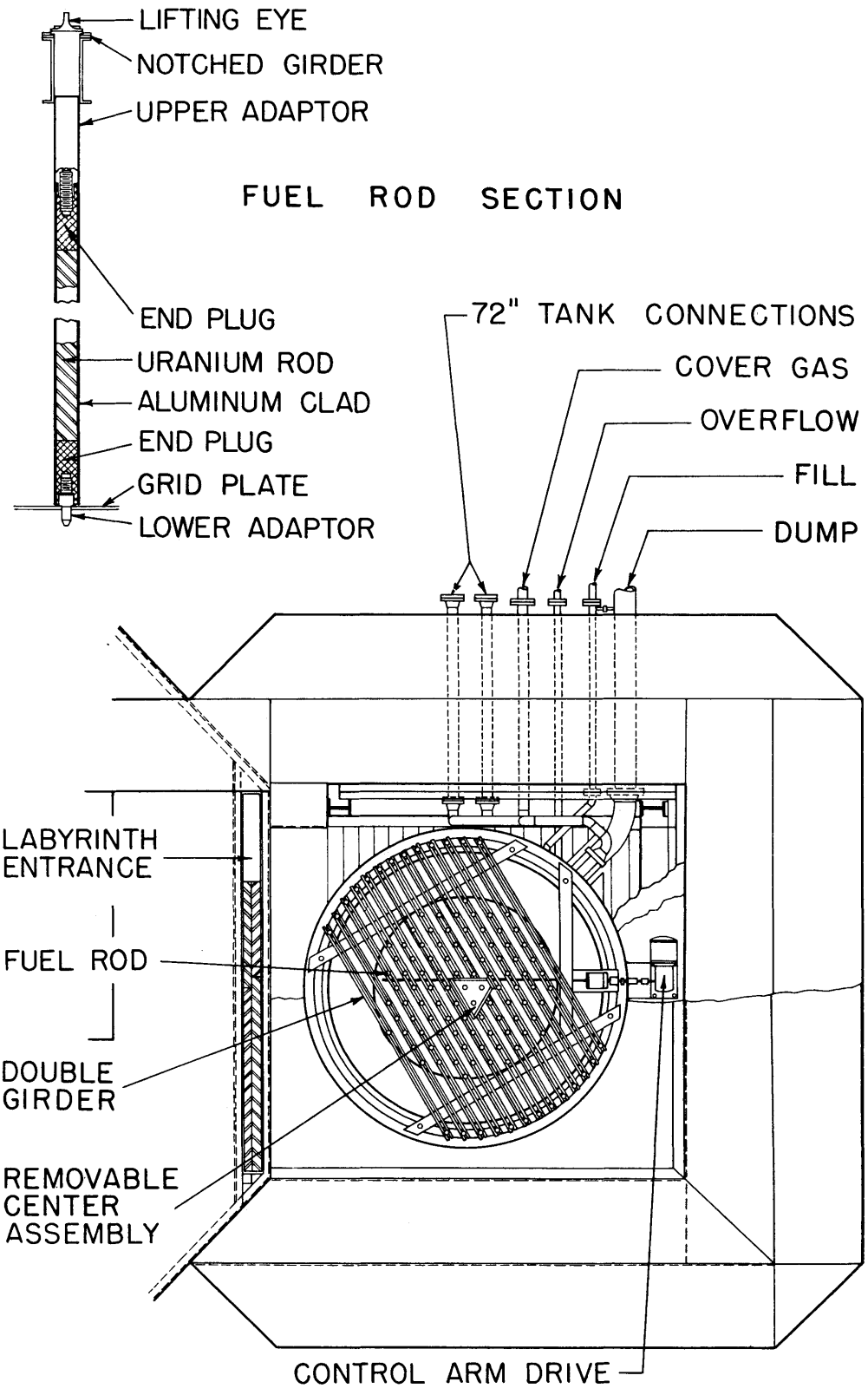

FIG. 3-2 PLAN VIEW OF THE SUBCRITICAL ASSEMBLY

The system has been designed so that tanks of different diameters can be used within an outer tank 72 inches in diameter. Figure 3.1 shows that the first tank used had a diameter of 48 inches. The function of the outer tank is to permit the use of liquid reflectors if necessary. In the first series of experiments, however, the inner tank was used as a bare system by surrounding it with a 0.021-inch sheet of cadmium, and by leaving the outer tank empty.

The fuel rods are held in place by double girders attached to support beams. The beams are supported by the upper flange of the outer tank, which rests on a steel ring. The ring is supported by the steel framework extending to the floor. The entire weight of the tanks and the fuel rods is thus supported from above; no load is supported by the graphite pedestal.

As shown in Fig. 3.2, the central girders support a removable three-rod cluster (center assembly). This unit is used for microscopic measurements such as those of δ_{28}, δ_{25}, ρ_{28} (the U^{238} cadmium ratio), conversion ratio, and for intra-cell flux plots. The fuel rods are accessible through a 10-inch hole in an eccentric rotary lid which is mounted on the tank lid. The hole is covered with a transparent, movable, plastic shutter. Both lids can be rotated and, with proper positioning, access to any position within the tank is permitted. To assure high purity of the heavy water, a glove box and plastic bag are used when access to the fuel rods or the three-rod cluster is necessary. The glove box is located above the 10-inch hole. The plastic bag is attached to the glove box and permits fuel rods to be moved into and out of the tank. In these operations, it is, of course, necessary to open the plastic shutter. When it becomes necessary to remove the lid for changes in the lattice configuration or for experimental purposes, the system is dried before reintroducing the heavy water into the 48-inch tank from the storage tank.

Details of the piping system, instrumentation, and shielding of the assembly can be found in NYO-9658.[H.3] Details pertinent to the experiments discussed in this thesis will be included in the appropriate sections.

In addition to the subcritical assembly, other MITR experimental ports were available for lattice project experimentation. In the work to be reported, the Medical Therapy Room Port was used primarily for the

experiments on the effect of neutron spectrum on P(t). Other ports were used on occasion and their use will be described in the appropriate sections.

Beyond the confines of the reactor containment shell, several areas were reserved for lattice project use. A set-up area containing a horizontally mounted, shielded, and ventilated hood was used for positioning foils in the three-rod cluster and for other work requiring the use of a hood. An air-conditioned counting room was also available for lattice project experimentation. The gamma-counting systems used in the experiments were set up in this area, and will be discussed in section 3.2.

3.2 MEASUREMENT OF δ_{28}

3.2.1 General Discussion

There are several aspects common to all existing methods of measuring δ_{28}. These will be discussed before considering the method used in this study and the differences between this method and earlier methods discussed in section 2.2.

In all existing methods, at least two foils of differing U^{235} content are irradiated, the usual combinations being a foil highly depleted in U^{235} and a foil of natural uranium or of the same enrichment as the fuel. The foils are irradiated in equivalent lattice positions or in positions for which a known normalization factor can be applied to the activity of one foil to compare it to the activity of the other foil. Upon removal of the foils from the fuel rod after completion of the irradiation, the relative fission product activity of the two foils is determined. This ratio can be related to δ_{28}.

To derive the relationship in its most general form, three subscripts denoting the isotopic concentrations of the uranium will be introduced. The subscript 1 will correspond to the isotopic concentrations of the depleted foil; 2, to those of the second foil; and 3, to those of the fuel. The measurement requires two foils of differing composition. The U^{235} concentration is as small as possible in the depleted foil. The U^{235} concentration of the second foil may equal the U^{235} concentration of the fuel, or it may be some other known enrichment. The usual enrichment in this case is the natural isotopic mixture present in naturally occurring uranium; often foils of the same enrichment as the fuel are not available. In the MIT measurements, the second

foil was always of natural uranium. We shall define $\gamma(t)$ as the ratio, at a time t after the irradiation, of the measured fission product activity in the depleted uranium foil to the activity of the second foil. The activities should, of course, be corrected for background, dead time, and differences in foil weights. For each foil, the fission product activity is the sum of the activities due to U^{238} and U^{235} fissions. Hence,

$$\gamma(t) = \frac{\mu_{28}(t)\, N_1^{28} \int_{E_T}^{\infty} \phi(E)\, \sigma_f^{28}(E)\, dE + \mu_{25}(t)\, N_1^{25} \int_0^{\infty} \phi(E)\, \sigma_f^{25}(E)\, dE}{\mu_{28}(t)\, N_2^{28} \int_{E_T}^{\infty} \phi(E)\, \sigma_f^{28}(E)\, dE + \mu_{25}(t)\, N_2^{25} \int_0^{\infty} \phi(E)\, \sigma_f^{25}(E)\, dE} . \qquad (3.2.1)$$

In this equation $\mu_{28}(t)$ is defined as the number of counts measured per U^{238} fission per unit time as a function of time after irradiation, and $\mu_{25}(t)$ is the number of counts measured per U^{235} fission per unit time as a function of time after irradiation. The quantities, $\mu_{28}(t)$ and $\mu_{25}(t)$, are different because the fission product yields are different for U^{238} and U^{235}. The neutron flux in the energy interval dE at energy E, averaged over the rod, is denoted by $\phi(E)dE$. The formulation of the problem is not affected by neglecting the spatial variation of the flux. The N's are the atom densities of U^{238}, (28), and U^{235}, (25), in the two foils; E_T is the U^{238} fission threshold energy. The lower limit of the integral containing E_T could have been written as 0, because the fission process in U^{238} is a threshold reaction. That is,

$$\int_{E_T}^{\infty} \sigma_f^{28}(E)\, \phi(E)\, dE = \int_0^{\infty} \sigma_f^{28}(E)\, \phi(E)\, dE , \qquad (3.2.2)$$

since,

$$\sigma_f^{28}(E) = 0 \qquad \text{for } E < 0 < E_T . \qquad (3.2.3)$$

The quantity δ_{28} is the ratio of fissions in U^{238} to fissions in U^{235} in the fuel, and can be written:

$$\delta_{28} = \frac{N_3^{28} \int_{E_T}^{\infty} \sigma_f^{28}(E)\, \phi(E)\, dE}{N_3^{25} \int_0^{\infty} \sigma_f^{25}(E)\, \phi(E)\, dE} . \qquad (3.2.4)$$

Using the following definitions:

$$P(t) = \frac{\mu_{25}(t)}{\mu_{28}(t)} , \qquad (3.2.5)$$

and

$$\frac{I_{28}}{I_{25}} = \frac{\int_{E_T}^{\infty} \sigma_f^{28}(E)\, \phi(E)\, dE}{\int_0^{\infty} \sigma_f^{25}(E)\, \phi(E)\, dE} , \qquad (3.2.6)$$

and dividing the numerator and denominator of Eq. 3.2.1 by $\mu_{25}(t)\, N_2^{25} I_{25}$, we get

$$\gamma(t) = \frac{\frac{1}{P(t)} \frac{N_1^{28}}{N_2^{25}} \frac{I_{28}}{I_{25}} + \frac{N_1^{25}}{N_2^{25}}}{\frac{1}{P(t)} \frac{N_2^{28}}{N_2^{25}} \frac{I_{28}}{I_{25}} + 1} . \qquad (3.2.7)$$

From Eqs. 3.2.4 and 3.2.6, it follows that

$$\frac{I_{28}}{I_{25}} = \frac{N_3^{25}}{N_3^{28}}\, \delta_{28} . \qquad (3.2.8)$$

Substitution of Eq. 3.2.8 into Eq. 3.2.7 yields

$$\gamma(t) = \frac{P(t) \frac{N_1^{28}}{N_2^{25}} \frac{N_3^{25}}{N_3^{28}}\, \delta_{28} + \frac{N_1^{25}}{N_2^{28}}}{\frac{1}{P(t)} \frac{N_2^{28}}{N_2^{25}} \frac{N_3^{25}}{N_3^{28}}\, \delta_{28} + 1} . \qquad (3.2.9)$$

Equation 3.2.9 can be rearranged to solve for δ_{28}:

$$\delta_{28} = \frac{P(t)\left[\frac{N_2^{25}}{N_3^{25}}\frac{N_3^{28}}{N_1^{28}}\gamma(t) - \frac{N_1^{25}}{N_1^{28}}\frac{N_3^{28}}{N_3^{25}}\right]}{1 - \frac{N_2^{28}}{N_1^{28}}\gamma(t)}. \qquad (3.2.10)$$

Expressions for the quantities N_3^{28}/N_1^{28} and N_2^{28}/N_1^{28} can be obtained. If it is assumed that

$$N_1^{25} + N_1^{28} = N_2^{25} + N_2^{28} = N_3^{25} + N_3^{28}, \qquad (3.2.11)$$

then

$$N_1^{28}(R_1+1) = N_2^{28}(R_2+1) = N_3^{28}(R_3+1), \qquad (3.2.12)$$

where

$$R_i = N_i^{25}/N_i^{28}. \qquad (3.2.13)$$

From Eq. 3.2.12, we get

$$\frac{N_3^{28}}{N_1^{28}} = \frac{1+R_1}{1+R_3} = a_3; \qquad \frac{N_2^{28}}{N_1^{28}} = \frac{1+R_1}{1+R_2} = a_2. \qquad (3.2.14)$$

Substitution of Eq. 3.2.14 into Eq. 3.2.10, gives

$$\delta_{28} = \frac{P(t)\left[\frac{N_2^{25}}{N_3^{25}}a_3\gamma(t) - S\right]}{1 - a_2\gamma(t)} = P(t)F(t), \qquad (3.2.15)$$

where

$$S = R_1/R_3, \qquad (3.2.16)$$

and F(t) is the ratio, at time t, after irradiation, of counts originating from U^{238} fission products to counts from U^{235} fission products in a foil of the same composition as the fuel. When the U^{235} concentration of foil 2 is the same as the U^{235} concentration of the fuel, $a_3 = a_2 = a$,

and Eq. 3.2.15 reduces to the familiar form,

$$\delta_{28} = P(t)\,\frac{a\gamma(t) - S}{1 - a\gamma(t)} = P(t)F(t). \qquad (3.2.17)$$

In all existing methods of determining δ_{28}, this formulation is used. The differences among the methods arise in the techniques used for measuring $\gamma(t)$ and $P(t)$. The functions $\gamma(t)$ and $P(t)$ may differ with different methods, but should yield the same value of δ_{28} for a given lattice when substituted into Eqs. 3.2.15 or 3.2.17.

The method developed in this study is based on the counting of gamma rays. Gamma-counting is also used in the Westinghouse and Savannah River Laboratory methods discussed in section 2.2. The choice of a gamma-counting rather than a beta-counting technique such as the one used at Brookhaven (also discussed in section 2.2) was made for several reasons.

1) Beta-counting methods are more sensitive to handling procedures because they require the use of catcher foils. As many as 12 Al catcher foils are used in a measurement of δ_{28},[K.7] and these thin foils must be carefully positioned to get consistent results. Special care must be taken not to wrinkle the foils when they are inserted into the fuel rod.

2) The results of experiments using beta-counting techniques are sensitive to the condition of the surface of the uranium foil, while gamma-counting results are not. Movement of fission products from the uranium foils to the catcher foils is affected by the oxide on the uranium foil surfaces, so that care must be taken to remove all oxide from the foil surfaces if beta-counting is used.

3) Gamma-counting methods are less sensitive to foil thickness. The energies of the gammas counted in all gamma-counting methods are great enough so that self-shielding is negligible in uranium foils several mils thick. Beta-counting methods could be devised which do not require the use of catcher foils, but self-shielding would still present a problem, and the results might depend on foil thickness.

As in all earlier methods, the method developed for measuring δ_{28} in the MIT lattice experiments requires two measurements. These are: (a) the measurement of $\gamma(t)$; (b) the measurement of $P(t)$. It is only

necessary to measure P(t) once. When a measurement of δ_{28} is required, the function $\gamma(t)$ is determined, and this function and the known function P(t) are substituted into Eq. 3.2.15 or Eq. 3.2.17 to obtain δ_{28}.

3.2.2 Measurement of $\gamma(t)$

The measurement of $\gamma(t)$ is made by means of a method similar to the Westinghouse technique. The counting setup is shown in Fig. 3.3. The following procedure was used.

1) The apparatus is calibrated for integral gamma-counting above 0.72 Mev. The reason for selecting 0.72 Mev will be discussed in 5) below. To do the calibrations, the 0.66 Mev gamma peak of Cs^{137} and the 0.84 Mev peak of Mn^{54} are located. The Pulse Height Selector (PHS) setting for 0.72 Mev biasing is then determined by linear interpolation. To locate the 0.66 Mev and the 0.84 Mev peaks, the integral bias curves for each of the calibration sources is determined. The curves of the differences between consecutive readings versus PHS setting are then plotted, and the PHS setting corresponding to the maximum point of each curve is taken as a calibration peak. The PHS interval between consecutive readings should be constant, and the combination of this interval and the counting time for each reading should be such that the difference curve can be determined accurately. Increasing the calibration source strength increases the number of counts in a given interval and therefore facilitates the calibration procedure.

2) The backgrounds of the foils to be irradiated are determined. If the foil has been irradiated within a period of a few days before the background measurement, the background might be a function of time, depending upon the irradiation conditions. It is, therefore, sound practice to keep track of the irradiation history of each foil.

3) The foils are positioned in the fuel rod. Figure 3.4 shows the foil arrangement used in the measurement of δ_{28}. The purpose of the Al foils is to prevent contamination by fission products from the fuel adjacent to the experimental foils. Measurements were made to determine the effect of fission product contamination and the effect of placing the two foils in adjacent positions. These measurements will be discussed in

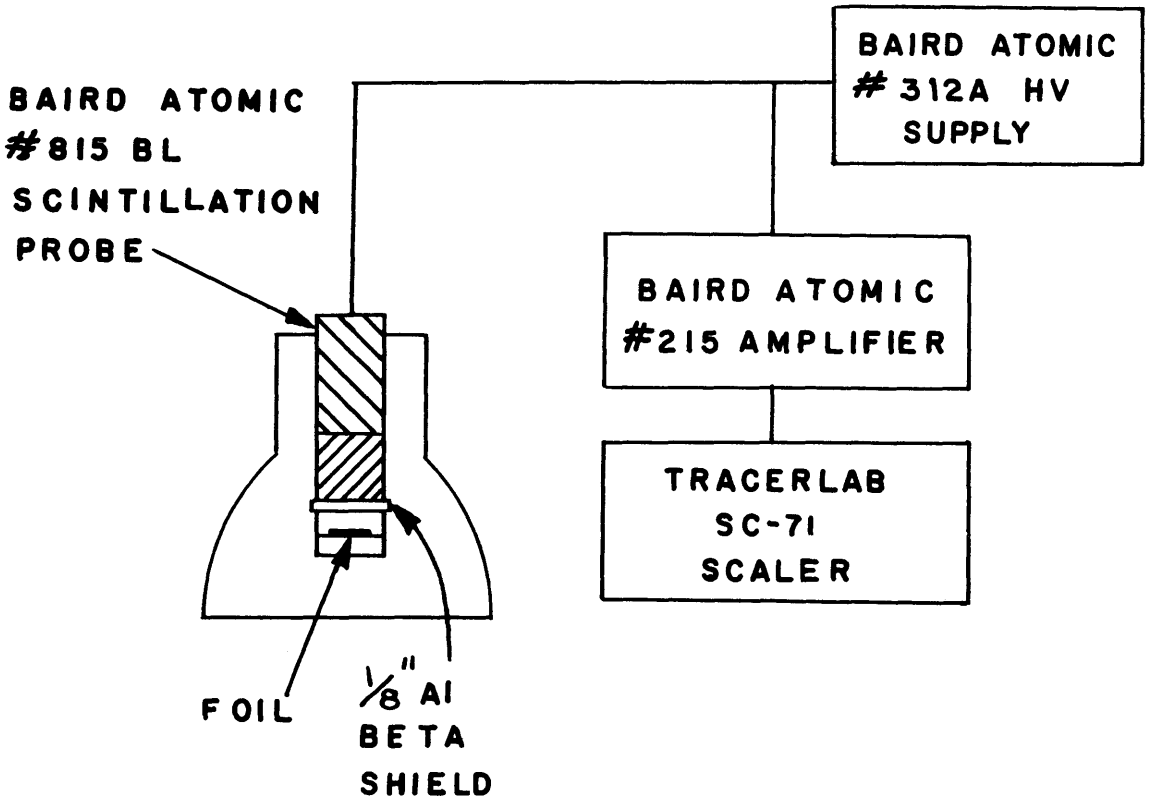

FIG. 3-3 EQUIPMENT FOR MEASURING GAMMA ACTIVITY OF THE FOILS

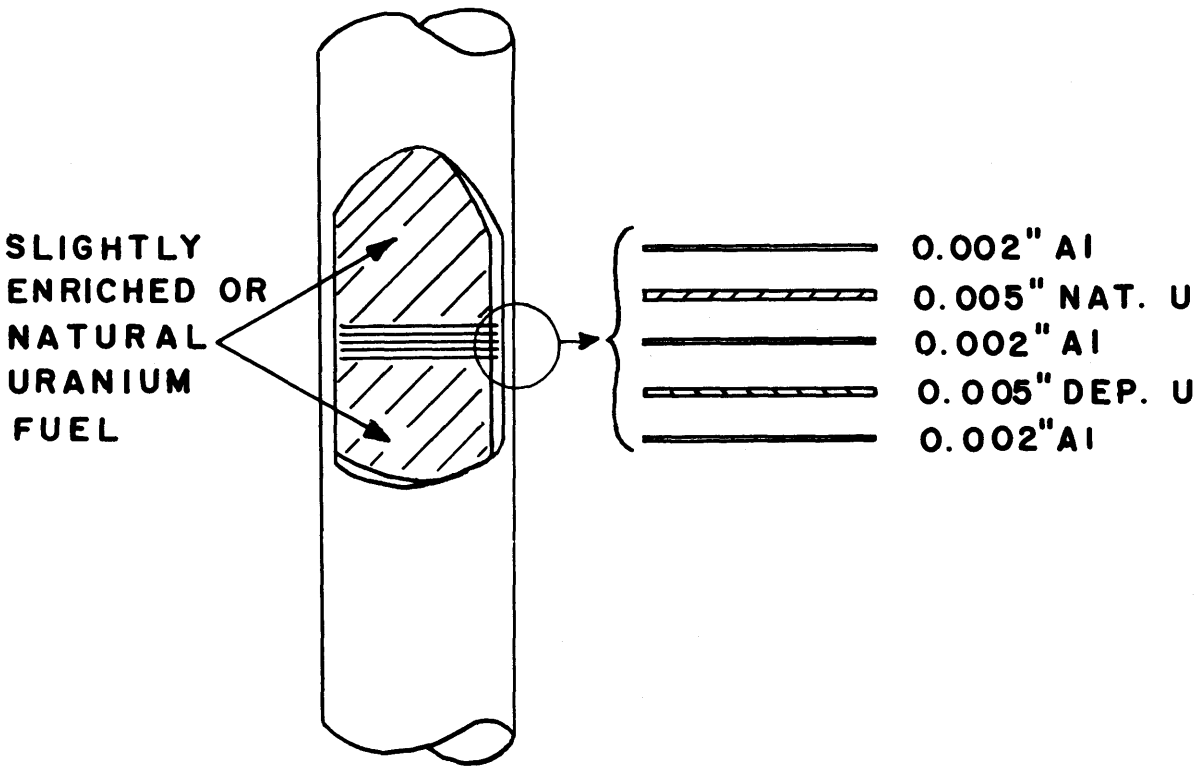

FIG. 3-4 FOIL ARRANGEMENT FOR δ_{28} MEASUREMENTS

section 3.3 and section 3.4.

4) The fuel rod or cluster is positioned in the subcritical assembly and the irradiation is begun. A standard irradiation time of 4 hours was used because this length of time met the requirements of the δ_{28} measurement as well as the requirements of experiments on resonance capture and thermal utilization which were often made at the same time as the fast fission measurements. The controlling factor in the selection of an irradiation time is the fission product activity of the depleted uranium foil which must be large enough to satisfy the statistical requirements of the experiment. The activity of the natural foil must also be considered. If it becomes too high, uncertainties in the dead time of the counting system may contribute significantly to the total experimental uncertainty. There is also a problem associated with pulse pileup for high activities, which is discussed in section 4.1.2 and Appendix E.

5) Upon completion of the irradiation, an adequate cooling time is allowed before removal of the fuel rod or cluster from the assembly. An "adequate" cooling time must satisfy two requirements:

(a) The radiation levels associated with the removal operation must be tolerable from the standpoint of radiation safety.

(b) The time must be short enough so that the count rate of the depleted uranium foil has not decayed to an intolerably low level.

A cooling period of 3 hours has been used for 4-hour irradiations. The maximum radiation level on the surface of the rods after a 3-hour cooling period was about 1r/hr, which was considered acceptable. The 3-hour cooling period satisfied the above conditions and also obviated an additional complication, which will be discussed briefly. Since the purpose of the experiment is to determine the ratio of fission product activity in the two foils, the number of counts coming from U^{238} capture reactions and subsequent beta decay must be small. Consider the capture reaction and the decay chain of the resulting U^{239} nuclide:

$$U^{238} + n \longrightarrow U^{239} \xrightarrow{23m} Np^{239} + \beta(1.2\ \text{Mev}) \xrightarrow{2.3d} Pu^{239} + \beta(0.72\ \text{Mev}) . \qquad (3.2.18)$$

The gammas associated with these beta decays have lower energies than the maximum beta energies; but even though a beta shield is used, there is bremsstrahlung with a maximum energy equal to the maximum energy of the betas. If counting starts before most of the U^{239} is allowed to decay, a significant fraction of the counts of the depleted foils may come from bremsstrahlung with energy above 0.72 Mev and originating from the U^{239} betas. The 0.72 Mev bias setting insures that no bremsstrahlung originating from the Np^{239} betas will be counted. A cooling period of three hours is long enough to insure a negligible contribution from the U^{239} beta activity.

6) The rod or cluster is removed from the assembly, and the foils are removed from the rod.

7) The foils are counted, with the discriminator setting at 0.72 Mev.

A measurement of δ_{28} could be made with only one measurement of the count rate of each foil, but the precision is improved by counting each foil several times The counting time for each measurement is chosen to give enough counts to satisfy the statistical requirements of the measurement. Counting intervals of 1 minute were sufficient to permit most 1-inch foils irradiated in the subcritical assembly to register at least 2000 counts for times up to about 8 hours after irradiation. Experiments with foils 1/4-inch in diameter usually required longer counting intervals for the depleted uranium foils.

The number of measurements of the count rate of a foil made after an irradiation usually depended on the number of foils irradiated during the experiment. It was common practice for each experimenter to make several experiments at the same time. This procedure reduced the total number of irradiations required, but increased the number of foils to be counted after a given irradiation. A general rule, however, was to make as many measurements of the count rates of the foils as possible.

8) The final operation is the reduction of the data. A data reduction code, written for the MIT IBM-7090 computer and discussed in Appendix D, was used to calculate δ_{28} from Eq. 3.2.15 or Eq. 3.2.17. The code makes all the count rate corrections and calculates and prints all quantities of interest, including an error analysis.

The above procedure for measuring $\gamma(t)$ is similar to the Westinghouse method (section 2.2). The major difference is in the selection of the bias setting. The Westinghouse technique requires a bias setting of 1.20 Mev, which makes the three-hour cooling period unnecessary. As soon as the rod can be removed from the assembly and the foils removed from the rod, the counting can begin. The advantage of using a setting of 0.72 Mev and waiting three hours is that the ratio of dose rate to the experimenter to count rate is reduced by a factor of about ten. By reducing the bias setting from 1.20 Mev to 0.72 Mev, the count rate is increased by an amount which just about compensates for the loss of fission product activity in the three-hour cooling period. But the radiation level associated with the rods three hours after irradiation is only about one-tenth the level at a half-hour after irradiation.

The workers at the Savannah River Laboratory have used bias settings as low as 0.5 Mev.[B.1] This procedure permits an even higher count rate, but requires a correction for the Np^{239} activity. The magnitude of this correction is difficult to determine, but should be small for times which are small compared to 2.3 days. In the MIT experiments, it was found that the activities resulting from four-hour irradiations and 0.72 Mev discrimination were satisfactory, and there was no need to go to lower bias settings.

Another advantage of using a 0.72 Mev bias setting rather than a 1.20 Mev setting is that the foils are counted at a longer time after irradiation with the result that the change in count rate per unit time is smaller. There is, therefore, a smaller uncertainty in count rates owing to uncertainties in time. The SRL method (see section 2.2), in which the foils are compared to foils irradiated in a standard position, goes one step further in eliminating uncertainties due to time. In this method, the uncertainty due to time is limited to the time uncertainty in the measurement of δ_{28} at the standard position. For several reasons, this method was not adopted at MIT: (1) there was no convenient standard position; (2) two additional foils had to be irradiated, counted, and analyzed for each experiment; and (3) the uncertainties due to time and bias setting were shown to be very small compared to other uncertainties in the measurement.

3.2.3 Measurement of P(t)

The method developed for measuring P(t) in this study differs from the earlier methods. As explained in section 2.2, the earlier methods all involve a fission chamber experiment for determining an absolute value of δ_{28}. Foils are irradiated within the fission chamber or at a position at which the flux is equal to the flux within the chamber, and are then gamma- or beta-counted. The absolute determination of δ_{28} with the fission chamber, coupled with the measurement of $\gamma(t)$ in the gamma- or beta-counting phase of the experiment, allows Eq. 3.2.15 or Eq. 3.2.17 to be solved for P(t).

The present method eliminates the need for a fission chamber experiment. Foils are irradiated in the usual manner and are gamma-counted. (Beta-counting with catcher foils could be used if desired.) The function $\gamma(t)$ is determined in the usual manner, as described in section 3.2.2. Research, which will be discussed in sections 3.14 and 4.9, has shown that the only important gamma ray with an energy above 1.2 or 1.3 Mev in the time interval from a week to several months after irradiation is the 1.60 Mev γ-ray from La^{140}. This nuclide has a 40h half-life, but reaches equilibrium with its parent, 12.8d Ba^{140}. The mass 140 chain has a high fission product yield, and 88 per cent of the La^{140} disintegrations result in the emission of a 1.60 Mev gamma ray. The ratio of the numbers of counts of the two foils at this energy is used to measure an absolute value of δ_{28}. This value of δ_{28} and the measured value of $\gamma(t)$ are inserted into Eq. 3.2.15 or Eq. 3.2.17 to determine P(t). The new method offers four advantages: (1) a direct measurement of δ_{28} within a fuel rod can be made; (2) the uncertainty in the measurement of δ_{28} is reduced; (3) measurements made at different laboratories can be compared more easily; (4) measured values can be brought up to date as improved fission product yield data become available.

We can define a quantity γ as the ratio of the numbers of counts from the two foils irradiated simultaneously in an interval which includes 1.60 Mev. This quantity is analogous to $\gamma(t)$, but is independent of time because gammas from only one fission product are counted, and the relative La^{140} activity of the two foils remains constant. An expression

analogous to Eq. 3.2.1 may be written:

$$\gamma = \frac{(\beta^{28})_{La^{140}} f(t)\, N_1^{28} I_{28} + (\beta^{25})_{La^{140}} f(t)\, N_1^{25} I_{25}}{(\beta^{28})_{La^{140}} f(t)\, N_2^{28} I_{28} + (\beta^{25})_{La^{140}} f(t)\, N_2^{25} I_{25}}. \qquad (3.2.19)$$

In this equation, $(\beta^{28})_{La^{140}}$ is the yield of La^{140} from the fission of U^{238}, and $(\beta^{25})_{La^{140}}$ is the yield from the fission of U^{235}; f(t) is a function of time which includes the buildup and decay of La^{140} and the counting efficiency for the 1.60 Mev gamma ray; the N's and I's have their usual meanings. The values used for $(\beta^{25})_{La^{140}}$ and $(\beta^{28})_{La^{140}}$ were 6.35 and 5.70, respectively.[N.2] The function f(t) could be written explicitly but, since it cancels out of Eq. 3.2.19, it is unnecessary to do so.

Expressions similar to Eqs. 3.2.15 and 3.2.17 can be derived. These are:

$$\delta_{28}^{*} = \left(\frac{\beta^{25}}{\beta^{28}}\right)_{La^{140}} \left\{\frac{N_2^{25}/N_3^{25}\, a_3\gamma - S}{1 - a^2\gamma}\right\} \qquad (3.2.20)$$

and

$$\delta_{28}^{*} = \left(\frac{\beta^{25}}{\beta^{28}}\right)_{La^{140}} \left\{\frac{a\gamma - S}{1 - a\gamma}\right\}. \qquad (3.2.21)$$

where δ_{28}^{*} is the notation that will be used for values of δ_{28} measured directly by using the La^{140} technique. The procedure for determining P(t) in this method follows.

1) The counting system, similar to the one shown in Fig. 3.5, is calibrated for the 1.60 Mev gamma ray. This peak is found directly by using the La^{140} peak from irradiated uranium foils. The channel width should be set to satisfy three conditions: (a) high ratio of counts to background, (b) low sensitivity to drift, (c) large count rate. Condition (a) is improved by decreasing the channel width and (b) and (c) are improved by

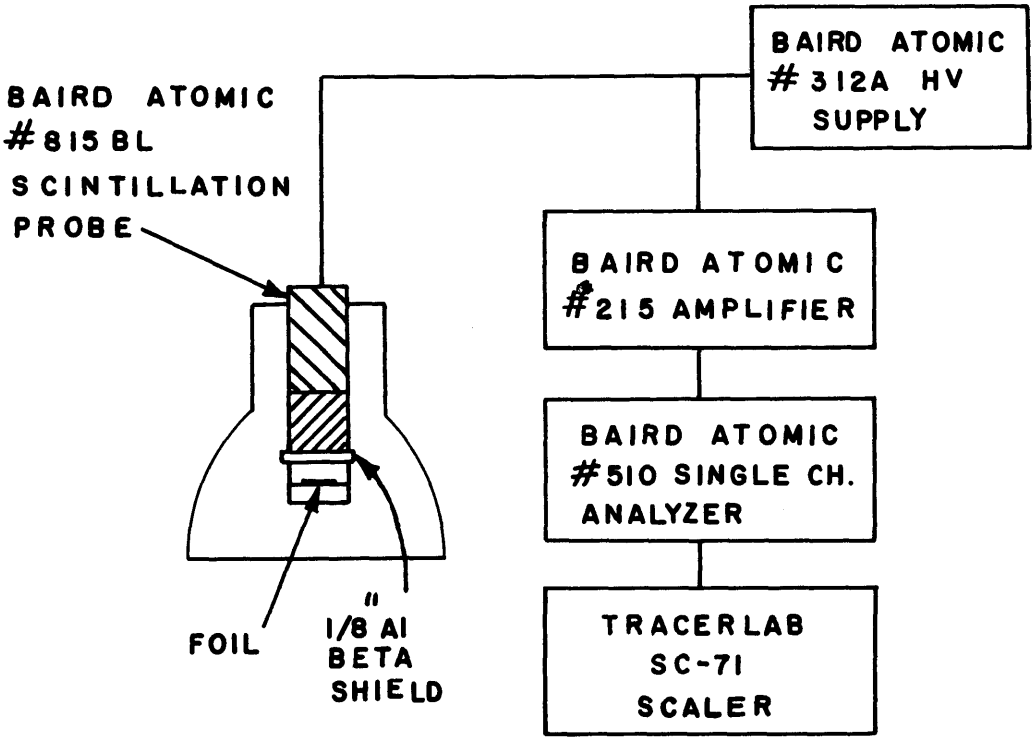

FIG. 3-5 EQUIPMENT USED TO MEASURE LA^{140} ACTIVITY OF THE FOILS

increasing the width, so that the chosen width should be a compromise among the three conditions. A width of 5.5 volts was used in the experiments and the calibrated base line setting varied from 53 to 54 volts. The width was, therefore, about 10 per cent of the base line value, and corresponds to about 0.16 Mev. All gamma rays with energies between about 1.52 Mev and 1.68 Mev were, therefore, counted.

2) The foil backgrounds are determined. These were about 11 counts a minute when a 1-3/4-inch × 2-inch NaI(Tl) crystal was used. About six counts per minute were from general background, not originating from the foils.

3) The foils are irradiated and $\gamma(t)$ is determined. The irradiation period was 4 hours, and $\gamma(t)$ was determined for a period from about 3-1/2 to 8-1/2 hours after irradiation. The measurement was repeated several times to improve the precision.

4) A different set of foils is used to measure the factor, γ. These foils are irradiated in the same position but for a much longer time. The foils used in 3) could be used for the measurement of γ, but it is neither necessary nor advisable to do so. A set of foils was irradiated for 22 hours. Two additional sets were irradiated to improve the precision of the measurement. The La^{140} activities in these foils were about 5-1/2 times as high as the activities in the foils irradiated for 4 hours, which explains why it is desirable to use this procedure.

5) After about a week, the 1.60 Mev activity of the foils mentioned in step 4) is counted. The counting is repeated daily for several weeks to improve the precision of the measurement. The system is calibrated daily and the background is checked periodically. It was found that the 22-hour irradiation resulted in initial depleted foil activities of about 10 times background, and initial natural foil (foil number 2) activities of about 200 times background. It was also found that 10-minute counting intervals for the natural foils and 30-minute intervals for the depleted foils gave reasonable numbers of counts. An advantage of using relatively short counting times is that the effect of drift is minimized.

6) The count rates are corrected for background, foil weights, and the slight differences in counting time (this correction should be small

because the effective half-life of La^{140} is 12.8 days), and γ is calculated. The value of γ measured on different days should be the same within reasonable statistical limits, and this turned out to be the case.

7) The quantity δ^*_{28} is calculated from Eq. 3.2.19 or Eq. 3.2.20; this result, and the value of $\gamma(t)$, are inserted into Eq. 3.2.15 or Eq. 3.2.17 and P(t) is determined.

The main advantage of the above method is that it provides a more accurate direct measurement of δ_{28} than the earlier fission chamber method. This permits a more accurate determination of P(t) and therefore more accurate measurements of δ_{28} for subsequent integral-counting experiments. An analysis of the errors and a discussion of the results are included in section 4.1.

Measurements of δ_{28} were made in heavy water moderated lattices containing one-inch diameter, natural uranium fuel rods. Additional experiments were made with 1-inch and 1/4-inch diameter single rods immersed in the heavy-water moderator. The results of these experiments are also discussed in section 4.1.

3.3 MEASUREMENT OF THE EFFECT OF FISSION PRODUCT CONTAMINATION ON THE FOIL ACTIVITIES

Figure 3.4 shows the foil arrangement used in a measurement of δ_{28}. The function of the Al foils is to prevent contamination of the uranium foil surfaces by fission products from adjacent fuel. An experiment was performed to determine the magnitude of the contamination that would result from the removal of an Al foil. The purpose of this experiment was to determine the error caused by faulty positioning of the Al foils.

The effect of fission product contamination is much more important for the depleted uranium foil than for the second, or natural uranium foil. The number of counts originating from the contamination would be approximately the same if each foil had a side exposed to fuel. The true count rate of the depleted foil is approximately twenty times smaller than the count rate of the natural uranium foil for the one-inch diameter rods, so that the ratio of true counts to counts originating

from contamination is smaller for the depleted uranium foil by approximately a factor of twenty. Figure 3.6 shows the foil arrangement for the experiment designed to measure this effect. The two adjacent depleted uranium foils were irradiated simultaneously. A side of one of the foils was exposed to fuel, while the other foil had both sides protected by Al. After a 4-hour irradiation, the fission product activities of the foils were measured. The results of this experiment are discussed in section 4.2.1.

3.4 INTERACTION OF ADJACENT FOILS IN THE MEASUREMENT OF δ_{28}

The use of adjacent uranium foils, separated only by a thin Al foil, as shown in Fig. 3.4, is desirable because it eliminates the need for normalizing the activities of foils irradiated in different positions. The possibility of a perturbation of the flux in one foil by the presence of another foil had to be investigated, however, before this method of foil positioning could be adopted. If foil 2 has the same U^{235} concentration as the fuel, it can be considered an extension of the fuel, and will not perturb the depleted uranium foil. In the experiments with the 1-inch diameter fuel rods, the fuel and the second foil were both made of natural uranium, so that this condition was fulfilled. The problem was, therefore, to investigate the degree of perturbation caused by the depleted foil on the fission rate of the natural uranium foil.

An experiment was designed to study this effect. Figure 3.7 shows the foil arrangement used to determine the extent of the perturbation caused by the depleted foil on the activity of the adjacent natural uranium foil. Two natural uranium foils were positioned below the foil sandwich and one above it. By comparing the activity of the natural uranium foil adjacent to the depleted foil, with the interpolated value at the same point determined from the activities of the other three natural uranium foils, a measure of the perturbation could be determined. The results of this experiment are discussed in section 4.2.2.

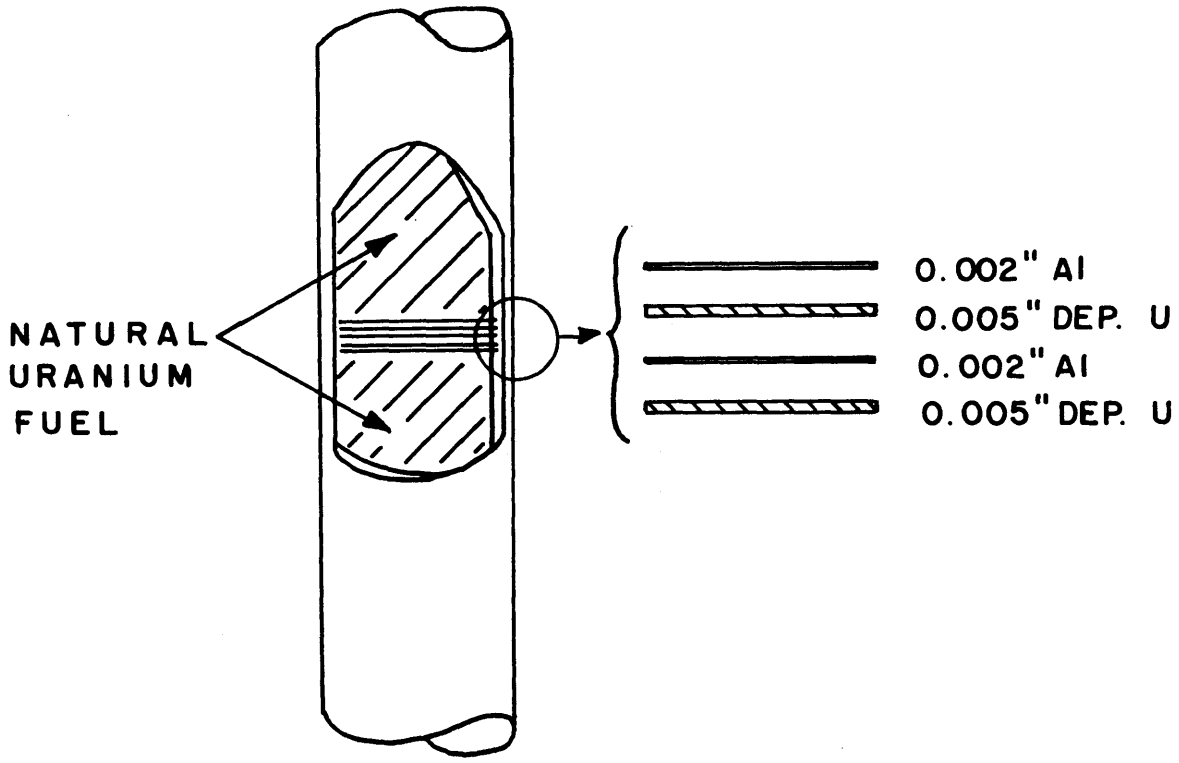

FIG. 3-6 FOIL ARRANGEMENT FOR CONTAMINATION EXPERIMENT

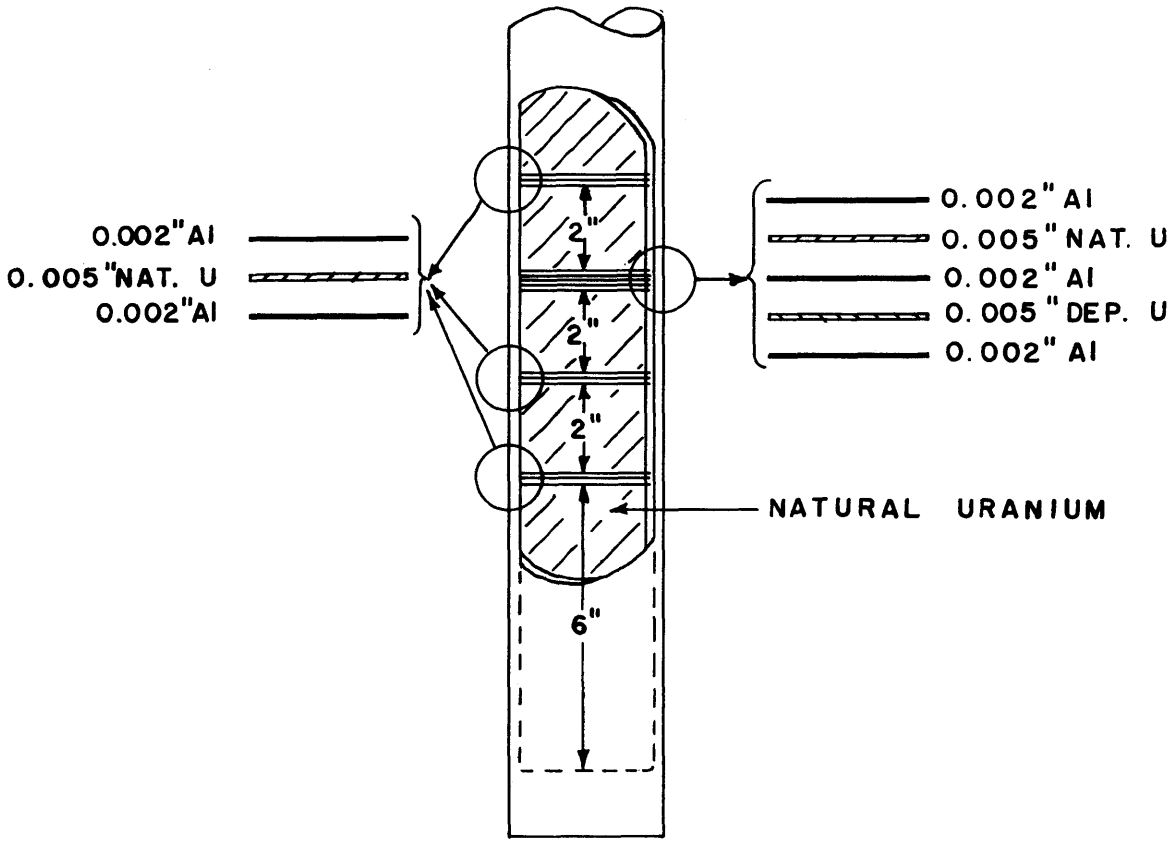

FIG. 3-7 FOIL ARRANGEMENT FOR INTERACTION EXPERIMENT

3.5 EFFECT OF COUNT RATE ON THE MEASUREMENT OF $\gamma(t)$

Measurements of $\gamma(t)$, the ratio of the depleted foil count rate to the natural foil count rate, showed discrepancies which could not be explained as statistical variations. It was noticed that $\gamma(t)$ was lowest for measurements in which the foil activities were the greatest. An experiment was designed to provide additional data for an analysis of this problem.

Figure 3.8 shows the foil arrangement used in the experiment. The rod was located in the central position of the 5-3/4-inch lattice. The neutron flux in the lattice is highest at the bottom of the tank and decreases with increasing height. The lowest foils were, therefore, irradiated at the highest neutron flux. The count rates of the highest and lowest sets of foils differed by a factor of about 3.5. The function $\gamma(t)$ was determined for each set of foils in the time interval from 228 minutes to 510 minutes after the irradiation. The results from this experiment were included in an analysis of the effect of count rate on the measurement of $\gamma(t)$. This analysis is discussed in section 4.1.2. Additional experimental work related to this problem is considered in Appendix E.

3.6 EFFECT OF THE RELATIVE POSITIONS OF THE DETECTOR AND THE FOILS ON THE FUNCTION P(t)

The effect on P(t) of the position of the uranium foils in relation to the NaI(Tl) scintillation detector, was first studied by Kinard and Baumann.[K.3] Changing the position at which the foils are counted changes the efficiencies for counting the gamma rays. The change in efficiency is a function of the gamma-ray energy, because the average angle at which the gamma rays enter the crystal is a function of the position at which the foils are counted; the efficiencies are a function of this angle and P(t) depends on the gamma-ray efficiencies, with the result that P(t) is a function of the relative positions of the detector and the foils. Kinard and Baumann found that this effect was negligible, and an attempt was made to reproduce their results.

Four sets of foils were irradiated for four hours in a rod in the

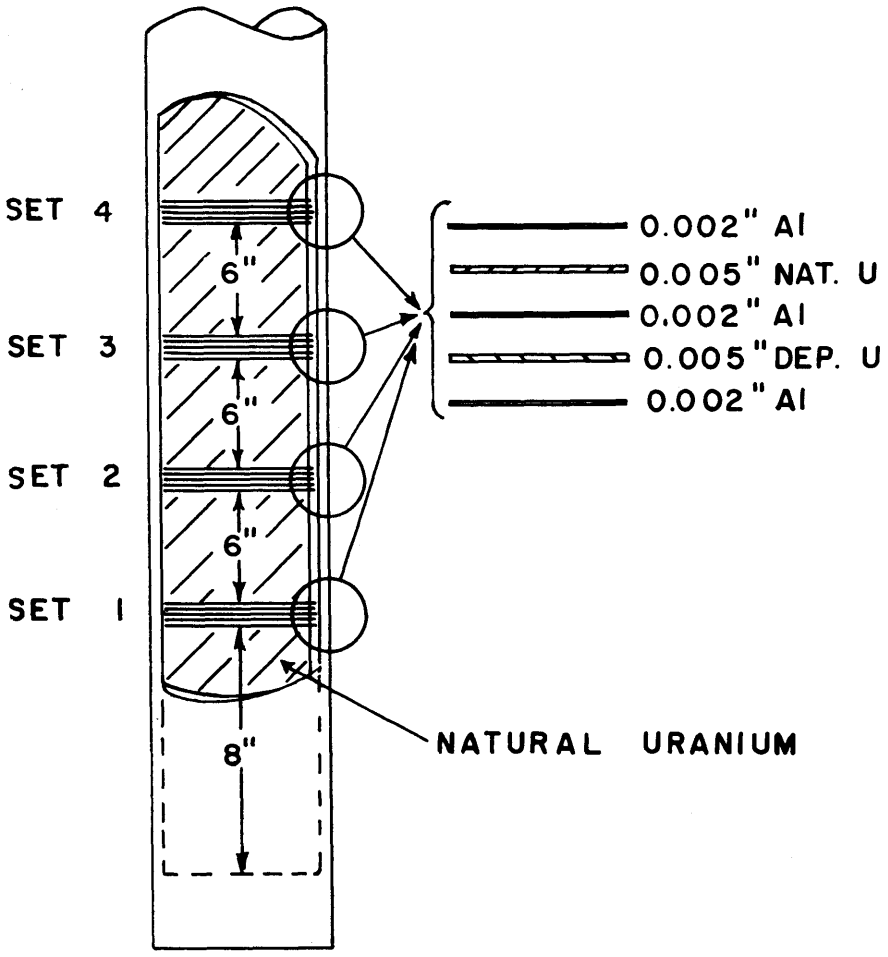

FIG. 3-8 FOIL ARRANGEMENT FOR COUNT RATE AND COUNTING POSITION EXPERIMENTS

triangular lattice with a 5-3/4-inch spacing. Each set of foils consisted of a one-inch diameter depleted uranium foil, and a one-inch diameter natural uranium foil. The foils were also used in a study of the effect of count rate on the measurement of $\gamma(t)$, (section 3.5). The positions at which the foils were irradiated are shown in Fig. 3.8.

The most active sets of foils (set 1 and set 2 in Fig. 3.8) were counted in the two positions shown in Fig. 3.9. Set 3 and set 4 were only counted in position 1. The natural uranium foils and most of the depleted foils were counted for 1-minute intervals. The first foil was counted at 228 minutes after the irradiation, and the counting period was terminated at 510 minutes after the irradiation. Near the end of the counting period, the count rates of the depleted foils counted at position 2 and the depleted foil from set 4 counted at position 1 were low, so 3-minute counting intervals were used for these foils. Each foil was counted 13 times during the experiment. The count rates were corrected for dead time, pulse pileup and background. Values of δ_{28} were then calculated from the foil activities and compared on the basis of the counting position. The results of this experiment are discussed in section 4.2.3.

With the exception of this experiment, all measurements of δ_{28} were made at position 1. By studying the effect of a change in counting position, it was possible to determine the effect on P(t) of a change in the average angle at which the gamma rays enter the crystal. This angle is also changed when foils of different sizes are counted at the same position. The experiment, therefore, gave an indication of the sensitivity of P(t) to foil size. This aspect of the problem is discussed in section 4.2.3.

3.7 TWO INDEPENDENT MEASUREMENTS OF δ_{28}

In this study, a new method for measuring δ_{28} has been developed and is described in section 3.2. An experiment was designed to compare values of δ_{28} measured by using the earlier double fission chamber technique, and by using the new method.

Foils and thin deposits of depleted and natural uranium on platinum were irradiated in a double-chamber fission counter designed and built by Mr. D. Shernoff as a Bachelor of Science thesis at MIT.[S.1] The

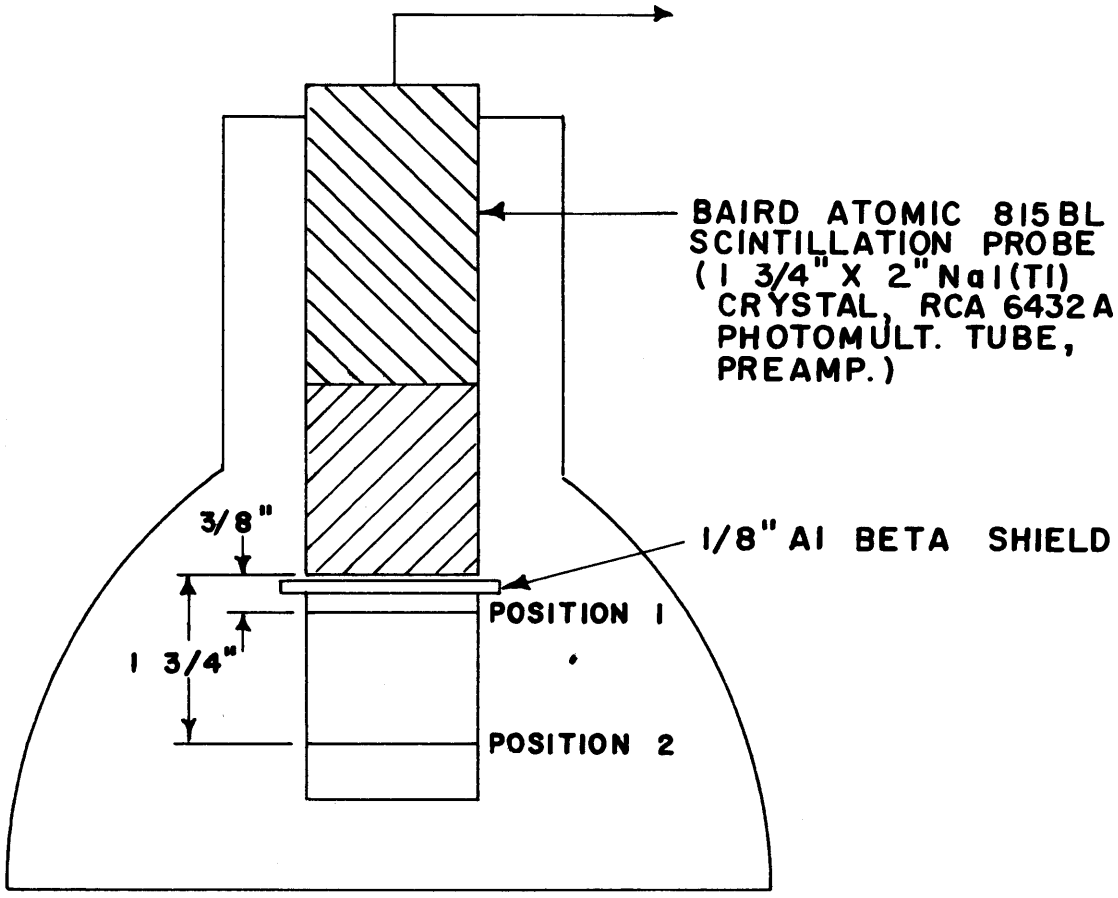

FIG. 3-9 COUNTING POSITIONS

experimental arrangement is shown in Fig. 3.10. A ratio of the number of fission reactions taking place in the depleted and natural uranium deposits was determined by comparing the count rates from the two chambers. Upon completion of the irradiation, the foils were removed from the fission counter. They were cooled for about one week, and then the relative La^{140} 1.60 Mev gamma-ray activity of the two foils, in an energy interval of 0.13 Mev centered at 1.60 Mev, was determined according to the procedure outlined in section 3.2. The ratio of the La^{140} activity of the foils was measured a total of 9 times during a two-week period following the first measurement. Values of δ_{28} were calculated from the 9 measured ratios and the average value was compared to the value determined by using the double-chamber fission counter. The results are discussed in section 4.3.

The uranium-platinum foils were prepared by using a technique similar to the Zapon spreading technique described by Graves and Froman in "Miscellaneous Physical and Chemical Techniques of the Los Alamos Project."[G.3] The first step in the procedure was the removal of oxide from the surfaces of a depleted or natural uranium foil. The oxide was removed by washing the foil in concentrated HNO_3. The foil was then washed in water, rinsed in distilled water, and dried. A piece of uranium metal was punched out of the foil, weighed, and dissolved in minimum concentration HNO_3. The solution was then evaporated to dryness, leaving uranyl nitrate in crystalline form. The uranyl nitrate crystals were dissolved in absolute ethyl alcohol, and added to a solution of one per cent Zapon (nitrocellulose) lacquer in lacquer thinner. The amount of Zapon solution was sufficient to insure a maximum uranium concentration of 5 mg per ml. Solutions were made from depleted and natural uranium. The foils were prepared by painting the solution onto the platinum and firing the foil in a furnace at a temperature in the range from 600° C to 900° C. The procedure was repeated until enough uranium had been deposited on the foil. The foil was wiped after each firing to remove any residue which might have been left on the surface; it was placed on a piece of felt during the wiping operation to prevent a loss of platinum by scraping. The amount of uranium deposited on the surface was determined by weighing the foil before and after the operation. A precision balance was used, and it was

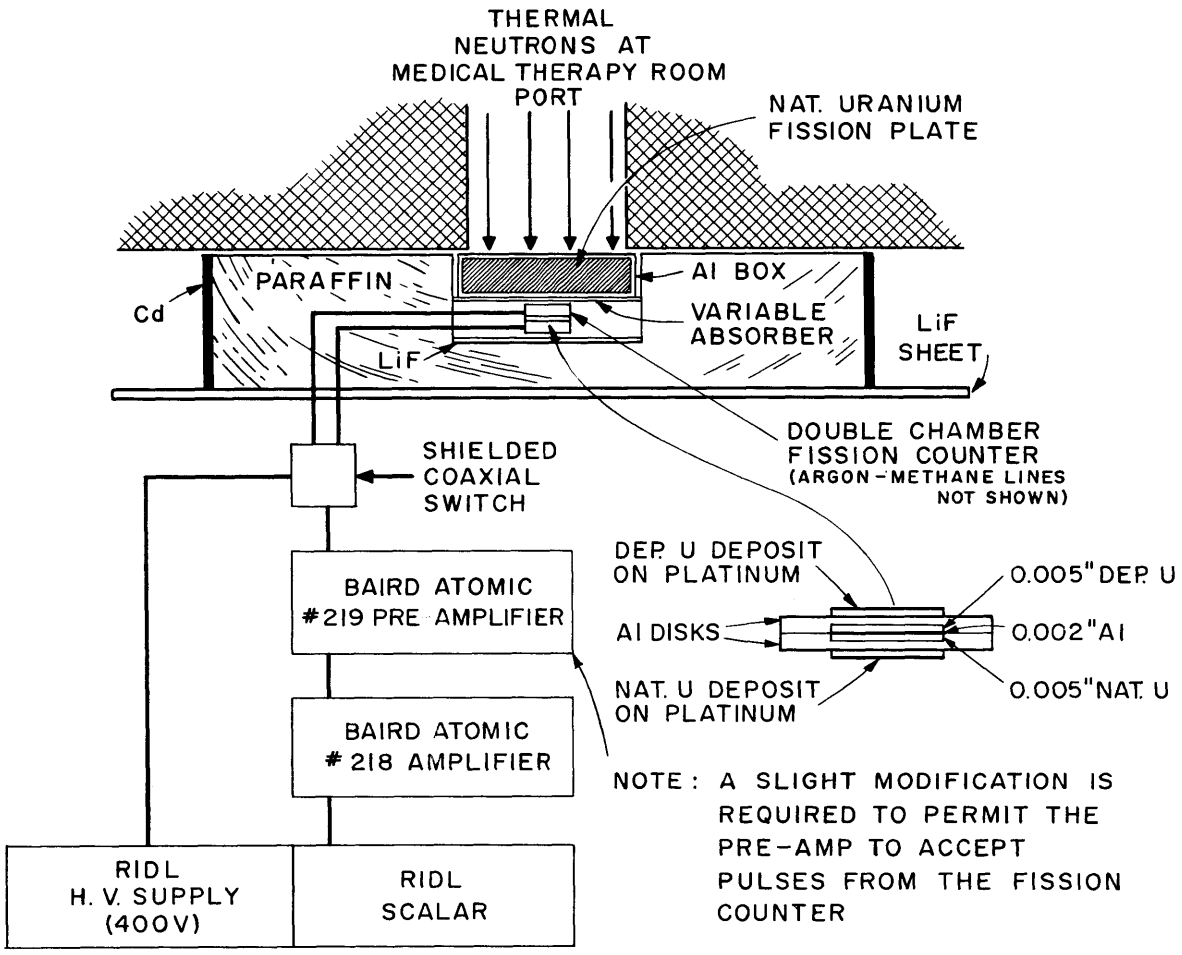

FIG. 3-10 MEASUREMENT OF δ_{28} BY USING A DOUBLE CHAMBER FISSION COUNTER

estimated that the uncertainty in the weight of the uranium deposited on the surface was about 1.0 per cent.

The effects of foil position within the chambers and the relative counting efficiencies of the two chambers were considered. Natural uranium foils were irradiated in both sides of the chamber and then counted for gamma rays above 1.20 Mev. The ratio of the gamma-ray activity of the two foils was compared to the ratio of the number of fissions counted in the chambers and the two values agreed to within one per cent. The activity of the foil furthest away from the Medical Therapy Room port was five per cent lower than the activity of the other foil, indicating a change in the neutron flux within the chamber. This flux change was considered in the calculations.

3.8 EFFECT OF THE NEUTRON ENERGY SPECTRUM ON THE MEASUREMENT OF P(t)

It has been shown that the fission product yields are different for resonance and thermal fissions.[R.2, R.5] The work by Regier et al. was done on Pu^{239} and Pu^{241}, and the work by Roeland et al. was done on U^{235} and U^{233}. A change in the neutron energy spectrum changes the ratio of resonance to thermal fissions, and the relative amounts of fission products will, therefore, depend on the energy spectrum of the neutrons inducing fission. The function P(t) depends on the yields of the fission products (see Appendix B); and, since these yields vary with the neutron energy spectrum, P(t) may be a function of the spectrum. In previous fast fission work, it has been assumed that this effect is small, and differences in P(t) caused by changes in spectra have always been neglected. An attempt was made to determine whether or not this effect is negligible.

Figure 3.11 shows the experimental arrangement used in this study. The function of the fission plate was to provide a source of fast neutrons. By varying the thickness of the thermal neutron absorber between the fission plate and the foils, the neutron energy spectrum could be changed. No attempt was made to normalize the measured P(t) functions. If there were measurable differences in these functions, they would appear as changes in the time behavior of the function.

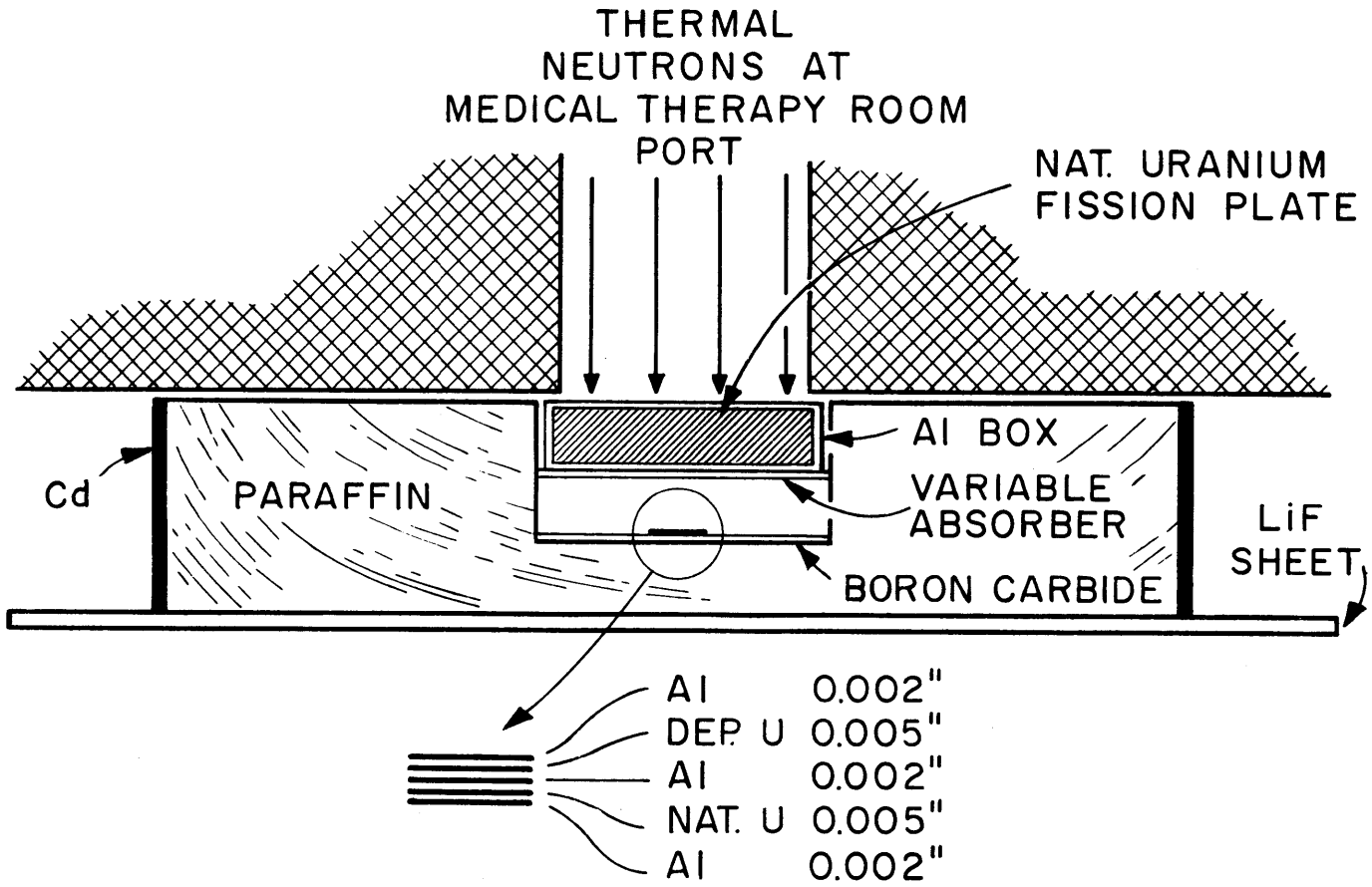

FIG. 3-11 EXPERIMENTAL ARRANGEMENT FOR STUDY OF EFFECT OF SPECTRUM ON P(t)

By irradiating depleted and natural foils in different spectra, and following the fission product gamma decay of the foils, a family of curves of $\gamma(t, \text{spectrum})$ was determined. From Eq. 3.2.17, it can be seen that this quantity is related to $P(t, \text{spectrum})$ as follows:

$$P(t, \text{spectrum}) = \frac{\delta_{28}(\text{spectrum})[1 - a\gamma(t, \text{spectrum})]}{a\gamma(t, \text{spectrum}) - S} = \frac{\delta_{28}}{F(t, \text{spectrum})}. \tag{3.8.1}$$

A family of curves of $F(t, \text{spectrum})$ was then determined. The time behavior of these curves was compared and the results are discussed in section 4.4.

The neutron energy spectrum was varied from a highly thermal spectrum with a value of δ_{28} equal to about 0.03 to spectra in which the thermal fission rate was decreased by factors of about 10 and 80. The values of δ_{28} for the latter neutron energy spectra were, therefore, about 0.3 and 2.4, respectively. The foils were counted with a bias setting of 1.20 Mev instead of 0.72 Mev. There were several reasons for using this discrimination level.

1) Since the foils were irradiated in the medical therapy room, rather than in the subcritical assembly, a cooling period was not needed for radiological safety reasons.

2) The P(t) function can be measured sooner after irradiation with 1.20 Mev biasing because there is no need to wait for the decay of the U^{239} activity.

3) The time dependence of P(t) for 1.20 Mev biasing is more pronounced than that for 0.72 Mev biasing, which increases the probability of seeing a change in the time dependence if there is one. The function P(t) varies by about 25 per cent in the time interval from one-half hour to two hours after irradiation for 1.20 Mev biasing; it varies by only about 10 per cent for 0.72 Mev biasing in the time interval from four to eight hours after irradiation. The use of 0.72 Mev makes the measurement of δ_{28} less sensitive to uncertainties in time and therefore, with the exception of these experiments, a bias setting of 0.72 Mev was preferable and was always used.

3.9 THE EFFECT OF SMALL CHANGES IN THE BIAS SETTING ON THE MEASUREMENT OF δ_{28}

An experiment was designed to study the effect of small changes in the bias setting on the measurement of δ_{28}. The purpose of this experiment was to determine how sensitive the measurement was to drift in the counting system.

A depleted and a natural uranium foil were irradiated for 4 hours, and counted alternately in the time interval from 3-1/2 to 6-1/2 hours after irradiation. The bias setting was alternated among 0.69 Mev, 0.72 Mev, and 0.75 Mev after each set of counts. The function F(t) was calculated for each discriminator setting, and the functions were examined for differences. The results are discussed in section 4.2.4.

3.10 MEASUREMENTS OF THE FAST FISSION RATE AS A FUNCTION OF POSITION WITHIN A FUEL ROD AND WITHIN THE MODERATOR

Calculations have shown that the number of fast fissions per unit volume as a function of radial position in a fuel rod is approximately constant.[W.1] The number of neutrons with sufficient energy to cause fast fission decreases rapidly in the moderator. Experiments were designed to study the fast fission rate as a function of position in a fuel element and the fast neutron flux as a function of position in the moderator.

Figure 3.12 shows the experimental arrangement used to measure the spatial variation of the fast flux in the moderator. Measurements were made for a single rod and for a rod in the 5-inch lattice. Cadmium-covered, depleted uranium foils, 1/4-inch in diameter, were attached to an aluminum foil holder. The cadmium covers were used to eliminate thermal fissions of U^{235}. An experiment was made to see if epicadmium U^{235} fissions could be detected in the depleted foils. Several cadmium-covered, 1/4-inch diameter, natural uranium foils were irradiated simultaneously with the depleted foils. The difference between the activities of the natural and depleted foils was due to epicadmium U^{235} fission. From the ratio of U^{235} in the natural and depleted foils, it was calculated that the number of U^{235} fissions in the cadmium-covered, depleted uranium foils was negligible.

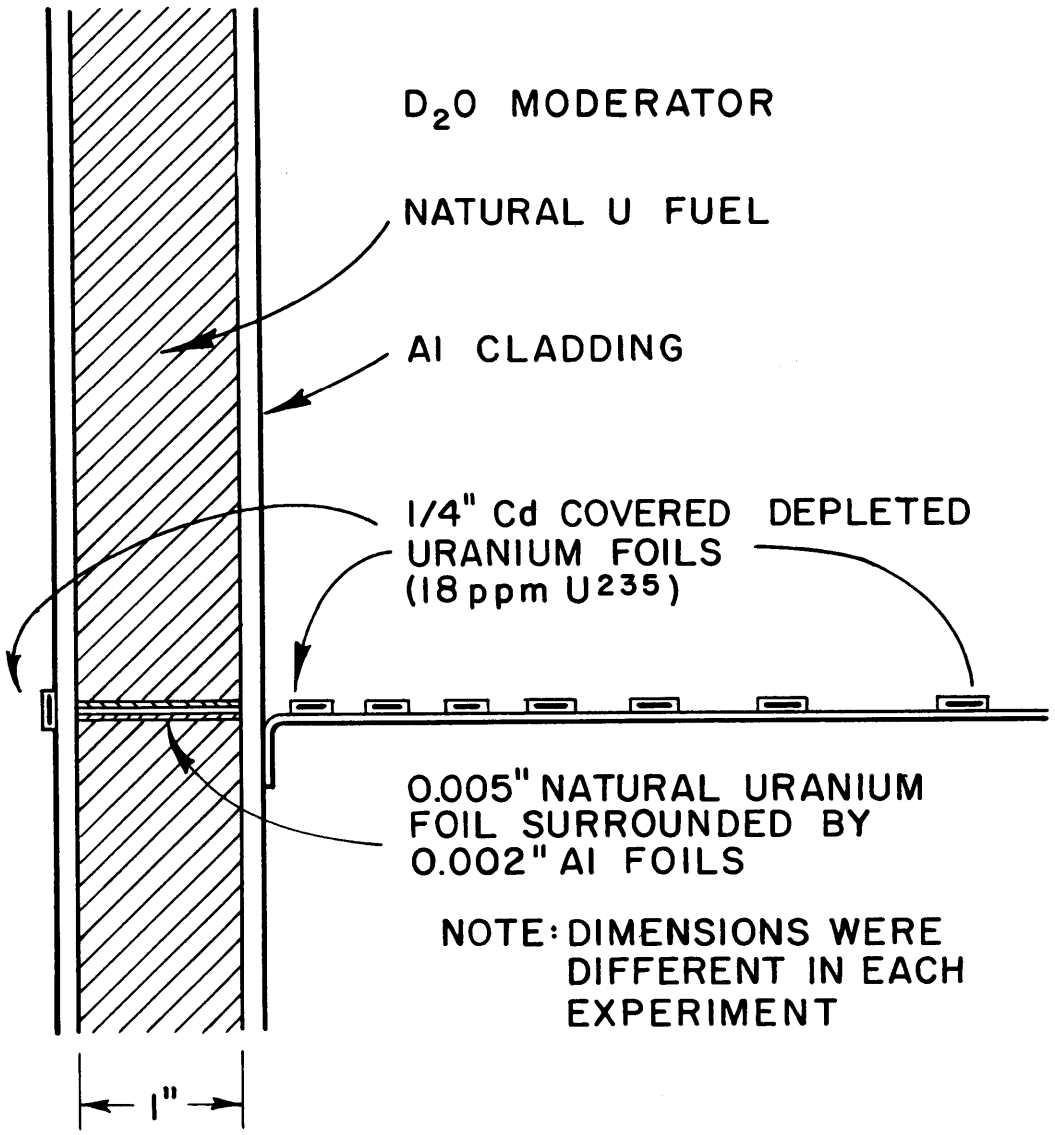

FIG. 3-12 FOIL ARRANGEMENT FOR FAST FLUX EXPERIMENT

The fast flux in the moderator was normalized to the average value in the fuel. A natural uranium foil was placed in the fuel rod at a position adjacent to the aluminum foil holder. Since the value of δ_{28} was known from previous measurements in a comparable arrangement, the fission product activity due to fast fissions could be calculated. The result was divided by the ratio of the weight of the 1-inch foil to the weight of the 1/4-inch foils. The fast flux was considered to be proportional to the U^{238} fission product activity of the 1/4-inch foils. The results of this experiment are discussed in section 4.5.

A measurement of the fast fission distribution was made in the 1-inch diameter rods. To correct for the U^{235} fissions in the depleted foil, it is also necessary to determine a thermal fission distribution. A natural and a depleted foil were irradiated in adjacent positions for 4 hours. After the irradiation, the foils were gamma-counted, and then 1/4-inch foils were punched out of the 1-inch foils. Three small foils were punched from each foil -- a foil at the center, one at the edge, and one in between. These foils were then gamma-counted and the results are discussed in section 4.5. A measurement of the fast flux as a ratio of radial position inside a fuel element was also made at the Brookhaven National Laboratory.[P.4] The Brookhaven method was based on the catcher foil technique, with 2.898- and 3.636-inch diameter, natural uranium rods embedded in graphite. After irradiation, 0.22-inch and 0.25-inch diameter foils were punched out of the Al catcher foils and beta-counted. The larger size of the BNL rods permitted 11 staggered points on the curve for the 3.636-inch rods. The measured fast fission distribution was almost flat. The thermal fission distribution showed the usual dip, which is about a factor of 5 from the edge of the foil to the center for the large 3.636-inch rods.

3.11 MEASUREMENT OF THE RATIO OF THE NUMBERS OF U^{235} ATOMS IN THE DEPLETED AND NATURAL URANIUM

The formulation of the equations for calculating δ_{28} assumes a knowledge of the isotopic composition of the uranium foils used in the

experiment. In the experiments with one-inch diameter rods, only natural uranium foils were used for the non-depleted foil, and no attempt was made to remeasure the well known enrichment of natural uranium. The enrichment of the depleted uranium was not known accurately, and an experiment was designed to measure the ratio of the numbers of atoms of U^{235} in the depleted and the natural uranium. The U^{235} concentration of the depleted uranium is equal to the product of this ratio and the U^{235} concentration of natural uranium. Figure 3.13 shows the experimental arrangement used for this measurement.

Bare and cadmium-covered foils of depleted and natural uranium were irradiated on a foil wheel immersed in the heavy water. The foil wheel was used to insure a constant average flux for the irradiation of each foil. The irradiation was made in the heavy water because the foils were used to measure δ_{25} and δ_{28} in the moderator at the same time. The foils were irradiated for 4 hours. After a 3-hour cooling period, they were removed and gamma-counted alternately. The counting intervals were 1 minute for the bare natural foil, 3 minutes for the bare depleted and natural cadmium-covered foils, and 10 minutes for the depleted cadmium-covered foil. The count rates, after subtracting background and correcting for dead time and pulse pileup, and with 0.72 Mev biasing, ranged from less than 100 cpm for the depleted cadmium-covered foil to between 300,000 and 400,000 cpm for the bare natural foil. Each foil was counted several times.

The method used to calculate the ratio of U^{235} atom density in the depleted and natural uranium was to correct the measured count rates for background, dead time, pulse pileup, weight differences, and count start time differences, and then substitute the corrected count rates into Eq. 3.11.1:

$$\frac{N_D^{25}}{N_N^{25}} = \frac{D - D_{cd}}{N - N_{cd}}, \qquad (3.11.1)$$

where N_d^{25} and N_n^{25} are the U^{235} atom densities in the depleted and natural uranium; D is the corrected count rate of the bare depleted foil; D_{cd} is the corrected count rate of the cadmium-covered, depleted uranium foil; and

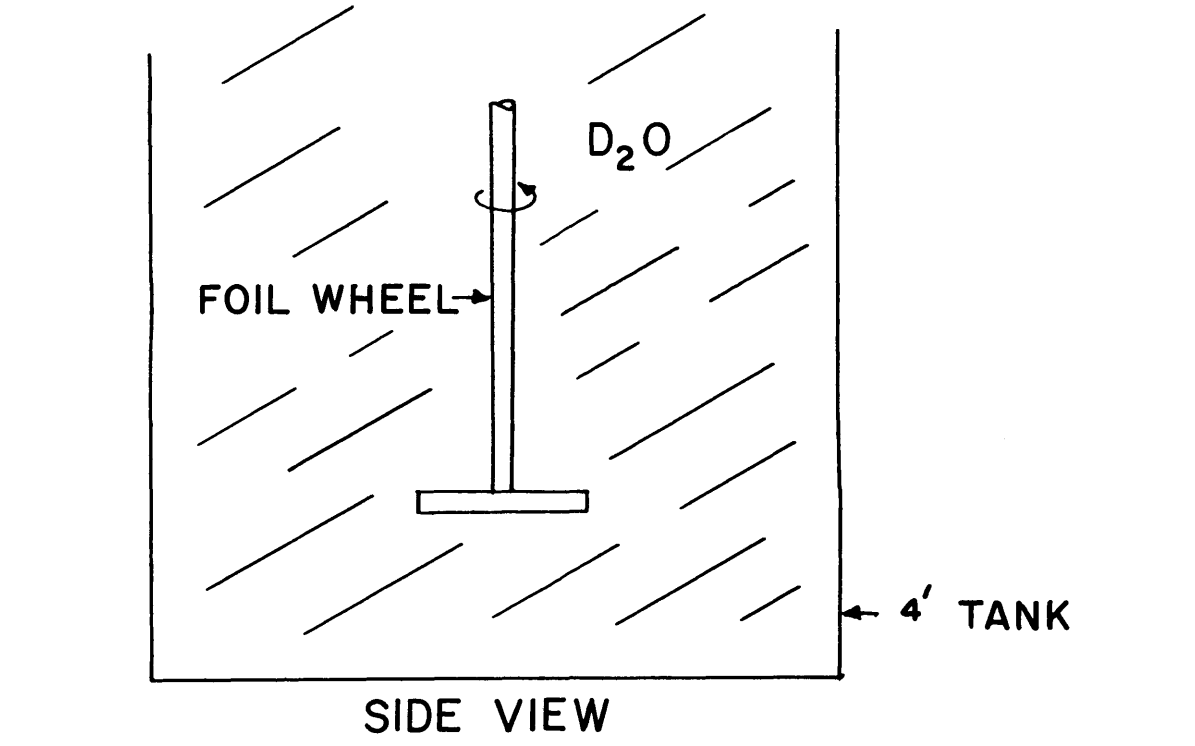

FIG. 3-13 FOIL WHEEL EXPERIMENT

N and N_{cd} are the same quantities for the natural uranium foils. The derivation of this equation is straightforward. Consider the following set of equations:

$$D = D_F + D_E + D_S , \tag{3.11.2}$$

$$D_{cd} = D_F + D_E , \tag{3.11.3}$$

$$N = N_F + N_E + N_S , \tag{3.11.4}$$

$$N_{cd} = N_F + N_E . \tag{3.11.5}$$

The D's and N's are the corrected count rates of the foils, the subscript F stands for fast fission (or fission in U^{238}), the subscript E stands for epicadmium fission in U^{235}, and the subscript S represents subcadmium fission in U^{235}. The neutron energy spectrum seen by each foil is the same; hence,

$$\frac{N_D^{25}}{N_N^{25}} = \frac{D_E + D_S}{N_E + N_S} = \frac{D_S}{N_S} . \tag{3.11.6}$$

Since

$$D_S = D - D_{cd} , \tag{3.11.7}$$

and

$$N_S = N - N_{cd} , \tag{3.11.8}$$

substitution of Eqs. 3.11.7 and 3.11.8 into Eq. 3.11.6 yields Eq. 3.11.1. The results of this experiment are discussed in section 4.6.

3.12 MEASUREMENT OF δ_{25}

The quantity δ_{25} is the ratio of the numbers of epicadmium to subcadmium fissions in U^{235}. Figure 3.14 shows the experimental arrangement used to measure this quantity. A natural and a depleted uranium foil are irradiated at a position surrounded by cadmium. At an equivalent position in an adjacent rod, natural and depleted bare foils are irradiated. Measurement of the fission product gamma-ray activities of these foils

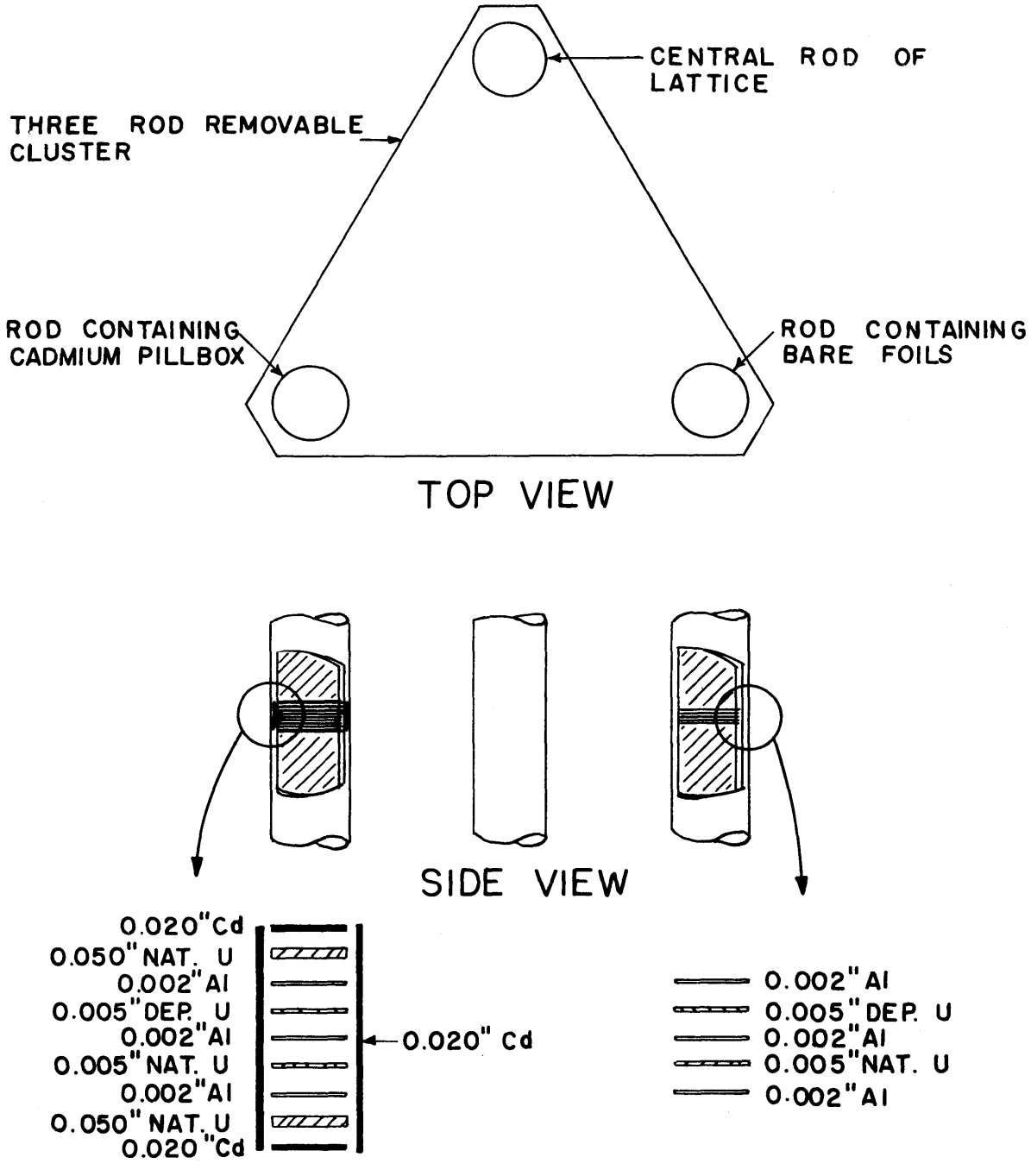

FIG. 3-14 FOIL ARRANGEMENT FOR δ_{25} MEASUREMENTS

after irradiation are then used to calculate δ_{25}.

The appropriate relationship for the determination of δ_{25} is:

$$\delta_{25} = \frac{\text{Epicadmium } U^{235} \text{ activity}}{\text{Subcadmium } U^{235} \text{ activity}}$$

$$= \frac{N_{cd} - D_{cd}}{N\left(1 - \delta_{28}/P(t)\right) - \left[N_{cd} - D_{cd}\right]}, \qquad (3.12.1)$$

where N_{cd} is the fission product activity of the cadmium-covered, natural uranium foil normalized to time t, N is the value for the bare natural uranium foil, and D_{cd} is the value for the cadmium-covered, depleted uranium foil. The value of δ_{28} is determined in the usual way from the activities of the natural and depleted bare foils. If δ_{28} is already known, it is unnecessary to include a bare depleted foil in the irradiation. The denominator of Eq. 3.12.1 is approximately equal to N. The other terms reduce N by an amount equal to the activities from U^{238} and epicadmium U^{235} fission in the bare natural uranium foil at time t.

Cadmium has a negligible effect on fast neutrons, but the number of fast fissions measured in the cadmium-covered depleted uranium foil was only about one-half of the number measured in the bare depleted foil. The reason for this is that the cadmium reduces the number of thermal fissions in the region near the depleted foil; hence, the number of fast neutrons being born in this region is reduced. The number of fast fissions in the depleted uranium foil is, therefore, reduced. In section 3.13, an experiment is described in which the effect of decreasing the number of fissions near the depleted uranium foil is measured.

Measurements of δ_{25} were performed in all the lattices studied. In addition, a value of δ_{25} was determined for a single, 1-inch diameter uranium rod in heavy water. The technique was to position bare natural uranium foils above and below the cadmium-covered natural and depleted uranium foils; the value of N was then determined by interpolation.

A measurement of δ_{25} was made in heavy water without any fuel present. The purpose of this measurement was to determine what

fraction of the epicadmium fissions in U^{235} results from neutrons that have been slowed down and what fraction results from neutrons from the thermal column. This measurement was made by using the same foils that were used in the measurement of the atom density of U^{235} in the depleted foil (section 3.11). With the notation of Eqs. 3.11.2 through 3.11.5, we have

$$(\delta_{25})_{\text{moderator}} = \frac{N_E}{N_S} . \tag{3.12.2}$$

If it is assumed that the numbers of fast fissions in the depleted and natural uranium foils are approximately the same, we get

$$N_E = N_{cd} - N_F = N_{cd} - (D_{cd} - D_E) . \tag{3.12.3}$$

From the measurement of the U^{235} concentration of the depleted foil, it is known that

$$\frac{D_E + D_S}{N_E + N_S} = \frac{D_S}{N_S} = \frac{D_E}{N_E} = 0.00246 . \tag{3.12.4}$$

Hence,

$$N_E = N_{cd} - (D_{cd} - .00246\, N_E) ,$$

or

$$N_e(1 - .00246) = N_{cd} - D_{cd} \approx N_E . \tag{3.12.5}$$

Since $N_S = N - N_{cd}$ (Eq. 3.11.8), it follows that

$$(\delta_{25})_{\text{moderator}} = \frac{N_{cd} - D_{cd}}{N - N_{cd}} . \tag{3.12.6}$$

The equipment used for the foil counting was the same as that used for measuring δ_{28}. The bias setting was 0.72 Mev, and the count rates of the cadmium-covered, natural and depleted foils were between 2,000 and 12,000 cpm in the time interval from 3-1/2 to 7 hours after a 4-hour irradiation of the 1-inch diameter rods. The cadmium-covered, natural uranium foil activity was 2 to 3 times the activity of the depleted cadmium-covered foil. The bare natural foil activity was more than an order of

magnitude greater. The results of the δ_{25} measurements are discussed in section 4.7.

Values of δ_{25} were also calculated from gold-cadmium ratios measured by Mr. A. Weitzberg[W.3] and are also considered in section 4.7. A third method for determining δ_{25} is to measure the fission product activity of bare and cadmium-covered foils of dilute U^{235}. Although this third method is adequate, the first method was selected because the foils could be used for several experiments simultaneously. For example, the bare and cadmium-covered depleted uranium foils were also used to measure ρ_{28}, a quantity used in the measurement of the resonance escape probability. The function of the 50 mil uranium buttons shown in Fig. 3.13 was to prevent streaming of resonance neutrons during this measurement. The bare depleted and natural foils were used in the measurement of δ_{28}.

3.13 EFFECT OF REMOVING FUEL FROM THE REGION NEAR A DEPLETED URANIUM FOIL

In section 3.12, it was mentioned that a cadmium-covered, depleted uranium foil had a fission product activity of about one-half that of a bare depleted foil in an equivalent position. It was explained that the reason for this was that the cadmium reduced the number of thermal fissions in the region near the foil, which decreased the number of fast neutrons being born in this region, which, in turn, reduced the number of fast fissions in the foil. An experiment was designed to study the influence of thermal fissions in the region near a depleted uranium foil on the fast fission rate in the foil.

Figure 3.15 shows the arrangement of the foils used in the experiment. Aluminum buttons of 1-1/4-inch length, 1/4-inch length, and 70-mil length were positioned adjacent to depleted uranium foils. This had the effect of removing 1-1/4 inches, 1/4 inch or 70 mils, respectively, of fuel from the region adjacent to the foils. In addition, 50-mil buttons and 20-mil Cd foils were positioned adjacent to a fourth depleted foil. This arrangement simulated the 50-mil uranium plus 20-mil Cd arrangement used in the measurement of δ_{25}. The natural uranium foils shown in Fig. 3.14 were used to calculate the depleted foil activities for unperturbed

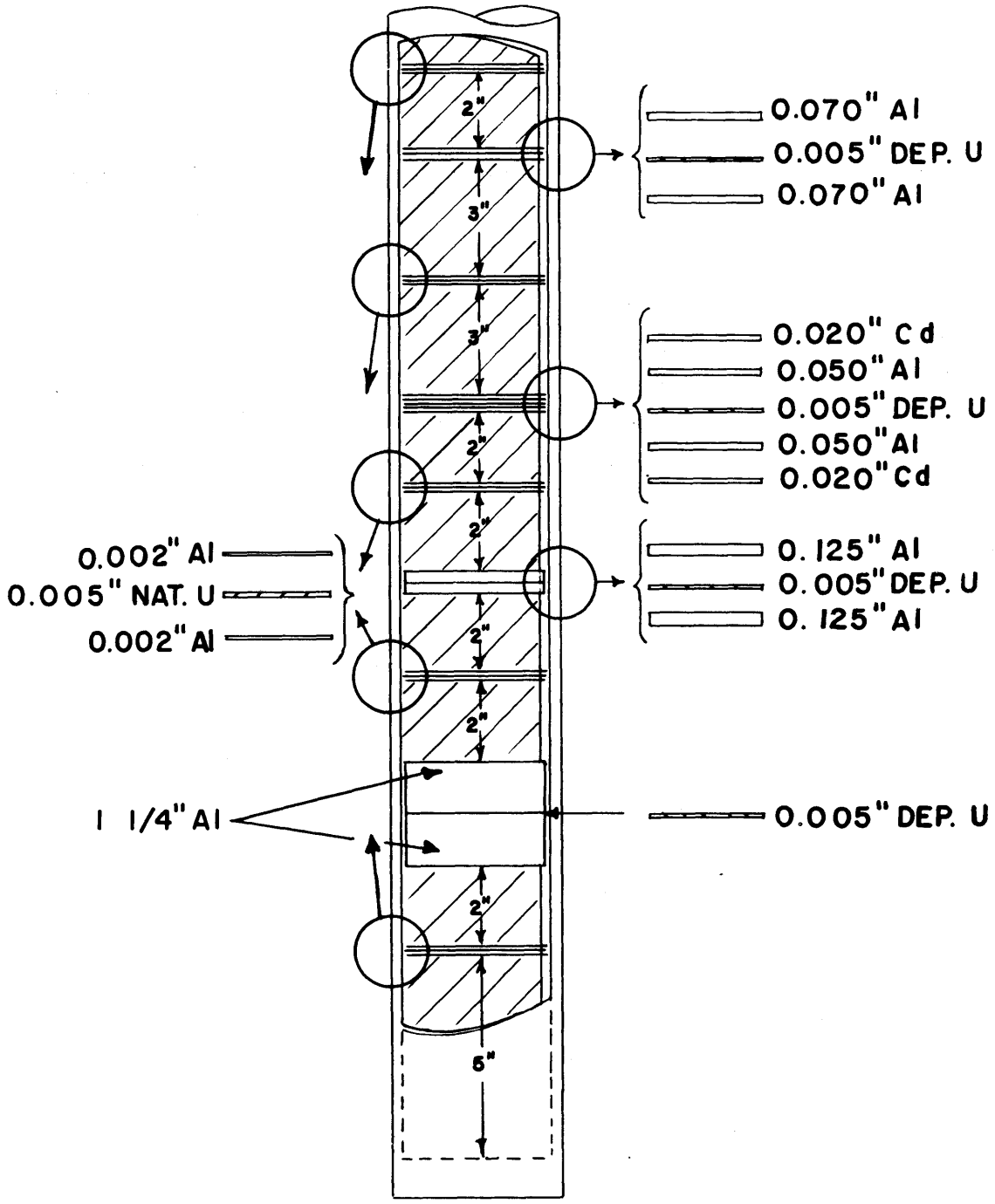

FIG. 3-15 FOIL ARRANGEMENT FOR EXPERIMENT ON THE EFFECT OF FUEL ADJACENT TO A DEPLETED URANIUM FOIL

depleted foils at the depleted foil positions. The natural foil activities at these positions were determined by interpolation; and by using the known value of δ_{28}, the depleted foil activity without Al or Cd spacers could then be calculated. The results of the experiment are discussed in section 4.8.

3.14 A STUDY OF THE FISSION PRODUCT GAMMA SPECTRUM

A study of the fission product gamma spectrum was undertaken to improve our understanding of the fast fission and related measurements. The experimental work was general in nature, with spectra measured for times from hours to months after irradiation. The approach to the problem was both experimental and theoretical. The theoretical work and the results of the experimental work are discussed in section 4.9. The experimental approach to the problem consisted of measuring the gamma spectrum of irradiated uranium foils in the energy range 0.4 Mev to 2.7 Mev. This range included all gammas of interest in the fast fission measurements.

A schematic diagram of the equipment used to measure the spectra is shown in Fig. 3.16. Standard settings were maintained to facilitate comparisons of spectra measured at different times. The calibration of the system was checked periodically by observing the positions of the following peaks:

Na^{22}	0.51 Mev annihilation peak
	1.28 Mev gamma peak
	1.79 Mev sum peak
Co^{60}	1.17 Mev gamma peak
	1.33 Mev gamma peak
	2.50 Mev sum peak
Cs^{137}	0.66 Mev gamma peak
Mn^{54}	0.84 Mev gamma peak

The system was linear within the range of interest, and the slight drift which is inevitable over long periods of time was compensated by small changes in the base line setting of the 256 channel analyzer.

The irradiation conditions were varied to satisfy the requirements

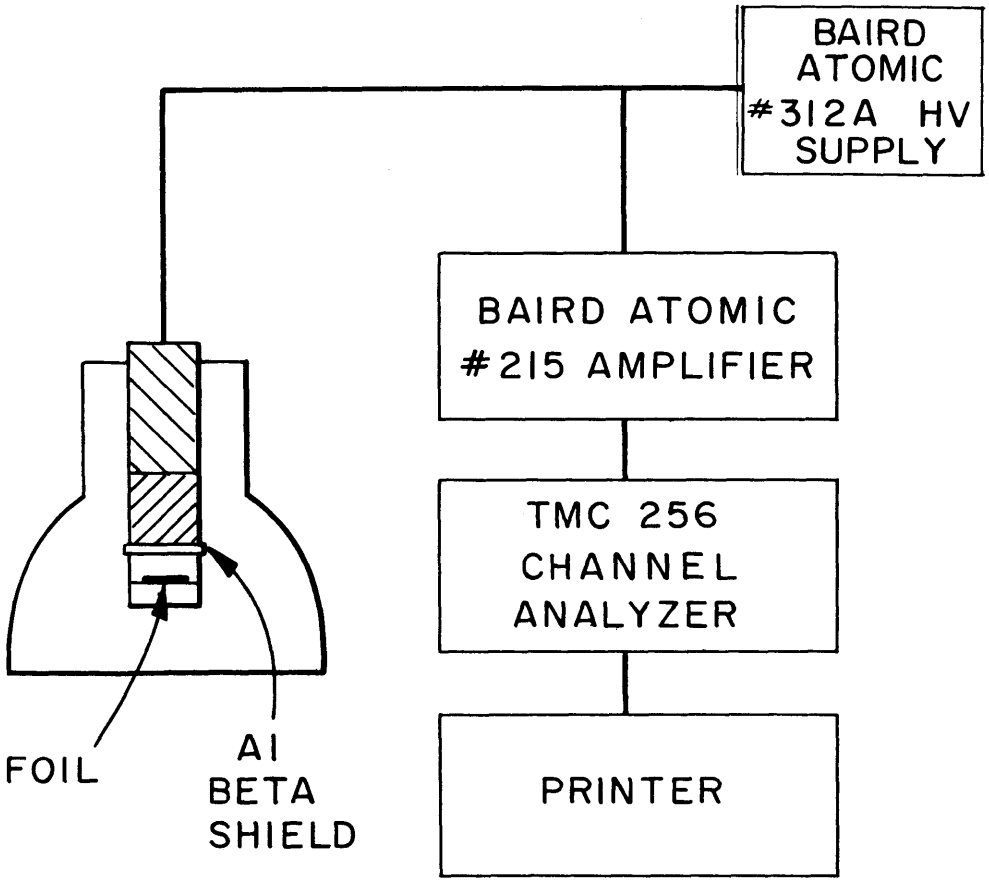

FIG. 3-16 EQUIPMENT FOR GAMMA SPECTRA STUDY

of the experiments. Much of the work was done before completion of the subcritical assembly so that most of the irradiations were made at reactor ports. The spectra for times longer than two months were obtained from a 0.070-gram U^{235} foil, irradiated for 2 hours at a flux of 5×10^{12} n/cm^2 sec. Most of the spectra for shorter times after irradiation were taken from 1-inch diameter foils irradiated at the Medical Therapy Room port of the MITR.

CHAPTER IV.
RESULTS AND CONCLUSIONS

4.1 MEASUREMENTS OF δ_{28}

The method used for the measurements of δ_{28} is described in section 3.2. Measurements were made in natural uranium rods, 1.01 inches in diameter, in three lattices moderated by heavy water, in a single, 1.01-inch natural uranium rod immersed in heavy water, and in a single, 0.25-inch diameter rod with a U^{235} concentration of 1.143 weight per cent immersed in heavy water. The results of these measurements are included in Table 4.4 and are summarized in Table 4.1.

Table 4.1. Average values of δ_{28} measured in the MIT Lattice Facility.

		V_m/V_f [a]	δ_{28}	Estimated Error of δ_{28}
Lattice	5-3/4" spacing	35.7	0.0583 [b]	0.0012
	5" spacing	26.2	0.0596	0.0017
	4-1/2" spacing	21.0	0.0597	0.0020
Single Rod	1" diameter		0.0559	0.0015
	1/4" diameter		0.0126	0.0004

(a) Ratio of the volume of heavy water to the volume of uranium.

(b) Used as δ^*_{28}, the standard value of δ_{28}.

4.1.1 Measurement of δ^*_{28}, the Standard Value of δ_{28}

A unique feature of the method developed for the measurement of δ_{28} is that the standard measurement of δ_{28} is made within a fuel rod. In the earlier methods, the standard measurement, which is used to normalize the other measurement, was made in fission chambers. The standard measurements in the present study were made in a one-inch

diameter, natural uranium fuel rod at the central position in a triangular lattice with a 5-3/4-inch spacing. Measurements of $\gamma(t)$ were also made in this lattice and were used to calculate P(t). The calculation of P(t) is discussed in section 4.1.3. Values of $\gamma(t)$ were measured for the other lattices and the single rods. Values of F(t) were calculated from Eq. 3.2.15 and were then multiplied by the appropriate values of P(t), obtained from the standard measurement of δ^*_{28}, to determine values of δ_{28}.

Three sets of depleted and natural uranium foils were irradiated in the 5-3/4-inch lattice. The ratio of the La^{140} 1.60 Mev activity of each set of foils was measured in three counting setups similar to the one shown in Fig. 3.5, and values of δ_{28} were calculated by means of Eq. 3.2.15. Setups 1 and 2 had different 1-3/4 × 2-inch scintillation probes, amplifiers and high voltage supplies; and setup 3 had a 3 × 3-inch probe, the high voltage supply from setup 1 and the amplifier from setup 2. The results of these measurements are given in Table 4.2 and Table 4.3.

Table 4.2. Standard Measurements of δ_{28} obtained with different counting setups.

	Number of Measurements	Average Value of δ_{28}	SD[(a)]	SDM[(b)]
Setup 1 (1-3/4" × 2" crystal)	40	0.0583	0.0020	0.00032
Setup 2 (1-3/4" × 2" crystal)	6	0.0573	0.0016	0.00065
Setup 3 (3" × 3" crystal)	10	0.0594	0.0021	0.00067
All setups	56	0.0583	0.0018	0.00024

(a) Standard deviation of the measurements.

(b) Standard deviation of the mean of the measurements. These quantities were determined by dividing the standard deviations by the square root of the number of measurements and are not the entire uncertainty of the values of δ_{28}, as will be explained in the discussion of the errors in section 4.1.4.

Table 4.3. Measurements of δ_{28} with setup Number 1.

Foil Set	Number of Measurements	Average Value of δ_{28}	SD[a]	SDM[b]
1	13	0.0584	0.0021	0.00058
2	13	0.0588	0.0017	0.00047
3	14	0.0578	0.0015	0.00040
All foils	40	0.0583	0.0020	0.00032

(a) Standard deviation of the measurements.

(b) Standard deviation of the mean of the measurements. These quantities were determined by dividing the standard deviations by the square root of the number of measurements and are not the entire uncertainty of the values of δ_{28}, as will be explained in the discussion of the errors in section 4.1.4.

The following conclusions may be drawn from these results:

1) The differences between the average values of δ_{28} measured in the three counting setups and the over-all average value are small. The largest difference among the values of δ_{28} is about 3.5 per cent and is between the results obtained with setups 2 and 3; it can be explained by considering the uncertainty in the backgrounds of the depleted foils. The foil backgrounds were measured in setup 1 but had to be estimated for setups 2 and 3 because these setups were built after the foils were irradiated. It was found that approximately half of the total background was from the room, the other half being attributed to the foil background. The ratio of these two components of the total background was approximately the same for each depleted foil. To calculate the backgrounds of the foils in setups 2 and 3, the values of the room and foil backgrounds for the same unirradiated foil were measured in the three setups. The backgrounds of the irradiated foils were then calculated from the following equations:

$$B^{2 \text{ or } 3} = B_R^{2 \text{ or } 3} + B_F^{2 \text{ or } 3}, \qquad (4.1.1)$$

where

$$B_F^{2 \text{ or } 3} = B_F^1 \times \left(\frac{B_F^{2 \text{ or } 3}}{B_F^1} \right)_{\text{unirradiated foil}} . \qquad (4.1.2)$$

In these equations, B is the total background, B_R is the room background and B_F is the foil background. The superscripts denote the counting setup. The room backgrounds, B_R, were measured for each setup, and B_F was calculated from Eq. 4.1.2 for each foil. Although the values of B^1 were known to about three per cent, it was estimated that the uncertainties in the calculated values of B^2 and B^3 were about 10 per cent. The count rates of the depleted foil (total minus background) in setups 2 and 3 ranged from 2.8 to 3.7 times background. It was, therefore, estimated that the uncertainty in the background added about 2.5 per cent to 3.5 per cent to the uncertainty of the measured values of δ_{28}. This uncertainty would not be apparent in the spread of the data because the same background was used for each measurement, and the 3.5 per cent difference in the measured values of δ_{28} obtained with setups 2 and 3 is therefore within reasonable statistical limits. The spread in the data is largely due to the counting statistics of the depleted foil which varied from 1.7 per cent to 2.3 per cent. The ratio of the count rate to background rate in setup 1 varied from 4.0 to 9.2 because the count rates in this setup were determined at earlier times after the irradiation than in setups 2 and 3. It was, therefore, estimated that the three per cent uncertainty in the backgrounds measured in setup 1 resulted in uncertainties of only 0.3 per cent to 0.7 per cent in the measured values of δ_{28}. It may be concluded that the measurement of δ_{28} is independent of the counting setup.

2) The differences among the average values of δ_{28} measured for the three sets of foils are small. The possibility of fission product contamination introduces an uncertainty associated with the foils. Experiments designed to study this effect are described in section 3.3 and the results are discussed in section 4.2.1. Contamination can occur if the Al foils protecting the depleted uranium foil surfaces from fission products

originating in adjacent fuel slip out of position. Since the results for the three sets of foils yield values of δ_{28} which are close, it is not likely that the depleted foils were contaminated, since the extent of the contamination would have had to be the same for each set of foils.

4.1.2 Consideration of the Function F(t)

The relationship between the functions F(t) and $\gamma(t)$ is:

$$F(t) = \frac{a\gamma(t) - S}{1 - a\gamma(t)} . \qquad (4.1.3)$$

A derivation of this relationship and definitions of the symbols are given in section 3.2.1. The quantity $\gamma(t)$ is the ratio of counts above 0.72 Mev from the depleted uranium foil to counts above 0.72 Mev from the natural uranium foil. Four measurements of $\gamma(t)$ were made in the 5-3/4-inch lattice and a comparison of the calculated values of F(t) indicated differences among the measurements which could not be explained by statistical variations. The values of F(t) were smallest for foils with the greatest activities, and the differences were smaller at longer times after irradiation. It was thought that the decrease in F(t) with increased foil activities was a result of the "pulse pileup" associated with the natural uranium foils. The term, "pulse pileup," refers to coincident pulses having individual energies lower than 0.72 Mev but which are counted because their total energy is greater than 0.72 Mev. It also refers to pulses which are counted owing to an apparent change in the baseline from the overshoot of previous pulses which decay with a time constant of about 200 microseconds. Experiments described in section 3.6 and Appendix E were performed to provide additional information for an analysis of the problem.

To analyze the effect of pulse pileup, it was assumed that: (1) the pileup problem could be neglected in the case of the depleted uranium foils; (2) the number of natural uranium foil counts originating from triple or higher order coincidences was negligible.

It follows from assumption (2) that the natural foil activity, N, may be written approximately as:

$$N = N_o + CN^2. \qquad (4.1.4)$$

where N_o is the count rate in the absence of pileup and the second term on the right represents the contribution of counts due to coincidences of two lower-energy photons. This equation is also applicable to the pulses resulting from overshoot of previous pulses as explained in Appendix E. The quantities N and N_o are both functions of time. Equation 4.1.4 can be divided by D, the number of depleted foil counts, which is also a function of time:

$$\frac{N}{D} = \frac{N_o}{D} + \frac{CN^2}{D} . \qquad (4.1.5)$$

Values of the ratio N/D were plotted as a function of N^2/D. All values measured within the interval from 230 to 290 minutes after irradiation for the four original measurements and the six additional measurements mentioned in section 3.6 were included on the curve. The time interval was long enough to include a large number of observations, but short enough so that it could be assumed that N_o/D was constant. The pileup effect decreases with time, owing to the decrease in the foil activities, so the earliest possible interval was chosen.

Figure 4.1 shows that the graph of N/D as a function of N^2/D is a straight line. The constant, C, is just the slope of the line. The values of N/D at time t were determined from the least square values of F(t) at time t by using Eq. 4.1.3, where N/D is equal to $1/\gamma(t)$. The values of N^2/D at time t were determined by multiplying the calculated value of N/D by N. The value of C, determined from Fig. 4.1, is:

$$C = \text{slope of line in Fig. 4.1} = 33 \times 10^{-6} \text{ seconds.} \qquad (4.1.6)$$

The uncertainty in C is approximately ± 10 per cent. The errors shown on Fig. 4.1 were determined from the root-mean-square errors of the values of F(t) used to calculate N/D. The value of C is surprisingly large and is considered in greater detail in Appendix E. With the model suggested in Eq. 4.1.4 and verified in Fig. 4.1, the data reduction code described in Appendix D was modified to correct the count rates for pulse pileup, and the values of F(t) were redetermined.

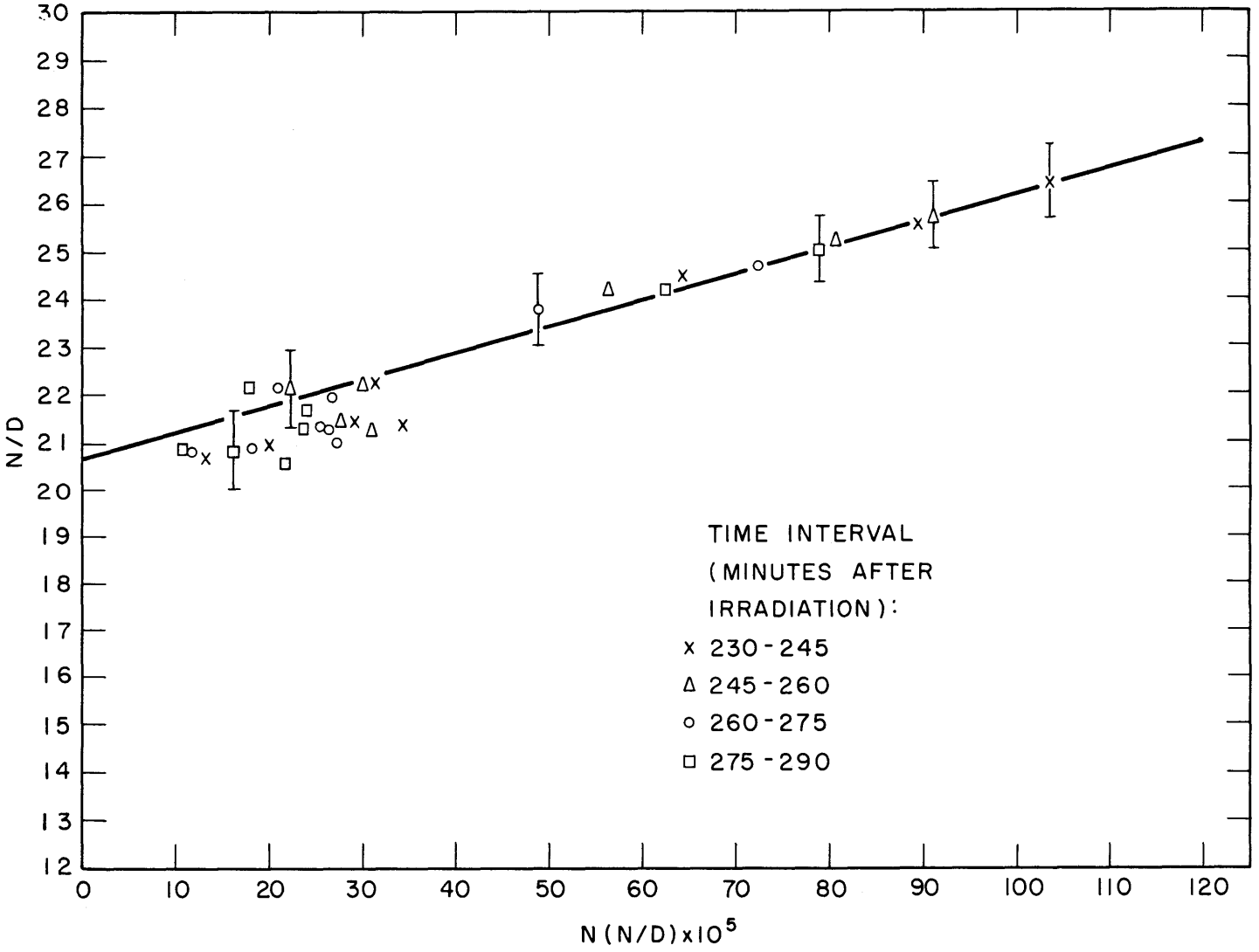

FIG. 4-1 RATIO OF NATURAL TO DEPLETED URANIUM FOIL ACTIVITY vs NATURAL ACTIVITY X THE RATIO (FOR MEASUREMENTS IN THE 5¾-INCH LATTICE)

4.1.3 Determination of P(t)

The function P(t) was determined by dividing δ^*_{28}, the standard value of δ_{28}, by average values of F(t) obtained with data from the irradiations in the 5-3/4-inch lattice. The data were grouped in 15-minute intervals and were averaged. If more than one data point for a particular irradiation fell within the same group, the average value was used and was considered as only one data point. The average value of the data points within each group was considered to be the value of F(t) at the midpoint of the time interval. The first interval was from 230 minutes to 245 minutes after the irradiations and the last interval was from 500 to 515 minutes after the irradiations. The number of data points within an interval varied from 2 to 9. Defining $P(t_i)$ as the value of P(t) for the i^{th} time interval,

$$P(t_i) = \frac{\delta^*_{28}}{F(t_i)} = \frac{0.0583}{F(t_i)} , \qquad (4.1.7)$$

where 0.0583 is the standard value of δ_{28} determined in the 5-3/4-inch lattice and discussed in section 4.1.1, $F(t_i)$ is the average value of F(t) for the i^{th} time interval determined by using the data from the 5-3/4-inch lattice, and t_i is the midpoint of the time interval. The function P(t) is shown in Fig. 4.2, and the uncertainties in the measurement of P(t) are discussed in section 4.1.4.

It is difficult to compare the measured P(t) curve with curves from previous work because the function is dependent upon many parameters which are usually different for different experiments. Since P(t) is a function of the particular conditions used in an experiment, it is not strictly correct to compare P(t) curves from different laboratories. The combination of P(t) and $\gamma(t)$ should yield the correct value of δ_{28} and comparisons should be made on the basis of values of δ_{28}. However, values of P(t), reported by Grof, Santandrea, and Ritz as part of the Yankee and Belgian Reactor-3 Critical Experiments program at the Westinghouse Reactor Evaluation Center, were determined for conditions which are similar to the conditions of the MIT measurements.[G.4] At 187 minutes

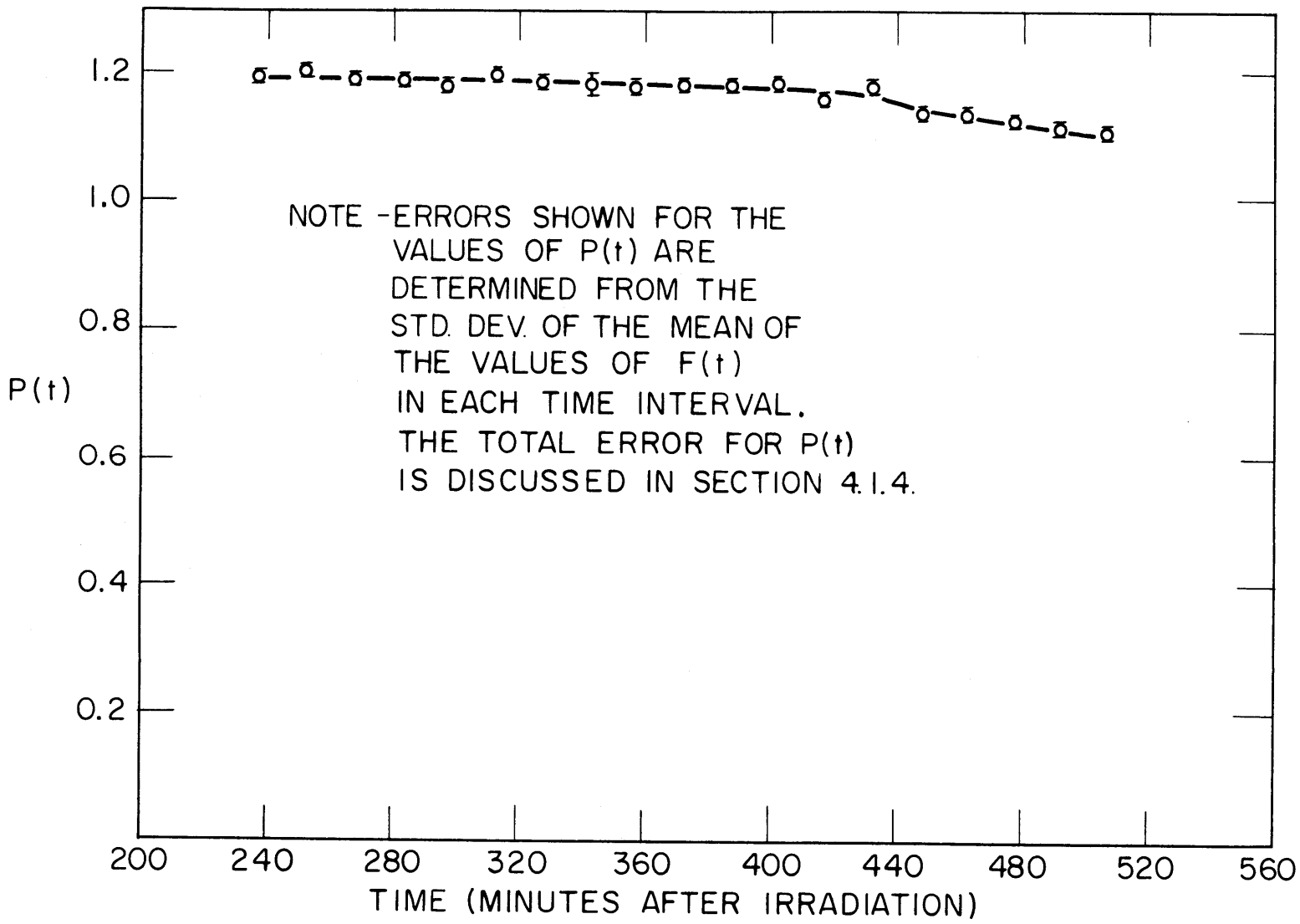

FIG. 4-2 P(t) VS. TIME

after irradiation, a value of 1.15 was reported for P(t) at a bias setting of 0.5 Mev and a value of 1.31 was reported for a bias setting of 1.20 Mev. In this study, with a bias setting of 0.72 Mev, a value of 1.19 was measured at 240 minutes after irradiation (Fig. 4.2), and additional work at MIT by Peak[P.2] indicates that P(t) is essentially constant from 180 to 240 minutes after an irradiation. The value of P(t) measured at MIT is therefore between the values reported by Grob et al. for a higher and a lower bias setting.

4.1.4 Measured Values of δ_{28} and an Analysis of the Uncertainties in the Measurements

With the exception of the value of δ_{28} given for the 5-3/4-inch lattice, the values in Table 4.1 are average values determined by using results for 2 to 5 measurements. The individual measurements and an analysis of the uncertainties in each measurement are given in Table 4.4.

The data from the measurements of δ_{28} made in the 5-3/4-inch lattice were used to determine P(t). The values of δ_{28} for the other lattices and single rods were determined by measuring values of $\gamma(t)$, calculating values of F(t), and multiplying these values by the appropriate values of P(t).

The uncertainty in δ_{28} was estimated by using the equation:

$$\left(\frac{\sigma(\delta_{28})}{\delta_{28}}\right)^2 = \left(\frac{\sigma F(t)}{F(t)}\right)^2 + \left(\frac{\sigma(P(t))}{P(t)}\right)^2 , \qquad (4.1.8)$$

where $\sigma(\delta_{28})$ is the estimated error in δ_{28}, $\sigma(F(t))$ is the estimated error in F(t), and $\sigma(P(t))$ is the estimated error in P(t). Two estimates of $\sigma(F(t))$ are given in Table 4.4 for each measurement; the calculations of these errors are discussed in Appendix D and the larger value was used to determine $\sigma(\delta_{28})$.

The value of $\sigma(P(t))$ was determined by using the equation:

$$\left(\frac{\sigma(P(t_i))}{P(t_i)}\right)^2 = \left(\frac{\sigma(\delta^*_{28})}{\delta^*_{28}}\right)^2 + \left(\frac{\sigma(F(t_i))}{F(t_i)}\right)^2 . \qquad (4.1.9)$$

Table 4.4. Values of δ_{28} measured in the MIT Lattice Facility

	δ_{28}	Number of Observations of F(t)	σ_1 (a) of F(t)	σ_2 (b) of F(t)	σ (c) of δ_{28}	N(240) (d)	T_i (e)	T_f (f)
5-3/4" Lattice	0.0580	13	0.0013	0.0010	0.0019	3.80×10^5 cpm	238 min	499 min
	0.0568	13	0.0012	0.0011	0.0018	2.48	232	492
	0.0602	13	0.0017	0.0012	0.0023	1.53	235	495
	0.0566	13	0.0017	0.0011	0.0022	1.05	228	487
	0.0589	13	0.0019	0.0014	0.0024	0.98	242	505
	0.0577	13	0.0018	0.0017	0.0023	0.65	245	510
	0.0591	25	0.0012	0.0010	0.0019	1.43	245	424
	0.0613	6	0.0010	0.0010	0.0018	1.42	261	350
	0.0584	9	0.0018	0.0009	0.0023	1.40	240	375
	0.0576	26	0.0005	0.0008	0.0016	3.40	237	428
5" Lattice	0.0595	8	0.0005	0.0011	0.0018	3.10	210	360
	0.0598	4	0.0015	0.0008	0.0021	1.50	246	366
4-1/2" Lattice	0.0616	5	0.0002	0.0008	0.0017	2.60	278	351
	0.0580	10	0.0005	0.0008	0.0016	3.00	252	367
	0.0594	5	0.0018	0.0010	0.0023	1.40	289	357
1" Single Rod	0.0545	8	0.0008	0.0015	0.0020	2.70	220	416
	0.0562	4	0.0013	0.0008	0.0019	1.90	243	355
	0.0545	8	0.0016	0.0015	0.0022	0.58	228	488
	0.0563	8	0.0009	0.0011	0.0018	1.40	232	495
	0.0568	8	0.0010	0.0007	0.0017	2.82	235	500
1/4" Single Rod	0.0123	4	0.00043	0.0005	0.0007	0.40	262	372
	0.0126	7	0.00073	0.0010	0.0010	0.21	184	460
	0.0131	7	0.00099	0.0008	0.0010	0.38	189	466
	0.0125	7	0.00082	0.0012	0.0012	0.28	194	478

(a) The RMS error of the least square curve fitted to the values of F(t).
(b) The average value of the error calculated for each point from counting statistics.
(c) The error in δ_{28} determined from the 2.5 per cent estimated error in P(t) and the largest of the two error estimates for F(t).
(d) The estimated natural foil count rate at 240 minutes after irradiation.
(e) The time of the initial measurement of F(t).
(f) The time of the final measurement of F(t).

where δ_{28}^{*} is the standard value of δ_{28} and the other terms are defined in the discussion of Eq. 4.1.7. The value of $\sigma(F(t_i))$ was estimated as the standard deviation of the mean of the measurements of F(t) in the i^{th} time interval. Values were determined for the 19 time intervals, and a maximum value of 0.0007 was calculated. The first term on the right side of Eq. 4.1.9 was estimated from the equation:

$$\left(\frac{\sigma(\delta_{28}^{*})}{\delta_{28}^{*}}\right)^2 = \left(\frac{\sigma(\beta^{25}/\beta^{28})}{(\beta^{25}/\beta^{28})_{La^{140}}}\right)^2 + \left(\frac{0.00024}{\delta_{28}^{*}}\right)^2 + \left(\frac{\sigma_B}{\delta_{28}^{*}}\right)^2 . \tag{4.1.10}$$

where $\sigma(\beta^{25}/\beta^{28})$ is the uncertainty in the ratio of the fission product yield of La^{140} from U^{235} and U^{238} fission, the quantity 0.00024 is the standard deviation of the mean of the 56 measurements of δ_{28}^{*} as shown in Table 4.2, and σ_B is the uncertainty in δ_{28}^{*} due to the uncertainties in the backgrounds of the depleted uranium foils. The uncertainty in δ_{28}^{*} due to the uncertainties in the natural foil backgrounds was negligible because the ratios of the natural foil count rates to the count rate of the background were about 20 times higher than the ratios for the depleted foils. The uncertainty due to the depleted foil background was taken as 0.7 per cent, which is the upper limit for the 40 measurements of δ_{28}^{*} made in setup 1, but is lower than the values for the 16 measurements made in setups 2 and 3. The uncertainty in the ratio of the fission product yields was estimated to be 2 per cent. The uncertainty in individual yield measurements usually vary from 3 per cent to 10 per cent, and the yields of La^{140} have been measured independently at several laboratories.[K.10] The 140 chain is one of the highest yield fission product chains and much work has been done on the measurement of the yields of this chain because it is often used to calibrate other measurements. In addition, the values are affected by measurements of the yields of other fission products through the normalization process used for the fission yield curves. Hence, the uncertainty in the ratio should be smaller than the uncertainties in the individual yield measurements. It should also be smaller than uncertainties in individual fission chamber

experiments because fission yield data include experiments based on many independent fission chamber measurements. The error in the fission chamber normalization of P(t) is the primary uncertainty for measurements of δ_{28}, and the published estimates of this uncertainty range from 4 per cent to 8 per cent, which is greater than the estimated uncertainty of the ratio, $(\beta_{25}/\beta_{28})_{La^{140}}$. The improvement associated with using this ratio over an individual fission chamber experiment was an important factor in the selection of the La^{140} method.

On substituting the estimated values of the uncertainties into Eq. 4.1.10, an uncertainty of 2.1 per cent was calculated for δ^*_{28}. The value of 0.0012 given in Table 4.1 for the 5-3/4-inch lattice was determined by multiplying 0.0583 by 0.021. Substituting the value of 0.021 and the value of 0.0007 for $\sigma(F(t_i))$ into Eq. 4.1.9, a value of 0.025 was calculated for $\sigma(P(t))/P(t)$. The time dependence of this quantity is small and was neglected. Values of $\sigma(\delta_{28})$ were then calculated by using Eq. 4.1.8 and the largest of the two estimates of $\sigma(F(t))$.

The values of $\sigma(\delta_{28})$ given in Table 4.1 are lower than the values given in Table 4.4, because they reflect the improvement in the accuracy associated with averaging the individual measurements. With the exception of the value included for the 5-3/4-inch measurement, Eq. 4.1.8 was used to calculate the errors given in Table 4.1. The error in F(t) was estimated to be either the average error given in Table 4.4 for each set of measurements divided by the square root of the number of measurement made in each set, or the standard deviation of the mean of the values of δ_{28} included in Table 4.4 for each set of measurements. The larger of the two values was used to determine the errors given in Table 4.1.

The measurements of δ_{28} tabulated in Table 4.4 include the lattice and single-rod experiments in which integral gamma-ray counting above 0.72 Mev was used. The question may be asked: What is the value of using an integral gamma-counting method when a more accurate value of δ_{28} can be measured directly by using the

La^{140} technique? There are several reasons for using this procedure.

1) Measurements based on the La^{140} technique require much longer irradiation and cooling times than the integral gamma-ray counting method.

2) The foils must be allowed to cool for at least a week, so that the activities of the fission products other than La^{140}, which emit gammas with energies near 1.60 Mev, become negligible.

3) The counting must be repeated many times to reduce the effect of statistical fluctuations. This problem arises from the low count rates associated with the 1.60 Mev La^{140} activity in the depleted foils.

4) The effective half-life of La^{140} is 12.8 days; after the measurements have been made, the foils must be cooled for several months before the La^{140} activity becomes small enough so that the foils can be reused. This problem is associated mainly with the depleted foils because the number of these foils available for experimentation is usually so small as to be a limiting factor in the measurements.

5) The uncertainty associated with the measurement of F(t) with the integral gamma-counting method can be reduced by repeating the experiment. The largest uncertainty in the measurement of δ_{28}^{*} is the estimated 2 per cent uncertainty in the value of $(\beta^{25}/\beta^{28})_{La^{140}}$. This value cannot be reduced by additional fast fission measurements. It can only be improved by additional work on fission product yields.

4.1.5 Analysis of the Results; Comparison with Other Experimental Results and Theory

The values of δ_{28} listed in Table 4.1 are averages of the measurements considered in Table 4.4, with the exception of the standard value measured in the 5-3/4-inch lattice. The uncertainties associated with these values are smaller than those of the individual measurements, and they reflect the improved precision obtained by repeating the experiments.

The differences between the lattice measurements and the one-inch diameter, single-rod measurement range from 4.3 per cent to 6.8 per cent (Table 4.1). These differences are attributed to the interaction fast effect and are small because the rod spacings in these lattices are greater

than the fast neutron mean free path in D_2O. One would expect to observe the largest value of δ_{28} in the 4-1/2-inch lattice, but the measured value in the 5-inch lattice is approximately the same as in the 4-1/2-inch lattice. However, this equivalence is not statistically significant. The interaction effect will be more important in the lattices of 1/4-inch diameter rods which will be studied later in the MIT lattice program. A qualitative discussion of the interaction fast effect is given in section 1.4.

Measurements of δ_{28} have not been made in lattices of one-inch rods and equivalent spacings at other laboratories, so that a comparison with other experiments can be made only on the basis of the single-rod measurements. The available results of similar single-rod measurements are collected in Table 4.5; calculated single-rod values of δ_{28} are also included for comparison with the experimental results.

Table 4.5. Comparison of single rod measurements and calculations of δ_{28}

	Diameter	Moderator	U^{235} Concentration	δ_{28}	Estimated Error of δ_{28}	Reference
ANL	0.96"	Graphite	0.7%	0.039		U.1, F.2
BNL	1.10	Graphite	0.7	0.059	0.0025	P.4, W.4 modified according to E.1[d]
	0.75	Graphite	1.0	0.042	0.0018	
	1.0[a]			0.054		
	0.25	Graphite	1.0	0.0121	0.0005	
SRL	1.00	D_2O	0.7	0.051	0.003	B.1
MIT	1.01	D_2O	0.7	0.0559	0.0015	
	0.25	D_2O	1.143	0.0126	0.0004	
Calculated values	1.01			0.0530[b]		
	.25			0.0141[b]		
	1.01			0.048[c]	+0.005 -0.001	

(a) Interpolated from the 1.10 and .75 inch measurements.
(b) Based on cross sections from (F.2).
(c) Based on cross sections from (C.1).
(d) Erdik (E.1) has recalibrated the BNL experiments and has suggested a 7 per cent reduction in values of δ_{28}.

As explained in section 1.4, the moderator and the difference in U^{235} concentration among the natural or slightly enriched uranium metal rods do not significantly affect the results of single-rod measurements of δ_{28}. No corrections were made for these effects, which are not taken into account in the calculation of the single-rod values of δ_{28}. A discussion of the calculations is given in Appendix F; however, the experimental results listed in Table 4.5 require comment.

1) The ANL (Argonne National Laboratory) value of δ_{28} is much lower than the other measured values and the calculated values. An examination of the ANL single-rod results (shown in Fig. 2.1) indicates that the value for the 0.96" diameter rod falls considerably below a curve fitted through zero and the values for rods with diameters of 1.96" and 2.96". The latter values agree reasonably well with results obtained at BNL with 1.93" and 2.90" diameter rods. Another value of δ_{28} can be obtained for one-inch rods by interpolating between zero and the ANL results for 1.96" and 2.96" rods; it is in the range from 0.05 to 0.06, which agrees with the other measurements and calculations. For these reasons, it seems likely that the measured ANL value of 0.039 is in error.

2) The interpolated BNL (Brookhaven National Laboratory) value of δ_{28} for one-inch diameter rods agrees with the MIT value within the limits of uncertainty of the former.

3) An SRL (Savannah River Laboratory) value of 0.045[F.4] for a one-inch diameter single rod was revised to 0.051 after it was discovered that the scintillation crystals used in the measurements were being affected by beta particles.[B.1] In a private communication from N. P. Baumann, three pieces of evidence are cited for the selection of 0.051:

(a) Later measurements with a corrected P(t) curve and a beta shield, yield values of 0.051. Baumann stated that workers at SRL plan to remeasure P(t), but currently think that their corrected curve is accurate to ± 5 per cent.

(b) The value of 0.051 agreed with the average value calculated from a compilation of single-rod measurements.[W.4]

(c) A value of 0.051 was calculated from the formula and cross-section values of Fleishman and Soodak (FS).[F.2]

The single-rod value of δ_{28} measured at SRL is 0.0044 lower than the value measured at MIT. This difference is slightly greater than the uncertainty of 0.003 quoted for the SRL value and is greater than the uncertainty of 0.0014 quoted for the MIT value. It has been shown in section 4.1.2 that pileup will decrease F(t). It was mentioned in Baumann's communication that the SRL workers had difficulties with pileup when they used a bias setting of 1.2 Mev. They noticed this by observing negative effective dead times and, as a result, went to a lower bias setting. The MIT results indicate that a pulse pileup problem may also exist at the lower setting. If this were the case, it would explain the discrepancy between the MIT and SRL results.

It should be mentioned that in Report NYO-9658, the MIT Heavy Water Lattice Research Project Annual Report,[H.3] a preliminary value of 0.051 for a one-inch diameter single rod was reported. This value was determined before the magnitude of the pileup effect was realized. After correcting the earlier measurements of P(t) for pileup and utilizing the improved measurement of δ_{28}^{*}, the MIT single-rod value was increased to 0.0559.

The average value of 0.051 mentioned in (b), above, includes the ANL value of 0.039. If this value is neglected, the average is increased. The calculation mentioned in (c) will be discussed in Appendix F.

(4) A comparison of the 1/4-inch single-rod values of δ_{28} from Table 4.5 shows that the MIT value falls between the BNL value and the value calculated by using FS cross sections. Values of δ_{28} were also measured at MIT for tight "miniature" lattices of 1/4-inch rods, and moderators of varying H_2O-D_2O content. The results of these experiments will be reported by Mr. John Peak.[P.2]

It is interesting to note that the BNL and MIT results are lower than the calculated value based on the FS cross sections for the 1/4-inch rod, but are greater than the calculated value for the 1-inch rod. Rief[R.3] predicts an increased backscatter effect for larger diameter rods (see section 2.3), and this effect is not included in the FS calculation. This effect tends to explain the inconsistency between the measured and calculated values of δ_{28}. Upon completion of his fast fission Monte Carlo code, Mr. Allard plans to calculate the magnitude of this effect for a variety of conditions.[A.1] It is anticipated that an experimental study of this effect will be carried out at MIT.

The inconsistencies between the measured and calculated values of δ_{28} point up the need for additional work on the cross sections used in the calculation and for additional measurements of δ_{28}. The measurements made at different laboratories by using the earlier fission chamber normalization technique, indicate discrepancies which are larger than the estimated errors quoted for the measurements. (See section 2.3). The method developed in this study for measuring δ^*_{28} was tested for consistent errors by using different sets of foils and different counting setups. However, it would be worth while to provide an additional test for consistency by repeating the measurements at a different laboratory. The measurement of δ^*_{28} could also be improved by additional research on the value of $(\beta^{25}/\beta^{28})_{La^{140}}$. Techniques have been devised for directly measuring the ratio of fission product yields from U^{235} and U^{238} fission.[B.4] It would be of value to make a high-precision measurement for the ratios of La^{140} or its parent, Ba^{140}.

4.2 FACTORS AFFECTING THE MEASUREMENT OF δ_{28}

4.2.1 Fission Product Contamination

An experiment designed to study the effect of fission product contamination on the activities of the uranium foils used in the measurement of δ_{28} was described in section 3.3. The increase in the count rate of a depleted uranium foil due to the exposure of one side of the foil to the adjacent fuel with no aluminum between the two surfaces was 19.5 per cent. The natural foil count rates were approximately 20 times higher than the depleted foil count rates, so that an increase of about 1 per cent would result from the exposure of the surface of a natural uranium foil to the adjacent fuel. Aluminum foils were used to protect the surfaces of the uranium foils in all the irradiations. The measurement, therefore, indicates that a positioning error of an Al foil, resulting in the exposure of 5 per cent of a depleted uranium foil surface, would result in an error of about 1 per cent because of fission product contamination from fission fragments originating in the adjacent fuel. A slight exposure of a natural uranium foil surface would introduce a negligible error in the measurement. Upon removal of the foils from the rod, an examination of the foil sandwich was always made to determine if exposure had occurred.

4.2.2 Interaction of Adjacent Foils

An experiment described in section 3.4 was designed to determine if a depleted uranium foil, placed in a position adjacent to a natural uranium foil, caused a measurable perturbation in the fission rate of the natural foil. The result of the experiment indicated that the magnitude of the perturbation could not be measured. The difference between the perturbed natural foil count rates and the interpolated values of the count rates were less than 1 per cent which was not considered to be significant. This result was used to justify the use of the foil arrangement shown in Fig. 3.4 for the measurements of δ_{28}.

4.2.3 Relative Position of the Foils and the Scintillation Detector

An experiment, designed to study the effect on P(t) of counting position, was described in section 3.6. The results of this experiment are summarized in Table 4.6.

Table 4.6. Values of δ_{28} measured at different counting positions.

Foil Set	Position	δ_{28}
1	1	0.0580
2	1	0.0568
3	1	0.0602
4	1	0.0566
		0.05765[a]
1	2	0.0589
2	2	0.0577
		0.05830[b]

(a) Average of position 1 measurements;
(b) Average of position 2 measurements.

There is a 1.5 per cent difference between measurements of δ_{28} made with set 1 foils at the two positions. The difference for the set 2 measurements is 2.6 per cent. The average difference for sets 1 and 2

is 2.0 per cent. The difference of the average values for the two positions is 1.1 per cent. A discussion of the errors associated with the measurements of P(t) and δ_{28} is included in sections 4.1.3 and 4.1.4. From these discussions it can be concluded that a difference of 1 or 2 per cent is not statistically significant. The same conclusion can be drawn from an examination of the spread in the data of Table 4.6. The effect of a change in the foil counting position on the function P(t) is, therefore, small, confirming the results of Kinard and Baumann.[K.3] On the basis of this result, Kinard and Baumann concluded that the effect on P(t) of changes in the foil size is small because the two effects are similar; they both change the average angle at which the gamma rays enter the crystal.

No attempt was made to study the effect of foil size on P(t). A change in foil size cannot be made with any assurance that the values of δ_{28} will be the same for the two different sets of foils. The smaller foils could be punched from a larger set, but even with this technique, the values of δ_{28} for the larger and smaller sets of foils would be different because the ratio of fission of U^{238} to fission of U^{235} is a function of position within a fuel rod, the value of δ_{28} being an average value. There is, therefore, no reason to assume that smaller foils punched from a larger set of foils will have the same value of δ_{28} as the larger set. For this reason, an attempt to measure P(t) with two sets of foils of different size would require two normalization experiments. The difference in P(t) that would arise from changes in foil size would, therefore, be more difficult to measure than the difference due to changes in counting position because of the additional uncertainties associated with the normalization experiments. Now, the effect on P(t) of changing the foil size is basically similar to the effect of changing the counting position; since the first effect cannot be measured as accurately as the second effect and, since the second effect was shown to be smaller than the uncertainty in the experiment, it was concluded that a correction due to the first effect would also be negligible.

4.2.4 Small Changes of the Bias Setting

It has been shown by Kinard and Baumann that P(t) is a function of the bias setting.[K.3] The effect of small changes of the bias setting on the measurement of δ_{28} was studied in an experiment described in section 3.9. This study was undertaken to determine the effect, on the measurement of δ_{28}, of the small amount of drift which might occur in the counting system between the time the system is calibrated and the time the foils are counted. Two sets of foils were irradiated and alternately counted at bias settings of 0.69 Mev, 0.72 Mev, and 0.75 Mev. The limits of 0.69 Mev and 0.75 Mev were about 5 times larger than variations from 0.72 Mev that might arise as a result of drift. Values of F(t) were determined for each bias setting and are given in Fig. 4.3 for the more active set of foils. A comparison of the results shows that there is no significant change in F(t) over the range considered. It was concluded that P(t) is insensitive to small changes in the bias setting, at a bias setting of 0.72 Mev. The measurements of δ_{28} should be, therefore, insensitive to the normal drift of the counting system.

4.3 TWO INDEPENDENT MEASUREMENTS OF δ_{28}

An experiment, described in section 3.7, was designed to compare measurements of δ_{28} based on two different methods: the earlier double fission chamber technique, and the La^{140} technique described in section 3.2. The value of δ_{28} determined from the La^{140} measurement was 2.3 per cent lower than the value determined from the double fission chamber experiment. The uncertainty in the La^{140} measurement was 2.1 per cent, the major part of this uncertainty being the 2 per cent attributed to the ratio of $(\beta_{25}/\beta_{28})_{La^{140}}$. It is recognized that this is an estimate but so also is the uncertainty of fission chamber measurements. The lowest published uncertainty in a fission chamber measurement is 4 per cent;[P.4] and the fission chamber measurements made during the course of this work are probably comparable to, but no more accurate than, those done elsewhere. It was concluded that the 2.3 per cent difference in the measurements was within the limits of the experimental uncertainty.

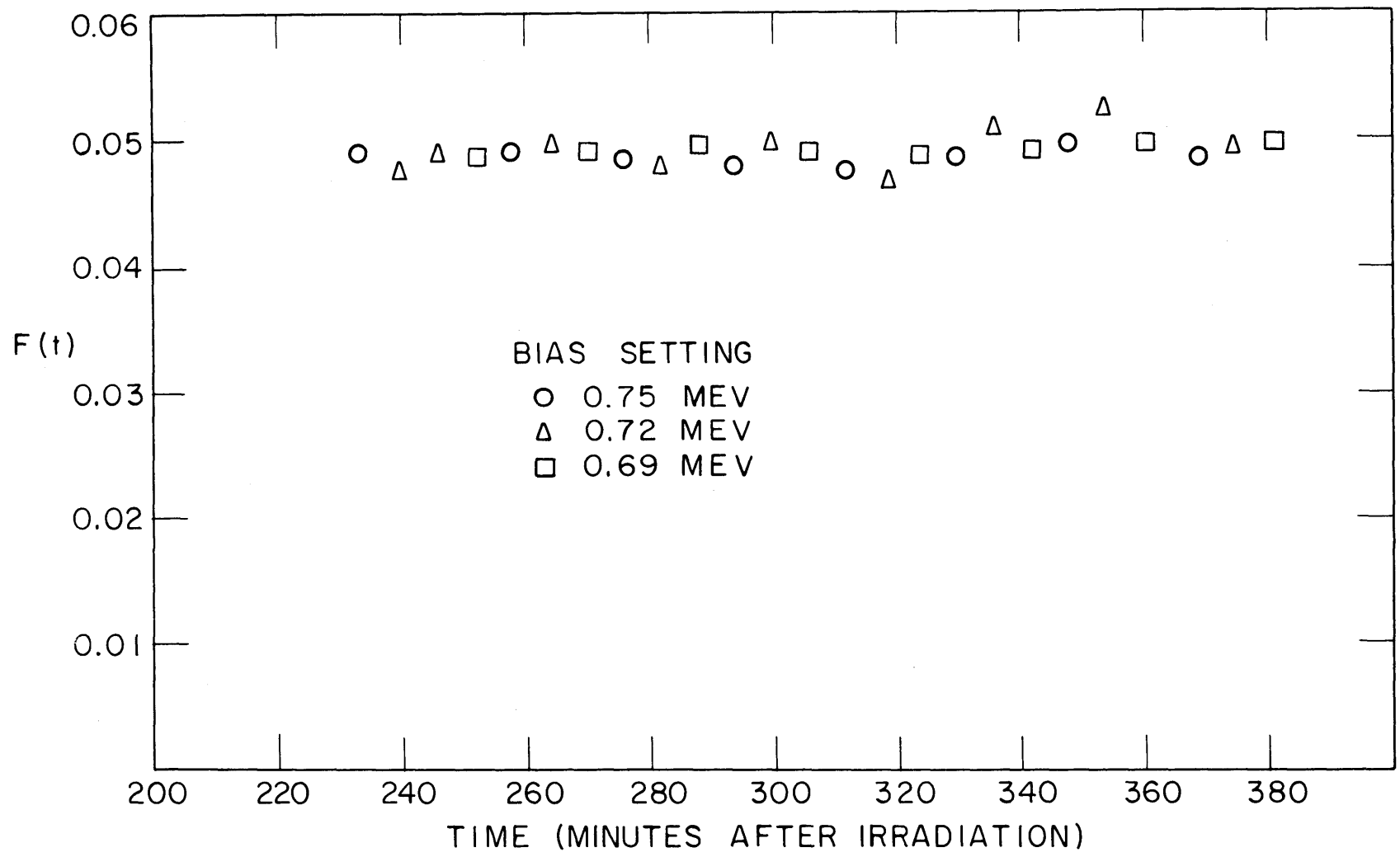

FIG. 4-3 VALUES OF F(t) VS. TIME FOR DIFFERENT BIAS SETTINGS

4.4 EFFECT OF THE NEUTRON ENERGY SPECTRUM ON THE FUNCTION P(t)

Experiments, designed to study the effect of the neutron energy spectrum on the function P(t), were described in section 3.8. No significant differences were observed in the time behavior of the functions, F(t, spectrum). It was, therefore, concluded that the changes in the fission product yields between thermal and resonance energy fission have a negligible effect on the function P(t).

Curves of F(t) are shown in Fig. 4.4 for two sets of foils. One set of foils was irradiated without an absorber between the fission plate and the foils, and the second set was irradiated using a boral absorber. Use of the boral absorber increased the value of F(t) by a factor of 10. The curves were normalized by multiplying the values of F(t) of the foils irradiated using the boral absorber, by a factor of 0.1. A comparison of the two functions as a function of time, indicates that the differences are less than the uncertainty in the measurements. Similar curves were also determined for the case in which F(t) was increased by a factor of 80. The results for this case also indicated negligible differences.

4.5 THE SPATIAL DISTRIBUTION OF FAST NEUTRONS AS A FUNCTION OF POSITION WITHIN A FUEL ROD AND WITHIN THE MODERATOR

Experiments designed to study the spatial distribution of fast neutrons in a fuel rod and in the moderator were described in section 3.10. The results of these measurements are shown in Figs. 4.5 and 4.6.

The distribution of fast neutrons in a fuel rod is considered in Chapter 20 of Weinberg and Wigner.[W.1] Calculations predict that the fast fission rate is approximately constant as a function of radial position within a fuel rod. Measurements made at BNL show an increase of less than 10 per cent in the fast fission rate near the surface of the rods, as compared to the rate at the rod centers.[P.4] A decrease

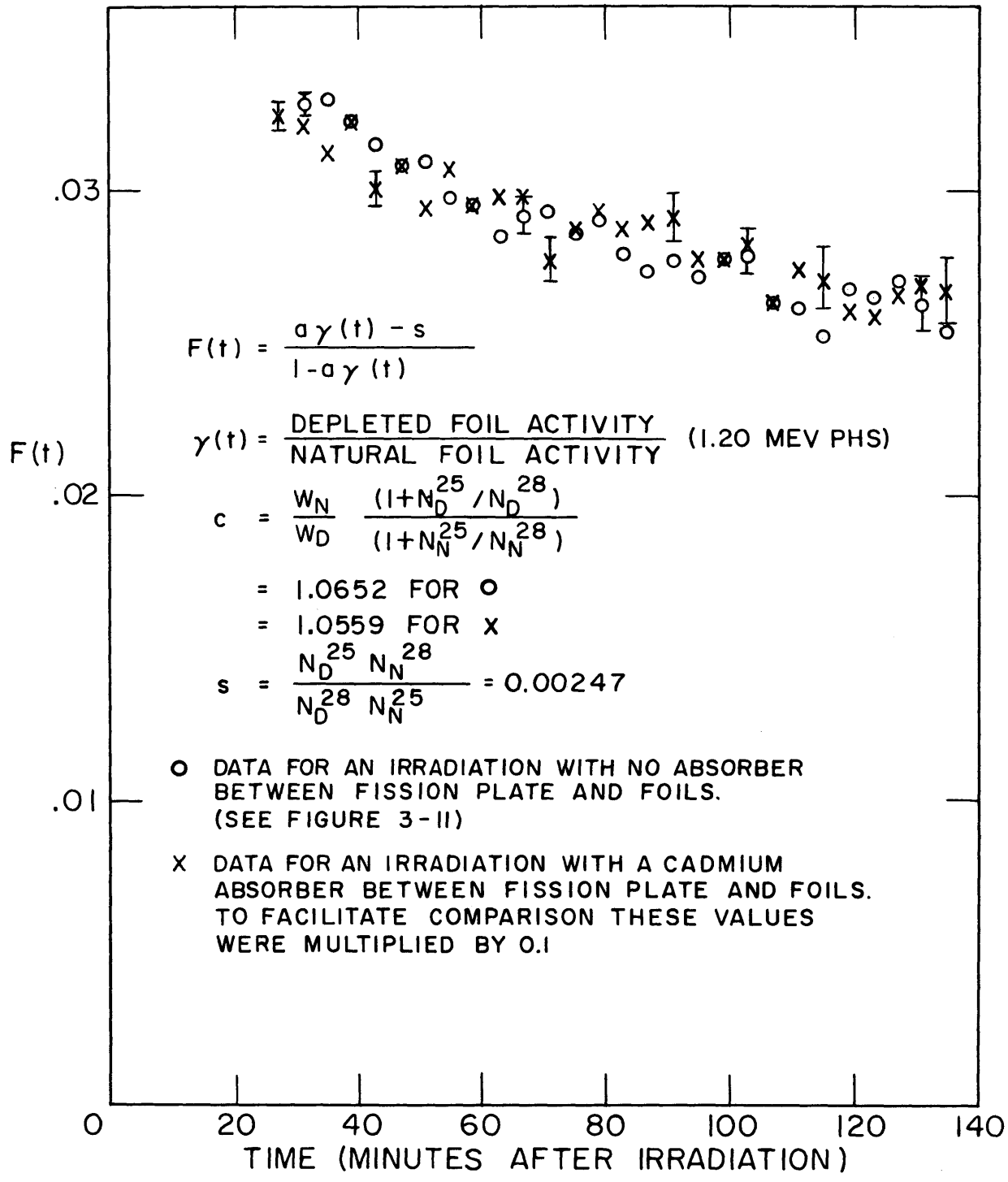

FIG. 4-4 F(t) VS. TIME FOR TWO IRRADIATIONS IN DIFFERENT SPECTRA.

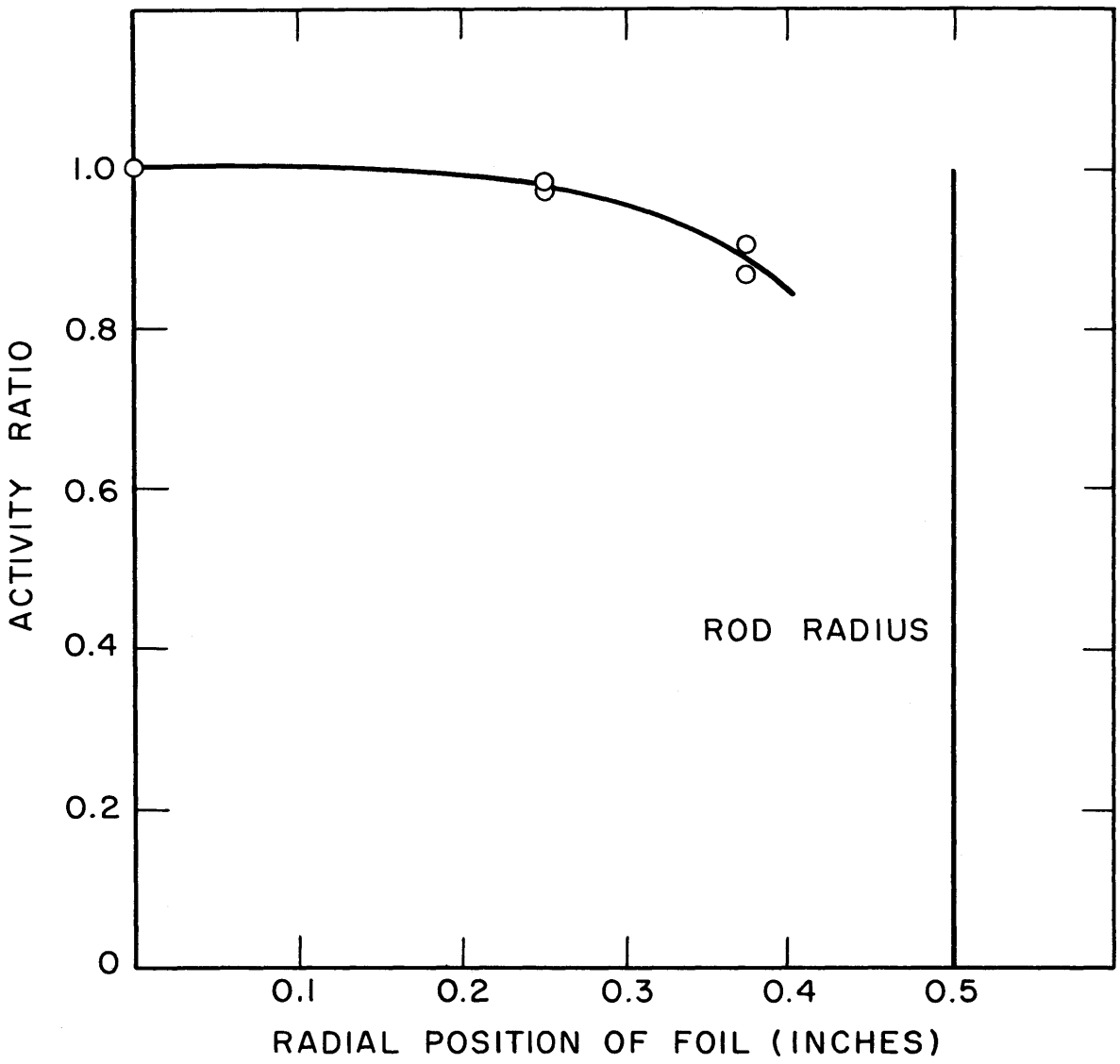

FIG. 4-5 RATIO OF FOIL ACTIVITY TO ACTIVITY OF A FOIL IRRADIATED AT THE ROD CENTER

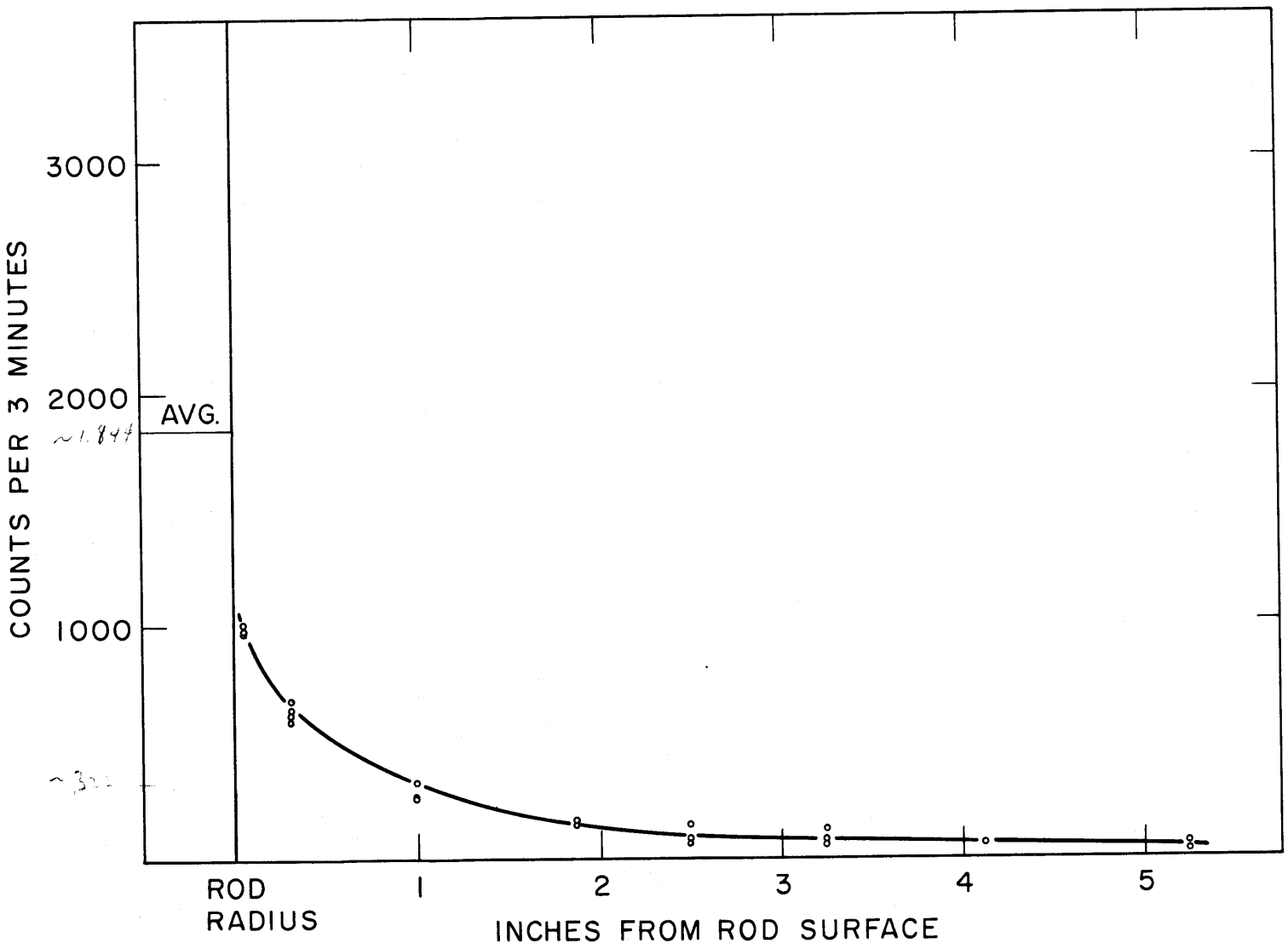

FIG. 4-6 FAST FLUX FOR SINGLE ROD IN D_2O

of 11 per cent between the foil irradiated at the rod edge and the rod center was observed for the MIT measurements. The BNL measurements were made in rods with diameters of 2.898 and 3.636 inches, respectively, while the MIT measurements were made in a 1.01-inch diameter rod. The difference between the MIT and BNL results can be explained by the fact that the thermal flux dip is much greater in the larger diameter rods. The thermal flux at the surface of the large rods was about five times the flux at the center of these rods; the corresponding ratio was only about 1.4 for the 1.01-inch rod.[B.3] The fast neutron source distribution was, therefore, much flatter for the 1.01-inch rod, increasing the number of fast fissions which occur near the rod center.

The fast neutron distribution in the moderator near a single natural uranium rod of 1.01 inches in diameter is shown in Fig. 4.6. The distribution measured near a rod in the 5-inch lattice was almost the same as the distribution near the single rod. This result is explained by the fact that the rod spacing in the 5-inch lattice is larger than the fast neutron mean free path in D_2O and indicates that the fast interaction effect should be small in the lattices considered in this study. Measurements of δ_{28} in the lattices verify that the interaction effect is small; lattice measurements of δ_{28} exceeded the single rod value by only 4.3 per cent to 6.8 per cent (Table 4.1).

4.6 MEASUREMENT OF THE RATIO OF U^{235} ATOMS IN THE DEPLETED AND NATURAL URANIUM

A description of the method used to measure N_D^{25}/N_N^{25}, the ratio of U^{235} atoms in the depleted and natural uranium, is given in section 3.11. This ratio was used to determine the constants a and S, which appear in the equations relating δ_{28} to P(t) and γ(t) (Eqs. 3.2.15 and 3.2.17). The measured value of N_D^{25}/N_N^{25} was 0.00246. This ratio corresponds to a U^{235} concentration of 17.7×10^{-6} in the depleted foil, and it was estimated that the uncertainty in the measurement was ± 5 per cent.

From Eq. 3.2.17, it can be seen that δ_{28} is nearly proportional

to $a\gamma(t) - S$. The calculated values of a and S were 0.992 and 0.00247, and values of $\gamma(t)$ for the one-inch diameter rods were usually about 0.045. The value of a is calculated from Eq. 3.2.14 and is insensitive to the value of N_D^{25}/N_N^{25}. The value of S is calculated from Eq. 3.2.16 and is nearly proportional to N_D^{25}/N_N^{25}. It can, therefore, be seen that δ_{28} is insensitive to the value of N_D^{25}/N_N^{25} when $a\gamma(t)$ is large compared to S. This condition is fulfilled when the U^{235} concentration of the depleted uranium is small, as is the case for the depleted uranium used in this study.

4.7 MEASUREMENTS OF δ_{25}

Measurements of δ_{25}, the ratio of the numbers of epicadmium to subcadmium fissions in U^{235}, were made in the natural uranium lattices, in a one-inch diameter single rod, and in the moderator. The method used to measure this quantity is described in section 3.12. The results of the measurements are summarized in Table 4.7.

Table 4.7. Measurements of δ_{25}.

	δ_{25}	$(\delta_{25})_{Au}$ [a]	$(\delta_{25})_{avg}$
4-1/2" Lattice	0.0479 ± 0.0019	0.048	0.048
5" Lattice	0.0340 ± 0.0030	0.041	0.037
5-3/4" Lattice	0.0268 ± 0.0010	0.026	0.026
1.01" Single Rod	0.0086 ± 0.0004		
Moderator	0.0035 ± 0.0002		

(a) Calculated from Au-cadmium ratios measured at MIT by Mr. A. Weitzberg (W.3).

The measured values of δ_{25} are compared to values calculated from dilute Au cadmium ratios measured at MIT by Mr. A. Weitzberg.[W.3] The equation relating δ_{25} and $R_{\text{dilute Au}}$ is:

$$\delta_{25} \cong \frac{0.327}{R_{(\text{dilute Au})} - 1} \qquad (4.7.1)$$

This equation is derived in the report, BNL-486, for a thermal reactor.[K.7] The two methods of determining δ_{25} agree for the 4-1/2-inch and the 5-3/4-inch lattices, but show a discrepancy of 0.007 for the 5-inch lattice. The results are plotted in Fig. 4.7 as a function of the ratio of moderator volume to fuel volume. An examination of the data indicates that a value of about 0.037 seems more reasonable for the 5-inch lattice than either of the measured values.

The measurements of δ_{25} for the single rod and for the moderator were used to determine where the neutrons causing epicadmium fission were born. In the 5-3/4-inch lattice, at a position of one foot above the bottom of the tank, approximately 13 per cent $\left(\frac{0.0035}{0.0268}\right)$ of the epicadmium fissions in U^{235} were caused by neutrons entering the tank from the thermal column, 19 per cent $\left(\frac{0.0086 - 0.0035}{0.0268}\right)$ were caused by neutrons born in the rod, and the remaining 68 per cent were caused by neutrons born in other rods. The fraction of neutrons born in other rods increases with decreasing moderator to fuel volume ratio because this change results in a hardening of the neutron energy spectrum.

The uncertainties included in Table 4.7 reflect counting statistics and the reproducibility of the measurements. Failure to position the foils adjacent to the Al sleeve shown in Fig. 3.13 would result in high values of δ_{25}, and this presented an additional uncertainty. Errors of this type were easy to observe, however, because they would result in unreasonably high values of ρ_{28}, as well as in δ_{25}; both measurements were made with the same depleted uranium foils. This problem can be avoided by re-using the same uranium fuel slugs and an Al spacer of the correct length to align the foils and the cadmium sleeve. This procedure was adopted after a correct combination of spacer and fuel slugs was determined. The value of δ_{25} reported for the 5-inch lattice is an average of two measurements, the value reported for the 5-3/4-inch lattice is an average of three measurements and the value reported for the 4-1/2-inch lattice is from only one measurement of δ_{25}. The fast fission rate is decreased by the presence of cadmium because the number of fast neutrons born near the foils is decreased. The magnitude of this effect is considered in section 4.8, but was not realized

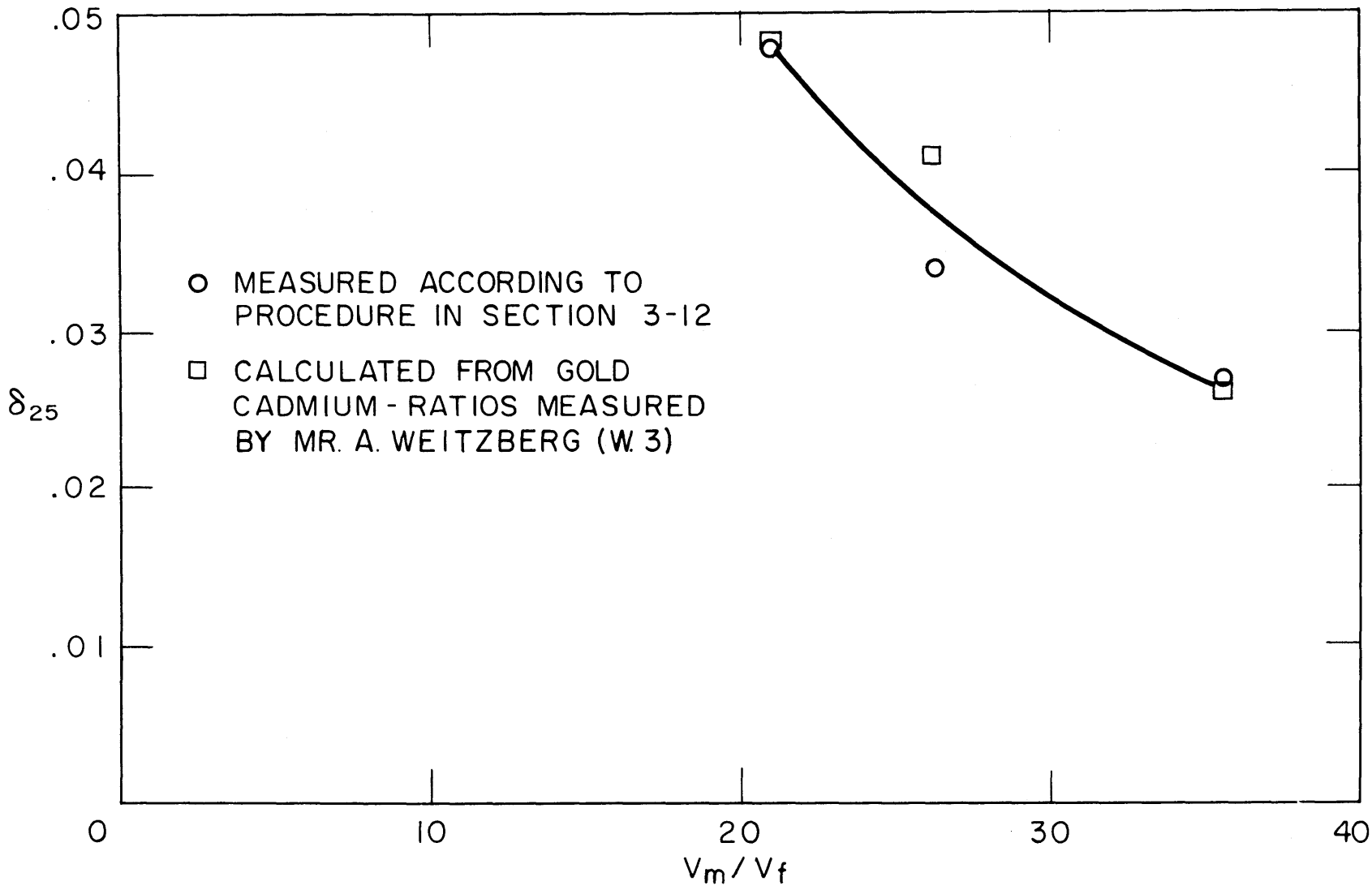

FIG. 4-7 δ_{25} VS. VOLUME OF MODERATOR TO VOLUME OF FUEL

for two previous measurements of δ_{25} in the 4-1/2-inch lattice. Measurements of the count rate of the cadmium-covered depleted foil were not made in these two experiments. The ratio of the number of counts for the natural uranium cadmium-covered foil and natural uranium bare foil agreed to within 2.8 per cent for the three measurements in this lattice, however.

4.8 EFFECT OF REMOVING FUEL FROM THE REGION NEAR A DEPLETED URANIUM FOIL

An experiment, designed to study the effect of removing fuel from the region near a depleted uranium foil, is described in section 3.12. The results of this experiment are shown in Fig. 4.8. The experiment was only performed once; the four points given in Fig. 4.8 for each value of Al thickness were determined by measuring the activity of each foil four times.

The effect of surrounding the depleted foil by 50 mil thick buttons of Al and 20 mil thick buttons of Cd, is to reduce the fast fission rate by 42 per cent. This foil arrangement is similar to the arrangement used in the measurement of δ_{25} as shown in Fig. 3.13. The equivalent thickness of Al required to make the same reduction is 0.2 inches.

4.9 A STUDY OF THE FISSION PRODUCT GAMMA-RAY SPECTRUM

Experiments, designed to study the fission product gamma-ray spectrum, were described in section 3.14. The experimental work was preceded by a survey of the fission products. The fission product gamma rays were classified according to their energies and effective half-lives. Other parameters of interest were the fission product yields and the gamma-ray abundances. The abundance of a gamma ray is defined as the percentage of decays of a radioactive species which result in an emission of the gamma ray. For the most part, the data were were gathered from three sources: Nucleonics, November 1960[N.2]; AECL-1225[H.1]; and the Nuclear Data Sheets.[N.1]

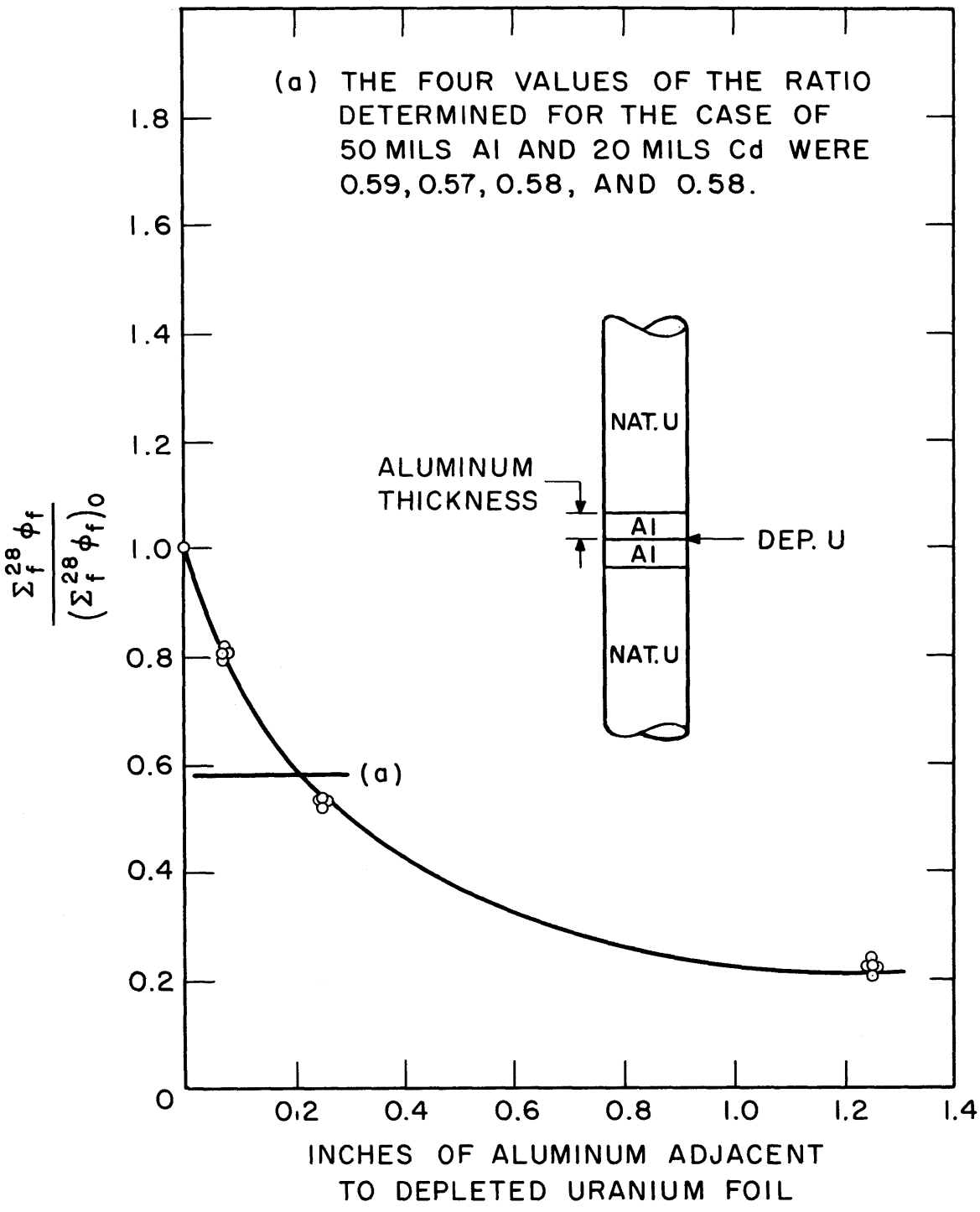

FIG. 4-8 RATIO OF FAST FISSION IN A FOIL ADJACENT TO ALUMINUM TO FAST FISSION IN A BARE FOIL.

4.9.1 Gamma-Ray Spectra as a Function of Time

The first phase of the experimental work consisted of observation of the gamma-ray spectrum as a function of time after irradiation. The purpose of this study was twofold.

1) It was to be used for comparison with the theoretical predictions. It was hoped that the decay of an irradiated uranium foil and thus P(t) could be explained on the basis of the fission product data, so that it was important to test the reliability of this data.

2) It was hoped that the study would uncover phenomena useful for fast fission measurements.

Figures 4.9 through 4.14 are typical of the spectra measured in this phase of the study. As can be seen, the spectra include distinct peaks and the complexity of the spectra decrease at increasing times after irradiation because the number of important gamma rays decreases with increasing time. It was found that the fission product survey provided very useful results: (1) all gamma rays of importance, as predicted, were observed; (2) all observed gamma rays could be identified.

An attempt was made to use the survey information to predict the time behavior of the fission products and the function P(t). The results of this analysis are given in Appendix B.

Observation of the distinct peak at 1.60 Mev for times greater than several days, led to adoption of the La^{140} method for measuring δ_{28}. Further experimental work was required before the method could be adopted, however. This work is discussed in section 4.9.2.

4.9.2 The La^{140} 1.60 Mev Gamma Ray

The possibility of using the La^{140} Mev gamma ray in the measurement of δ_{28} appeared as a result of the gamma-ray spectrum research discussed in section 4.9.1. The nuclide La^{140} has a fission product yield of 6.35 per cent for fission of U^{235} and 5.70 per cent for fission of U^{238}. The direct yield of La^{140} is negligible[G.5]; the quoted yields are the total yields for the preceding nuclides in the 140 chain. The abundance of the 1.60 Mev gamma is 88 per cent; the abundance of a

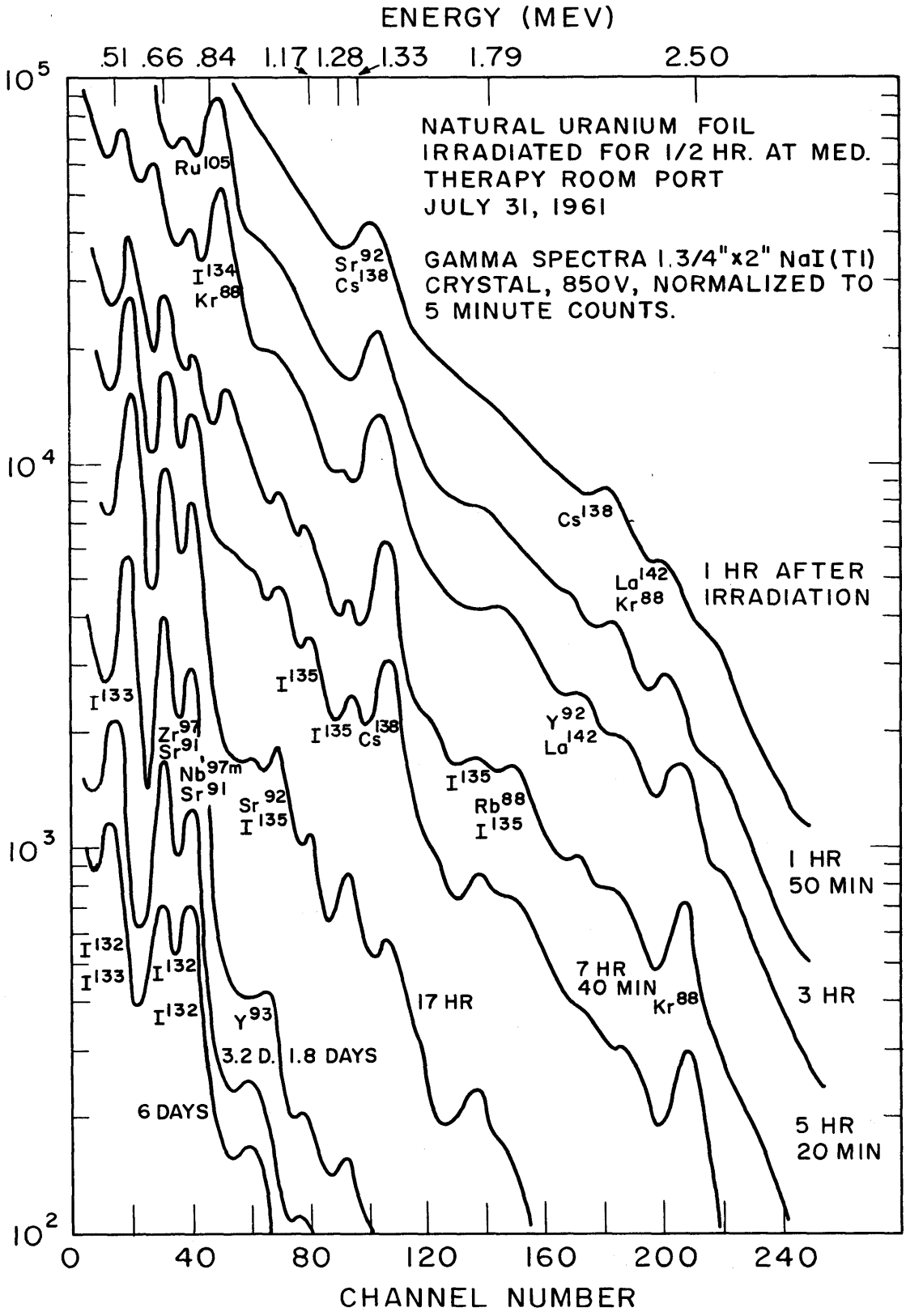

FIG. 4-9 NATURAL URANIUM FISSION PRODUCT GAMMA SPECTRA

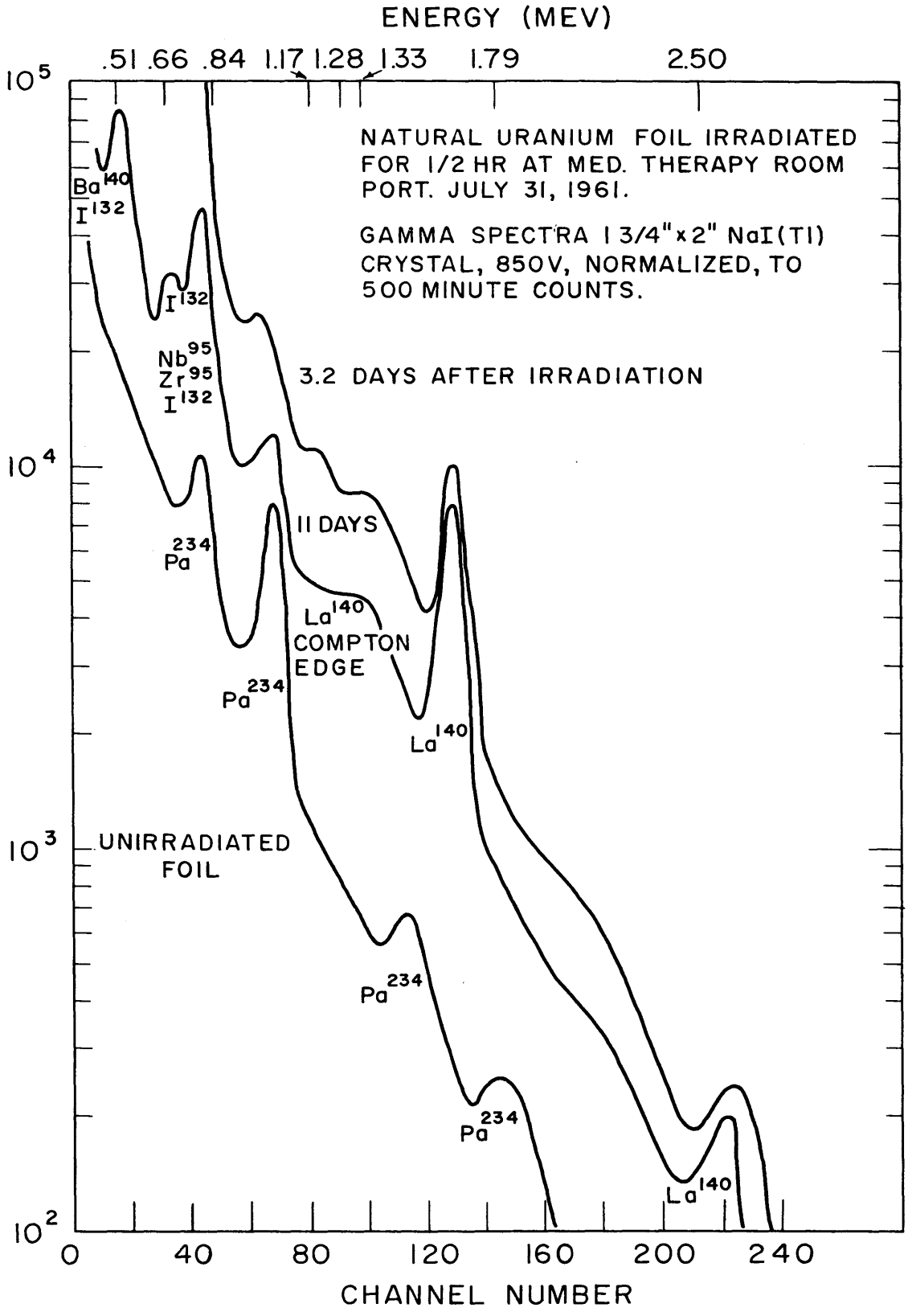

FIG. 4-10 NATURAL URANIUM FISSION PRODUCT GAMMA SPECTRA

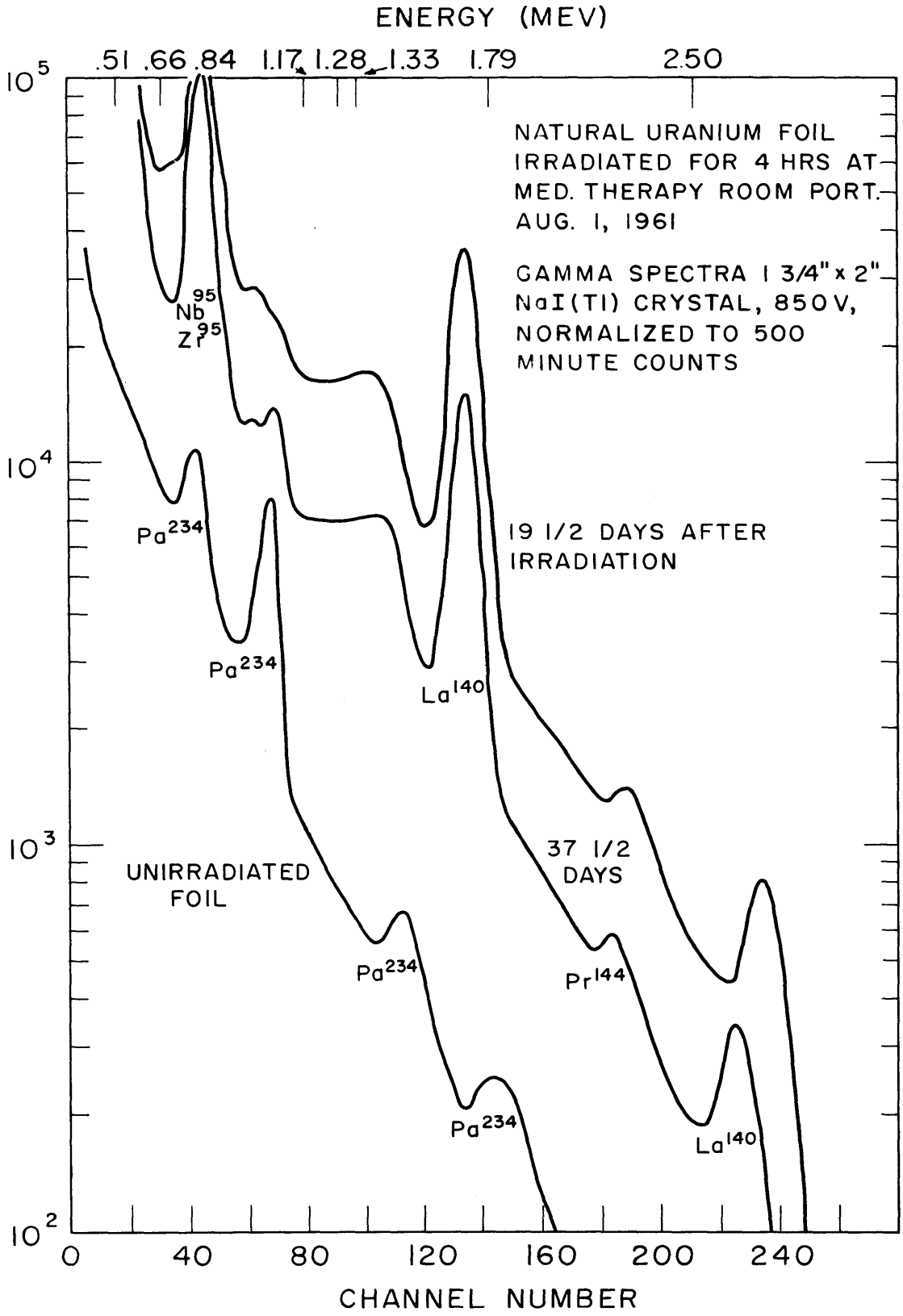

FIG. 4-11 NATURAL URANIUM FISSION PRODUCT GAMMA SPECTRA

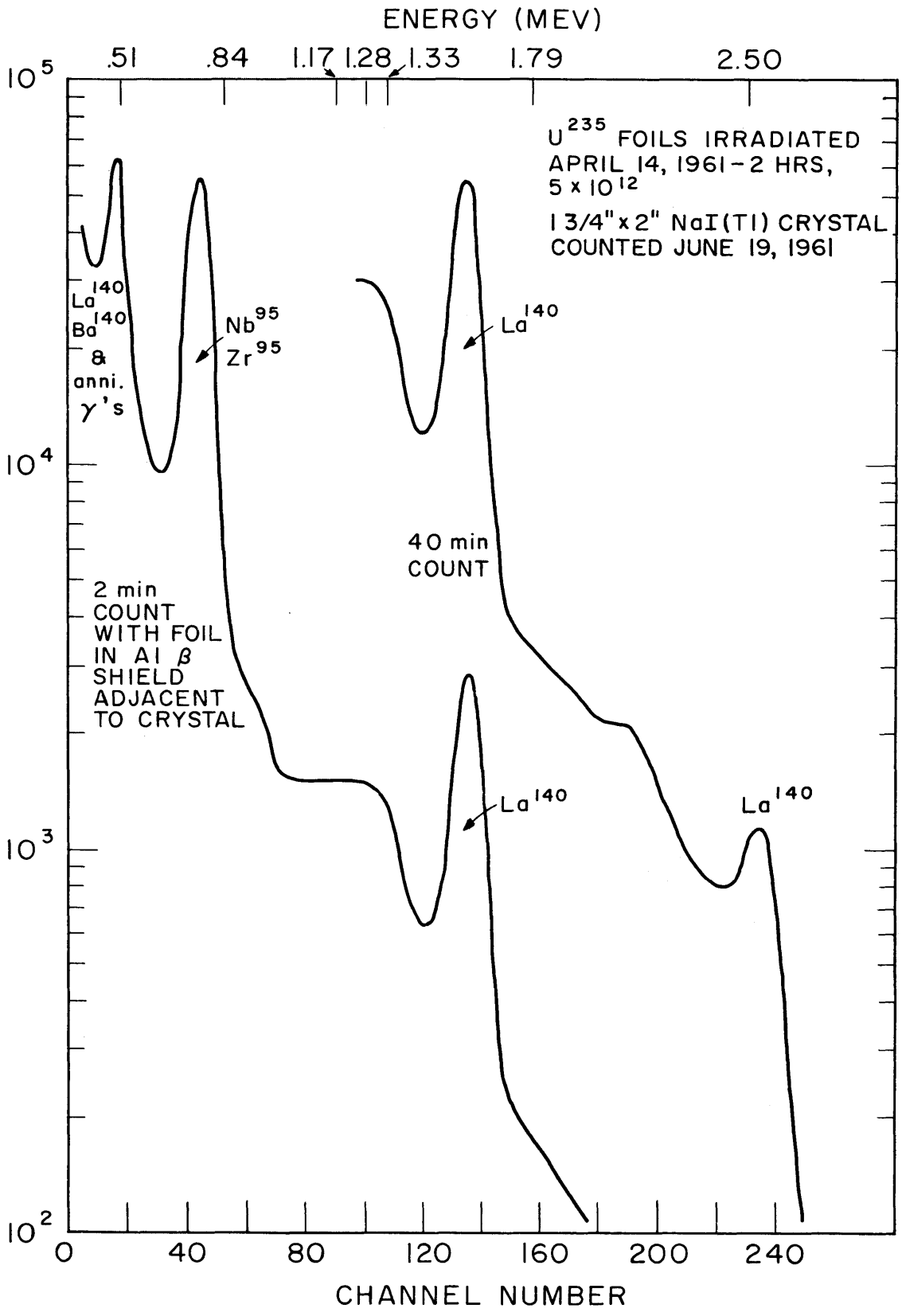

FIG. 4-12 U^{235} FISSION PRODUCT GAMMA SPECTRA

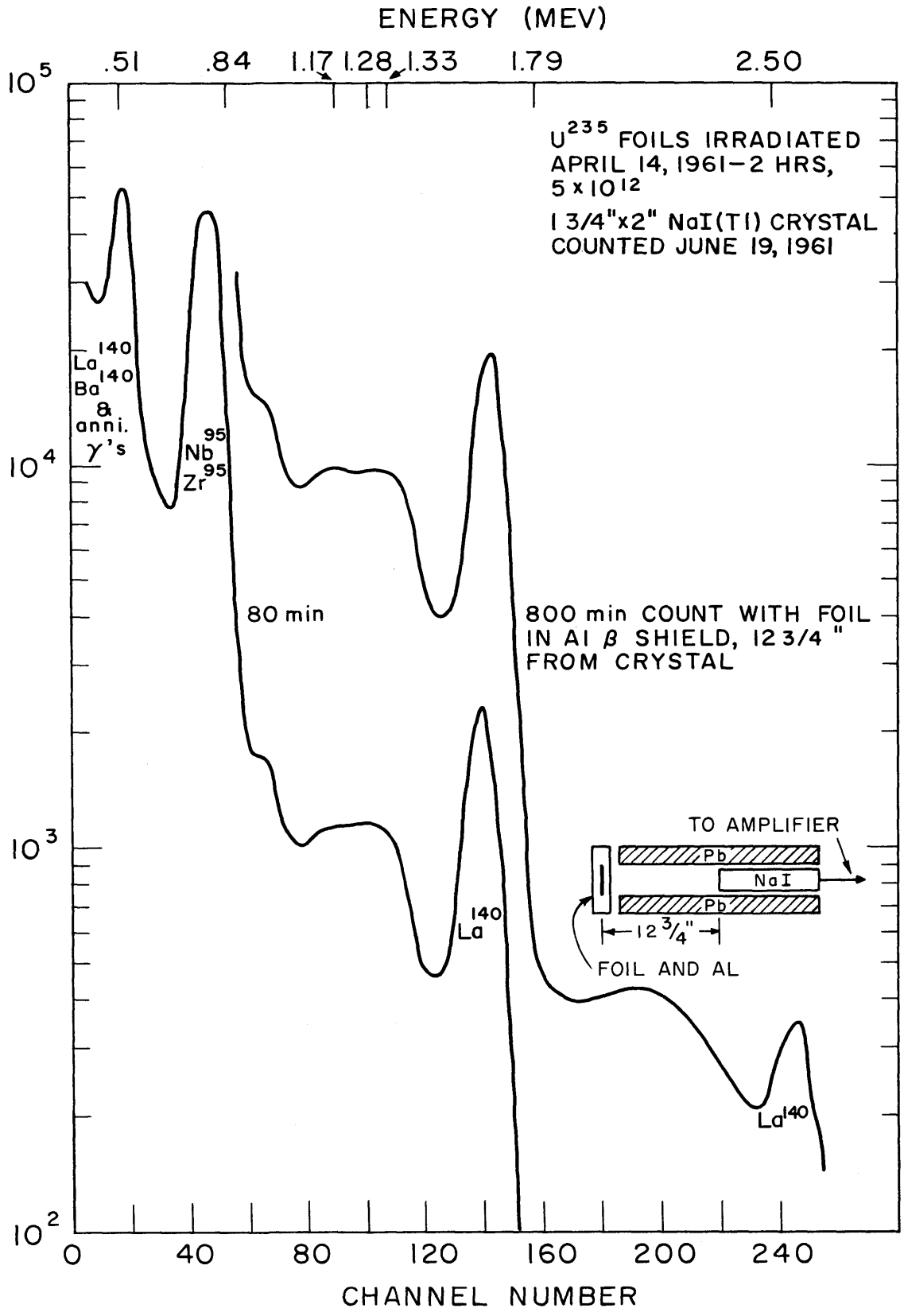

FIG. 4–13 U^{235} FISSION PRODUCT GAMMA SPECTRA

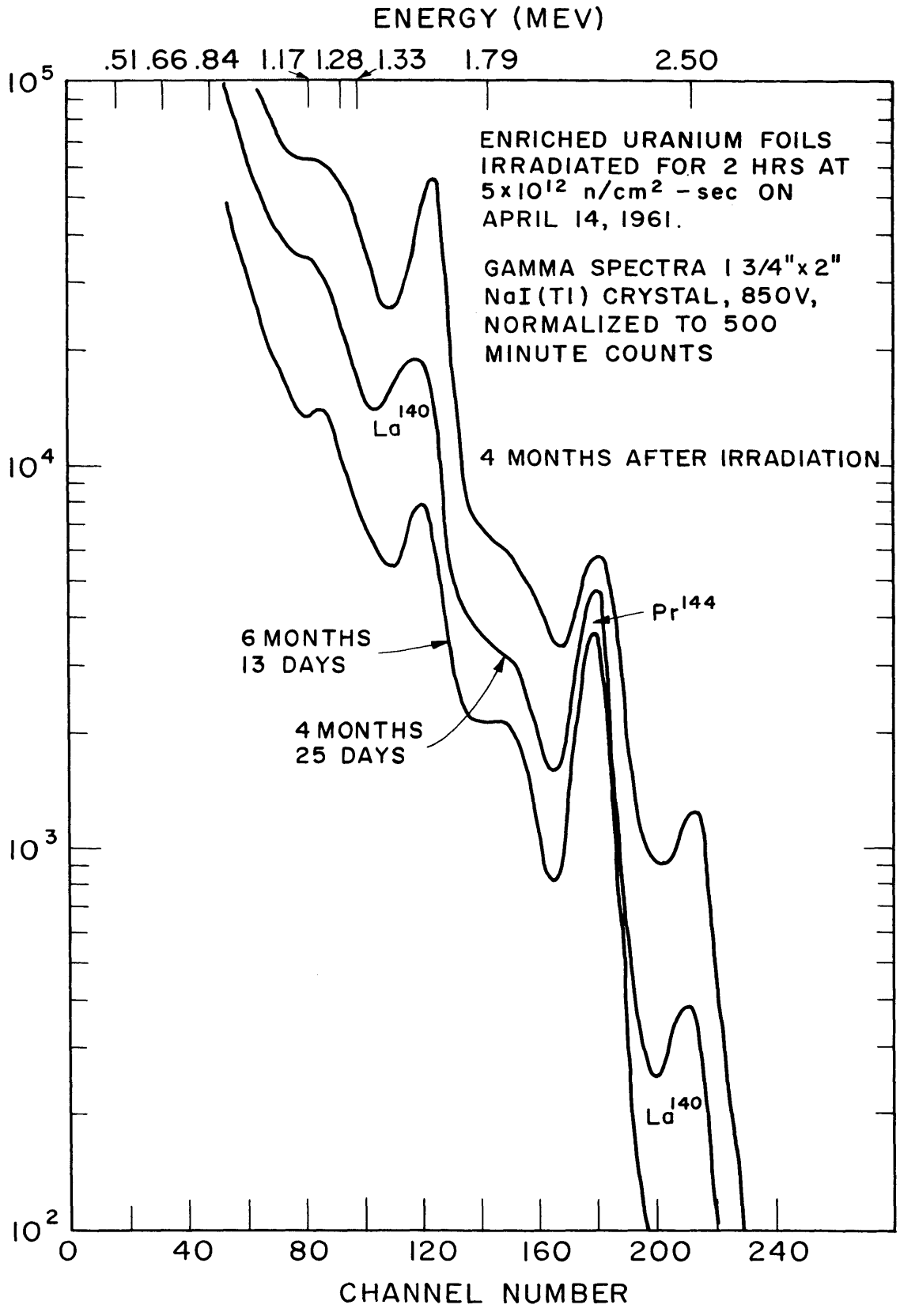

FIG. 4-14 U^{235} FISSION PRODUCT GAMMA SPECTRA

gamma ray is defined as the number emitted per 100 disintegrations of the nuclide. The half-life of La^{140} is 40.2 hours, but it reaches equilibrium with its parent, 12.8-day Ba^{140}. The survey of the fission products, mentioned in section 4.9.1, showed that there are very few fission product gamma rays with comparable or longer effective half-lives in the higher energy range. There are a few higher energy La^{140} gamma rays, the most important being the 2.52 Mev gamma with an abundance of about 2 per cent. There are several high-energy gammas associated with 14.6 d Eu^{156}, 210 d Rh^{102}, 1.02 y Rh^{106}; but in each case, the yield and abundance are low. The only other high-energy gamma ray of any significance is the 2.18 Mev Pr^{144} gamma, which has a high yield (5.6 per cent), but a low abundance (0.8 per cent); Pr^{144} reaches equilibrium with Ce^{144} which has a half-life of 285 days.

Within a week, La^{140} is in equilibrium with Ba^{140}, and the important high-energy gamma rays of shorter effective half-life are negligible. These include gammas from 32 m Cs^{138}, 52 m I^{134}, 1.3 h La^{142}, 1.3 h Kr^{87}, 2.8 h Kr^{88}, 2.8 h Rb^{88}, 3.6 h Y^{92}, 6.7 h I^{135}, 10.4 h Y^{93}, and 17 h Zr^{92}. One would thus expect to see a large distinct peak at 1.60 Mev, with negligible background due to other fission products. This property was observed experimentally as shown in Figs. 4.10 and 4.11. The spectra were obtained with the natural uranium foils containing the fission fragments in a position adjacent to the detector crystal. Spectra were also observed several months after an irradiation of U^{235} foils (Figs. 4.12, 4.13, 4.14). It was thought that a significant number of counts registered in the channels above 150 in Fig. 4.12 were due to lower energy La^{140} gammas and Compton scattered gammas in coincidence with the 1.60 Mev gamma ray. To test this hypothesis, the foil was placed in a position about one foot away from the detector. The spectrum was measured (Fig. 4.13) and, as expected, the relative number of counts above the 1.60 Mev peak was reduced. The relative heights of the 1.60 Mev peak and the 2.52 Mev peak remained the same, however, because these are both true peaks rather than sum peaks. The spectra were compared to the La^{140} spectra in the report IDO 16408.[H.2]

Although the counting arrangements were different, an obvious similarity exists between the irradiated uranium spectrum after about a week and the spectrum of La^{140} above 1.20 Mev.

At the time the spectra in Figs. 4.12 and 4.13 were observed, the Pr^{144} peak at 2.18 Mev was barely discernible; these observations were at about 2 months after irradiation. Figure 4.14 shows spectra observed between 4 and 6 months after irradiation; in these, the Pr^{144} peak becomes important. The Pr^{144} peak shown in Fig. 4.11 includes residual Pr^{144} activity from many previous irradiations with the same foil.

The above results indicated that if uranium foils are observed by using a single channel analyzer centered on the 1.60 Mev peak in the time range from a week to several months after irradiation, one will see predominantly La^{140} 1.60 Mev gamma rays. The only other significant possibilities are pulses from the Compton scattered gamma rays of Pr^{144} and the higher energy La^{140} gammas and, of course, background. The effect of Pr^{144} has been calculated to be negligible for several months after irradiation, and the spectra confirm this. Gammas from Eu^{156}, Rh^{102} and Rh^{106} were not observed and were calculated to be negligible. Perturbations in the peak, caused by different La^{140} coincidence rates at different counting positions, do not affect the results if all foils are measured at the same or approximately the same position. The background is measurable and anything from La^{140} is helpful. A measurement of the half-life of the 1.60 Mev peak yielded a value of 12.8 ± 0.4 days, which was further evidence that the counts originate from decays of La^{140}.

The results from the study of the 1.60 Mev fission product gamma-ray peak formed the basis of a new technique for measuring δ_{28}. This method is discussed in section 3.2.3.

APPENDIX A
TREATMENT OF FAST FISSION IN THE FOUR FACTOR FORMULA

The multiplication factor, k, can be determined by first calculating a multiplication factor for an infinite lattice, k_∞, and then modifying k_∞ to include the effects of neutron leakage. Now, k_∞ is not an invariant reactor parameter but depends upon the theory used to define it. A common method of treating k_∞ is to define it as the product of four factors:

$$k_\infty = \eta f p \epsilon \, . \qquad \text{(A.1)}$$

The first factor, η, is the number of neutrons produced per thermal neutron absorbed in the fuel. The second factor, f, is the ratio of the number of thermal neutrons absorbed in the fuel to the number absorbed in the entire system. The third factor, p, is the resonance escape probability, which may be defined in several ways; and the fourth factor, ϵ, is the fast fission factor, which may also be defined in several ways. The calculation of k_∞ thus becomes a problem of calculating each factor.

Definitions of k_∞ and the four factors must be compatible with Eq. A.1. The definitions of η and f do not vary among different formulations; but several definitions are used for k_∞, p and ϵ, and compatibility conditions can be determined for the definitions.

Two important definitions of k_∞ are the following: (1) the ratio of the total number of neutrons produced to the total number of neutrons absorbed in an infinite lattice, denoted by $k_{\infty 1}$; (2) the ratio of the number of thermal neutrons produced to the number of thermal neutrons absorbed in an infinite lattice, denoted by $k_{\infty 2}$. These definitions can be expressed in multigroup notation for an infinite, homogeneous system with n groups:

$$k_{\infty 1} = \frac{\sum_{i=1}^{n} \nu_i \Sigma_{fi} \phi_i}{\sum_{i=1}^{n} (\Sigma_{ci}+\Sigma_{fi})\ \phi_i}, \tag{A.2}$$

and

$$k_{\infty} = \frac{f_n\left(\sum_{i=1}^{n} \nu_i \Sigma_{fi} \phi_i\right) + \sum_{i=1}^{n} \Sigma_{i\to n} \phi_i}{(\Sigma_{cn}+\Sigma_{fn})\ \phi_n}, \tag{A.3}$$

In these equations, the n^{th} group is the thermal energy group, f_i is the fraction of neutrons born in the i^{th} group, ν_i is the number of neutrons emitted per fission in the i^{th} group, Σ_{ci} and Σ_{fi} are the macroscopic capture and fission cross sections for the i^{th} group, $\Sigma_{i\to n}$ is the slowing-down cross section from the i^{th} group to the thermal group, and ϕ_i is the flux of the i^{th} group. The quantities $k_{\infty 1}$ and $k_{\infty 2}$ are different, and it will be shown that $k_{\infty 1}$ is closer to unity than $k_{\infty 2}$.

The two quantities, $k_{\infty 1}$ and $k_{\infty 2}$ can be considered as eigenvalues of multigroup equations:

$$-\Sigma_i \phi_i + \sum_{j=1}^{i-1} \Sigma_{j\to i} \phi_j + \frac{f_i}{k_{\infty 1}} \sum_{j=1}^{n} \nu_j \Sigma_{fj} \phi_j = 0, \tag{A.4}$$

and

$$-\Sigma_i \phi_i + \frac{1}{k_{\infty 2}}\left[\sum_{j=1}^{i-1} \Sigma_{j\to i} \phi_j + f_i \sum_{j=1}^{n} \nu_j \Sigma_{fj} \phi_j\right] = 0. \tag{A.5}$$

In these equations,

$$\Sigma_i = \Sigma_{ci} + \Sigma_{fi} + \sum_{j=i+1}^{n} \Sigma_{i\to j}, \tag{A.6}$$

where $\Sigma_{i\to j}$ is the slowing-down cross section from the i^{th} to the j^{th} group. For i equal to n, $\Sigma_{i\to j}$ is not applicable, and is set equal to zero.

On summing Eq. A.5 over all groups after substituting Eq. A.6 into Eq. A.5, and using the fact that

$$\sum_{i=1}^{n} f_i = 1, \tag{A.7}$$

we can see that

$$k_{\infty 2} = \frac{\sum_{i=1}^{n} \nu_i \Sigma_{fi} \phi_i + \sum_{i=1}^{n-1} \sum_{j=i+1}^{n} \Sigma_{i \to j} \phi_i}{\sum_{i=1}^{n} (\Sigma_{ci} + \Sigma_{fi}) \phi_i + \sum_{i=1}^{n-1} \sum_{j=i+1}^{n} \Sigma_{i \to j} \phi_i}. \tag{A.8}$$

Substitution of

$$\sum_{i=1}^{n-1} \sum_{j=i+1}^{n} \Sigma_{i \to j} \phi_i = A \tag{A.9}$$

gives

$$k_{\infty 2} = \frac{\sum_{i=1}^{n} \nu_i \Sigma_{fi} \phi_i + A}{\sum_{i=1}^{n} (\Sigma_{ci} + \Sigma_{fi}) \phi_i + A}. \tag{A.10}$$

Comparison of Eqs. A.10 and A.2 shows that $k_{\infty 2}$ differs from $k_{\infty 1}$ and is always closer to unity than $k_{\infty 1}$. The quantity $k_{\infty 2}$ was defined as the ratio of the number of thermal neutrons produced to the number of thermal neutrons absorbed, but Eq. A.8 shows that it can also be interpreted as the ratio of the total number of neutrons entering all groups to the total number of neutrons leaving all groups.

With the standard definitions for η and f, the product ηf can be expressed by means of the relation

$$\eta f = \frac{\nu_n \Sigma_{fn}}{\Sigma_{cn} + \Sigma_{fn}}. \tag{A.11}$$

Equations A. 11, A. 2, and A. 3 can be substituted into Eq. A. 1 to determine the compatibility conditions:

$$(p\epsilon)_1 = \frac{k_{\infty 1}}{\eta f}, \tag{A.12}$$

$$(p\epsilon)_1 = \frac{\sum_{i=1}^{n} \nu_i \Sigma_{fi} \phi_i}{\sum_{i=n}^{n} (\Sigma_{ci} + \Sigma_{fi})\, \phi_i} \cdot \frac{\Sigma_{cn} + \Sigma_{fn}}{\nu_n \Sigma_{fn}}; \tag{A.13}$$

$$(p\epsilon)_2 = \frac{k_{\infty 2}}{\eta f}, \tag{A.14}$$

$$(p\epsilon)_2 = \frac{f_n\left(\sum_{i=1}^{n} \nu_i \Sigma_{fi} \phi_i\right) + \sum_{i=1}^{n} \Sigma_{i\to n} \phi_i}{\nu_n \Sigma_{fn} \phi_n}. \tag{A.15}$$

The energy spectrum of the neutrons emitted in fission is such that f_n may be taken equal to zero, and Eq. A. 15 reduces to:

$$(p\epsilon)_2 = \frac{\sum_{i=1}^{n} \Sigma_{i\to n} \phi_i}{\nu_n \Sigma_{fn} \phi_n}. \tag{A.16}$$

Equations A. 13 and A. 15 show that the product $p\epsilon$ depends on the definition of k_∞. Furthermore, after k_∞ has been defined, either p or ϵ is arbitrary. This result indicates why several definitions of ϵ have appeared in the literature (section 1. 1). For this reason, experimentalists use the unambiguous quantity, δ_{28}, the ratio of the fission rate in U^{238} to the fission rate in U^{235}. When ϵ has been defined, δ_{28} can be related to ϵ by an equation of the form:

$$\epsilon = 1 + C\delta_{28} \tag{A.17}$$

where C is a constant involving nuclear properties of U^{235} and U^{238}.

APPENDIX B
AN ANALYSIS OF THE FUNCTION P(t)

In this report, P(t) has been defined as the ratio of the count rate of gamma rays above 0.72 Mev, per fission of U^{235}, and at time t, to the count rate, above 0.72 Mev, per fission of U^{238}, and at time t. The technique used to measure this function is described in section 3.2, and the results are discussed in section 4.1. The function was also estimated independently from nuclear data by using the following procedure.

1) The survey of fission product gamma rays described in section 4.9 was used to determine which nuclides emit gamma rays with energies greater than 0.72 Mev that would be important at times greater than 3 hours after an irradiation.

2) The nuclides were divided into three groups: (1) those with half-lives long compared to the half-lives of the preceding nuclides in their decay chains, (2) those with half-lives short compared to a half-life of a preceding nuclide in their decay chains, and (3) those with half-lives comparable to the half-life of a preceding nuclide in their decay chains.

3) Values of the fission product yields, the effective half-lives, the important gamma rays with energies above 0.72 Mev, and the abundances of these gamma rays were tabulated for each nuclide, and are given in Table B.1. The effective half-life of a nuclide in group 1 or group 3 is defined as the actual half-life of the nuclide; the half-life of a nuclide in group 2 is defined as the half-life of its longest lived parent. The total abundance of the gamma rays is defined as the number emitted with energies greater than 0.72 Mev per hundred disintegrations of the nuclide. Measured values of abundance were not available for all the gamma rays included in Table B.1, and it was therefore necessary to estimate certain values.

Table B.1. Fission products emitting gamma rays of interest in the measurements of δ_{28}.

Fission Product	Yield from U-235 Fission[a]	Yield from U-238 Fission[a]	Group	Effective Half Life[b]	Half Life of Parent Nuclide (Group 3)	Total Abundance[c]	Gamma Ray Energies (Mev)[d]
Kr^{88}	3.6	2.3	1	2.8 h		90	0.85, 1.55, 2.19, 2.40
Rb^{88}	3.6	2.3	2	2.8 h		42	0.90, 1.39, 1.84, 2.11, 2.68
Sr^{91}	5.8	3.7	1	9.7 h		69	0.75, 0.93, 1.02, 1.41
Sr^{92}	6.0	4.2	1	2.6 h		90	1.37
Y^{92}	6.0	4.2	3	3.5 h	2.6 h	20	0.93, 1.44, 1.84
Zr^{95}	6.2	5.7	1	65 d		70[e]	0.72, 0.76
Nb^{95}	6.2	5.7	3	35 d	65 d	99	0.77
Nb^{97m}	5.7	5.7	2	17 h		100	0.75
Ru^{105}	0.9	4.1	1	4.5 h		63[e]	0.72, 0.87, 0.97
I^{132}	4.4	4.4	2	3.2 d		126	0.78, 0.96, 1.16, 1.40, 1.96
I^{134}	7.8	6.4	3	52 m	43 m	100[f]	0.86, 1.07, 1.14, 1.45, 1.62
I^{135}	6.1	5.7	1	6.7 h		132	0.86, 1.04, 1.14, 1.28, 1.46, 1.72, 1.80
Cs^{138}	5.7	6.0	3	32 m	17 m	129	0.87, 1.01, 1.43, 2.21, 2.63
La^{140}	6.4	5.7	2	12.8 d		147	0.75, 0.81, 0.87, 0.92, 1.60, 2.52
La^{142}	6.0	5.1	1	1.4 h		50	0.90, 1.05, 1.43, 1.54, 1.75, 1.92, 2.08, 2.40, 2.57
Pr^{144}	5.6	4.5	2	285 d		1.1	1.49, 2.18

(a) Estimated from curve on page 202 and data on pages 203-208, Nu, Nov., 1960(N. 2). (b) Defined in paragraph 3. (c) Defined in paragraph 3, estimated using data from refs. (N. 1), (N. 2), and (H. 1). (d) Neglecting lower abundance gamma rays. (e) Estimated using only one-half the abundance of 0.72 Mev gamma rays. (f) No data available for estimate of I^{134} abundance.

4) The count rate per nuclide was determined from the equations given below. A similar set of equations is derived in Chapter 15 of reference E. 2.

$$(N\lambda)_{1i} \quad \text{or} \quad (N\lambda)_{2i} = C_i e^{-\lambda_i t}, \tag{B.1}$$

and

$$(N\lambda)_{3i} = D_i e^{-\lambda_i t} + E_i\left(e^{-\lambda_i(p)t} - e^{-\lambda_i t}\right), \tag{B.2}$$

where $(N\lambda)_{1i}$ or $(N\lambda)_{2i}$ is the activity of the i^{th} nuclide in group 1 or group 2, and $(N\lambda)_{3i}$ is the activity of the i^{th} nuclide in group 3. The quantity, λ_i, is the effective decay constant of the i^{th} nuclide, and $\lambda_i(p)$ is the decay constant of the parent of the i^{th} nuclide in group 3. The constants C_i, D_i, and E_i are defined by the equations:

$$C_i = K\beta_i\left(\sum_{j=1}^{n} A_{ij}\right)\left(1 - e^{-\lambda_i T}\right), \tag{B.3}$$

$$D_i = K\beta_i\left(\sum_{j=1}^{n} A_{ij}\right)\left[1 - \frac{\lambda_i}{\lambda_i - \lambda_i(p)}\left(e^{-\lambda_i(p)t} - \frac{\lambda_i(p)}{\lambda_i} e^{-\lambda_i T}\right)\right], \tag{B.4}$$

$$E_i = K\beta_i\left(\sum_{j=1}^{n} A_{ij}\right)\left(1 - e^{-\lambda_i(p)T}\right)\left(\frac{\lambda_i}{\lambda_i - \lambda_i(p)}\right), \tag{B.5}$$

where K is a proportionality constant, β_i is the yield of the i^{th} nuclide, A_{ij} is the abundance of the j^{th} gamma ray with energy above 0.72 Mev emitted by the i^{th} nuclide, and T is the irradiation time. The variation of counting efficiency with energy was not included in the calculation. The photoelectric absorption decreases with increasing gamma-ray energy, but the fraction of the Compton scattered gamma rays absorbed at energies above 0.72 Mev increases with increasing energy. To the first order, these effects balance, and it was thought that a more exact model was not reasonable because the accuracy of the calculation

was limited by the large uncertainties associated with the estimated abundance values. With a value of T equal to 4 hours, a value of K equal to 1, and with U^{235} fission product yields, count rates were calculated from Eqs. B.1 and B.2 and are listed in Table B.2. The value of K was taken as 1 because relative, rather than absolute, count rates were of interest.

5) A decay curve measured for a natural uranium foil which had been irradiated for four hours was compared to the curve obtained from the calculated values given in Table B.2. Although P(t) was measured in the time interval from about 4 to 8 hours after an irradiation, the comparison was made for the time interval from 3 to 1,200 hours after an irradiation. The longer time interval was used to provide a more stringent test of the validity of the model used in the calculation. The results of the comparison are shown in Fig. B.1, and indicate reasonable agreement between the measured and calculated curves. The irregularities in the curves are real and result from the gamma activity of type 3 nuclides.

6) The calculation described in 4) was repeated with values of β_i for U^{238}.

7) The values calculated in 4) were divided by values calculated in 6), to obtain values of P(t) in the time interval from 3 to 10 hours after an irradiation:

$$P(t) = \frac{\sum_{\text{all groups}} N\lambda_i(t) \text{ (with } U^{235} \text{ yields)}}{\sum_{\text{all groups}} N\lambda_i(t) \text{ (with } U^{238} \text{ yields)}} . \qquad \text{(B.6)}$$

The calculated and measured curves of P(t) are compared in Fig. B.2. Both curves indicate that P(t) decreases slightly within the range of interest, and the curves agree within 4.5 per cent. The major uncertainties in the calculation of P(t) are in the values of the fission product yields and in the total abundances of the gamma rays. A value of 10 per cent was estimated for the uncertainty in the calculated values of P(t), so that the 4.5 per cent discrepancy is within the uncertainty limits of the calculation.

Table B.2. Calculated values of the relative nuclide count rates.[a]

Hours After Irradiation	Kr^{88} and Rb^{88}	Sr^{91}	Sr^{92}	Y^{92}	Zr^{95}	Nb^{95}	Nb^{97m}	Ru^{105}	I^{132}	I^{134}	I^{135}	Cs^{138}	La^{140}	La^{142}	Pr^{144}	Total
3	137	85.8	163	54.0	0.78		75.2	16.3	19.0	191	202	28.0		59.0	0.0025	1031
4	110	75.0	125	49.6	0.78		72.0	13.9	18.9	101	181	7.62		35.6	0.0025	790.4
5	85.2	69.8	95.3	45.3	0.78		69.0	11.9	18.8	47.7	163	2.09		21.2	0.0025	630.1
6	65.2	64.6	73.0	42.7	0.78		66.6	10.1	18.7	23.7	147	0.572		12.8	0.0025	525.8
8	40.0	57.9	42.3	31.2	0.78		61.5	7.42	18.5	5.50	119	0.042		4.62	0.0025	388.8
10	24.5	49.4	30.8	23.3	0.78		56.5	5.40	18.3	1.19	99		1.28	1.29	0.0025	311.7
15	7.15	34.9	6.64	10.7	0.78		46.0	2.47	17.8		58.8		1.87	0.078	0.0025	187.2
20	2.04	23.8	1.78	4.87	0.77		37.8	1.14	17.4		35.4		2.55		0.0025	127.5
30	0.18	11.7	0.150	0.81	0.77		25.1	0.235	12.5		12.8		3.23		0.0025	67.5
50		2.81			0.76		11.2		7.82		1.66		4.60		0.0025	28.85
100		0.079			0.74	0.084	1.47		3.19		0.01		6.04		0.0025	11.61
200					0.715	0.148	0.025		0.209				5.88		0.0025	6.98
500					0.627	0.333							3.06		0.0024	4.02
1000					0.501	0.476							0.99		0.0024	1.96
1400					0.420	0.518							0.405		0.0023	1.35

(a) Using U^{235} yield values.

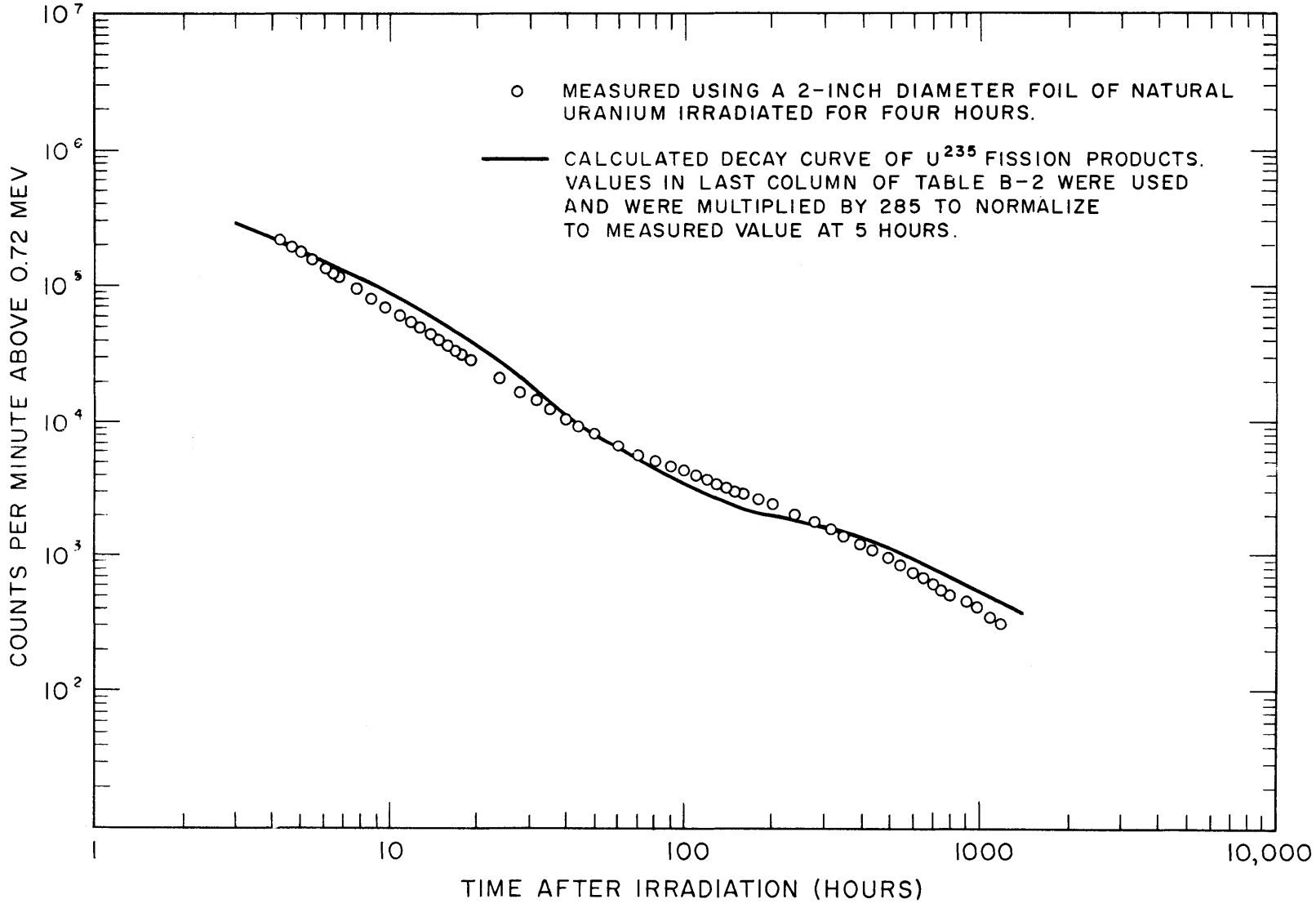

FIG. B-1 INTEGRAL GAMMA RAY DECAY CURVE - MEASURED AND CALCULATED

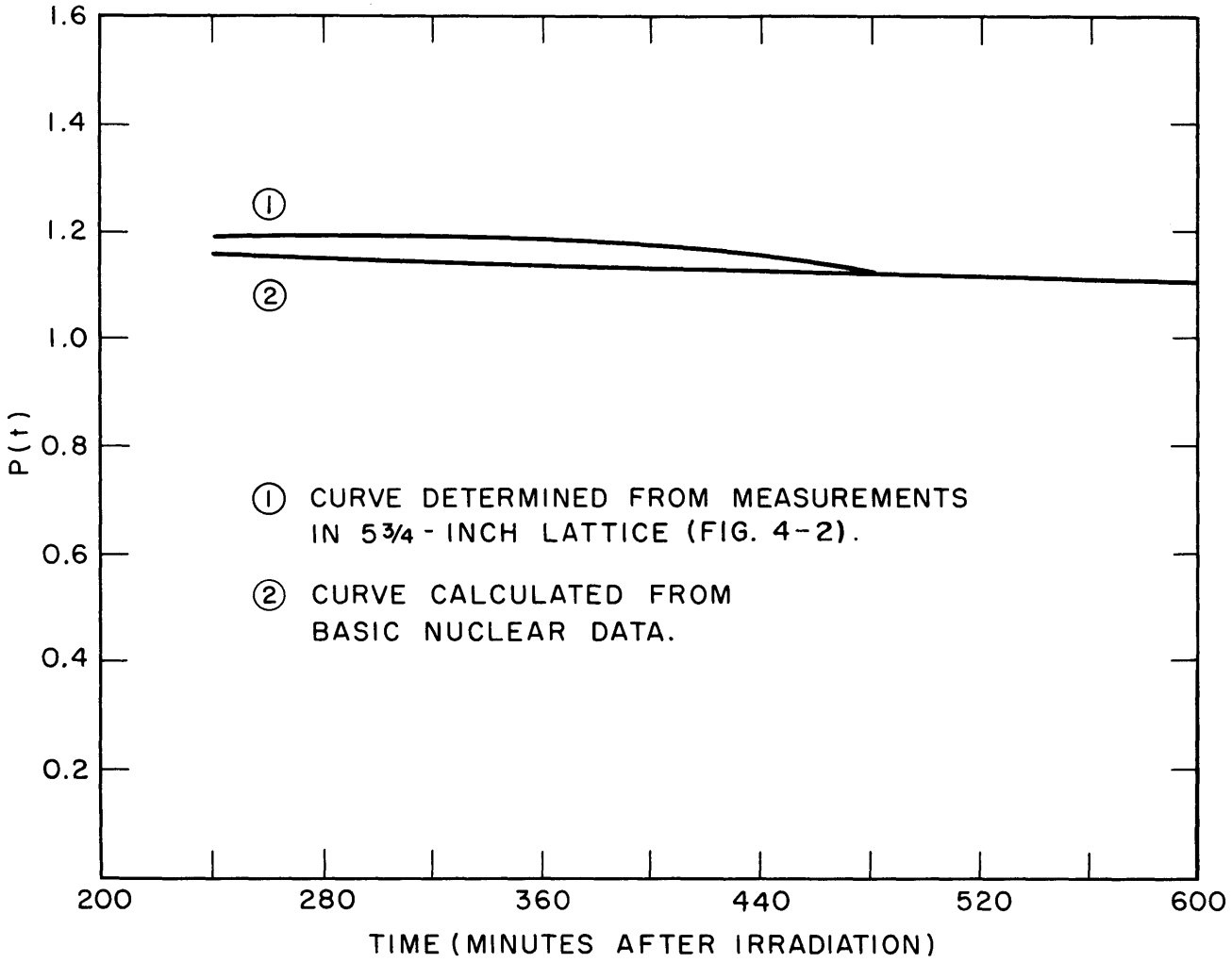

FIG. B-2 P(t) vs TIME. COMPARISON OF MEASURED AND CALCULATED CURVES.

APPENDIX C

DIFFERENCES IN δ_{28} FOR EXPONENTIAL AND INFINITE ASSEMBLIES

The interaction fast effects measured in three D_2O-natural uranium lattices were small (section 4.1.5). The fast fission effect is therefore primarily a single-rod phenomenon. On the basis of this result, an estimate was made of the differences between values of δ_{28} measured in infinite and exponential assemblies similar to the MIT lattices. Consider two idealized cases: (1) a single rod of infinite length, in which the flux is not a function of axial position; (2) a single rod of infinite length, in which the flux is an exponentially varying function of axial position.

Case 1 is similar to the situation that would be observed in an infinite assembly, and case 2 is similar to the situation that would be observed in an exponential assembly.

Consider an experiment in which a uranium foil with the same radius as that of the rod and with thickness t is irradiated, inside the rod, at z = 0. The fission rate of the U^{235} is given by

$$R_f^{25} = At\Sigma_f^{25}\phi(0), \qquad (C.1)$$

where $\phi(0)$ is the average value of the neutron flux in the foil. The fission rate of the U^{238} in the foil depends on the rate at which fast neutrons are produced by fission of U^{235} inside the rod, on the probability that these neutrons will reach the foil at z = 0, and on the fission cross section of U^{238}. We denote by $d^{-|\kappa_f z|}f(z)$ the average probability that a fast neutron born at an axial position z reaches the foil at z = 0. This probability is given a rather complicated expression, as will be seen below, and involves integrations over the areas of the disk and foil and geometrical factors. The fission rate of the U^{238} in the foil may then be written:

$$R_f^{28} = t\Sigma_f^{28} \int_{-\infty}^{\infty} A\Sigma_f^{25}\nu_{25}\phi(z)\, e^{-|\kappa_f z|} f(z)\, dz. \qquad (C.2)$$

An expression for δ_{28} is obtained by dividing Eq. C.2 by Eq. C.1:

$$\delta_{28} = \Sigma_f^{28}\nu_{25} \int_{-\infty}^{\infty} \frac{\phi(z)}{\phi(0)}\, e^{-|\kappa_f z|} f(z)\, dz. \qquad (C.3)$$

This equation neglects those neutrons produced by fission of U^{238}, those that escape into the moderator and are scattered back into the foil, as well as the radial variation of the thermal flux on the rate of fission of U^{238}. The inclusion of these effects would change the absolute values of δ_{28} by a few per cent but would not significantly affect the relative values (in an exponential experiment and an infinite lattice) because the number of neutrons reaching the foil from z would still be very nearly proportional to the average thermal neutron flux at z.

The difference between the expressions for δ_{28} in the two cases arises from the function $\phi(z)$. In the first case (infinitely long rods),

$$\phi_1(z) = \phi(0)\,, \qquad (C.4)$$

throughout the rod. In the exponential assembly,

$$\phi_2(z) = \phi(0)\, e^{-\kappa_t z}, \qquad (C.5)$$

where $1/\kappa_t$ is the relaxation length of the axial flux. Then,

$$(\delta_{28})_1 = \Sigma_f^{28}\nu_{25} \int_{-\infty}^{\infty} e^{-|\kappa_f z|} f(z)\, dz\,, \qquad (C.6)$$

and

$$(\delta_{28})_2 = \Sigma_f^{28}\nu_{25} \int_{-\infty}^{\infty} e^{-\kappa_t z}\, e^{-|\kappa_f t|} f(z)\, dz\,. \qquad (C.7)$$

Now, the relaxation length $1/\kappa_t$ for an exponential assembly is large compared to the mean free path of fast neutrons in the rod. Most of the neutrons reaching the foil are, therefore, born within a few centimeters of the foil, and in this range, the exponential term may be approximated by the linear expression:

$$e^{-\kappa_t z} \approx 1 - \kappa_t z \tag{C.8}$$

Substitution of this expression into Eq. C.7 yields

$$(\delta_{28})_2 \approx \Sigma_f^{28} \nu_{25} \int_{-\infty}^{\infty} (1-\kappa_t z)\, e^{1|\kappa_f z|} f(z)\, dz\,. \tag{C.9}$$

Substituting Eq. C.6 into Eq. C.9,

$$(\delta_{28})_2 \approx (\delta_{28})_1 - \Sigma_f^{28} \nu_{25} \kappa_t \int_{-\infty}^{\infty} z e^{-|\kappa_f z|} f(z)\, dz \tag{C.10}$$

The function, $e^{-|\kappa_f z|} f(z)$, which is discussed below, is a symmetric function so that the integral vanishes and

$$(\delta_{28})_2 \approx (\delta_{28})_1\,. \tag{C.11}$$

The uncertainty in the relation in Eq. C.11 is determined by the error caused by neglecting higher-order terms in Eq. C.8. The next term in the expansion of the exponential can be used to estimate the difference between $(\delta_{28})_2$ and $(\delta_{28})_1$:

$$(\delta_{28})_2 - (\delta_{28})_1 \approx \Sigma_f^{28} \nu_{25} \frac{(\kappa_t)^2}{2} \int_{-\infty}^{\infty} z^2 e^{-|\kappa_f z|} f(z)\, dz\,. \tag{C.12}$$

Equation C.12 suggests that differences between values of δ_{28} for exponential and infinite lattices are small if the quantity κ_t is small. Values of κ_t in the MIT exponential assembly were calculated to be about 0.023 cm^{-1} from axial flux plots measured by Mr. P. Palmedo.[P.1]

The difference between values of $(\delta_{28})_1$ and $(\delta_{28})_2$ was determined by comparing values calculated by using Eqs. C.6 and C.7. Values of $e^{-|\kappa_f z|} f(z)$ were determined by numerical integration of the following equation,

$$e^{-|\kappa_f z|} f(z) = \frac{1}{\pi R^2} \int_0^R 2\pi r\, dr \int_0^R 2r'dr' \int_0^{\pi} \frac{d\theta e^{-|\kappa_f s|}}{4\pi s^2}\,, \tag{C.13}$$

where r is a radial distance on one disk, r′ is a radial distance on the second disk, θ is the angle between r and the projection of r′ on the first disk, and s is the distance between r and r′. The distance s is related to the other quantities:

$$s^2 = z^2 + r^2 + r'^2 - 2rr' \cos \theta . \qquad (C.14)$$

The element of area $r'd\theta dr'$ subtends a solid angle $\frac{r'd\theta dr'}{4\pi s^2} \cos \phi$, where ϕ is the angle between the normal and s. The factor, $\cos \phi$, has been omitted from Eq. C.13. The justification for this omission is that neutrons reaching $r'd\theta dr'$ from r, enter the foil at an angle ϕ and therefore travel a distance $t/\cos \phi$ within the foil if they are not involved in a reaction. If the factor $1/\cos \phi$ is included in the $e^{-|\kappa_f z|} f(z)$ term, it cancels the factor $\cos \phi$. This procedure results in a discrepancy between the definition of $e^{-|\kappa_f z|} f(z)$ and the values used in the calculations of δ_{28}. However, by including this effect, the solution is made more rigorous and the mathematical complexity is reduced. The validity of Eq. C.13 was tested at large values of z and at z equal to zero. For large values of z,

$$e^{-|\kappa_f z|} f(z) \approx \frac{e^{-|\kappa_f z|} R^2}{4z^2} \qquad (\text{for } \frac{z}{R} \gg 1) . \qquad (C.15)$$

It can be seen that Eq. C.13 reduces to Eq. C.15 for large values of z/R, and the values determined by numerical integration of C.12 agree with values determined by using C.15. In the limit z = 0, if the $\cos \phi$ term is included in Eq. C.13, the equation should yield a value of 1/2. This procedure was followed and a limit of 1/2 was obtained. The values obtained by this method therefore appear to be sufficiently accurate for the calculation considered here.

Numerical integration of Eq. C.6 and Eq. C.7, with values of $e^{-|\kappa_f z|} f(z)$ determined by using Eq. C.13, yielded values of $(\delta_{28})_1$ and $(\delta_{28})_2$ which were different by less than 0.5 per cent for parameters typical of the MIT lattices. This difference results in an error of less than 0.01 per cent in the value of k_∞.

The analysis can be extended to lattices in which the interaction fast effect is important.[P.2] Peak has compared the interaction fast effect in an infinite assembly and in an assembly with an exponential axial flux distribution and a J_o radial flux distribution. The rods surrounding the rod of interest were considered as line sources of fast neutrons and the resulting equations were integrated with the aid of an IBM 7090 computer. The difference between values of the interaction fast effect in finite and infinite lattices were shown to be significant if the finite system is small.

APPENDIX D
A COMPUTER PROGRAM FOR REDUCING THE δ_{28} DATA

A Fortran program has been written for reducing the experimental data needed for the determination of δ_{28}. One case requires approximately one minute of IBM 7090 time; if more than one case is submitted to the computer, each additional case requires less than a tenth of a minute. The program can also be used for any problems requiring a least square polynomial fit of no more than eleven coefficients to a set of no more than one hundred data points. A flow diagram (Fig. D. 1) and a listing of the program are included at the end of the appendix.

D.1 DESCRIPTION OF THE CALCULATION

The calculation of F(t) or δ_{28}, from the experimental data, is described below. The relationships between symbols used in this discussion (external symbols) and symbols used in the program (internal symbols) are given in Table D. 1.

1) Values of constants required in the calculation, control constants, values of the count rates of the depleted and natural uranium foils, and the times at which the foils were counted are submitted to the computer. A discussion of the program input is included below.

2) The values of the count rates of the depleted foil, $D(t_D)$, measured at times t_D, and the values of the count rates of the natural foil, $N(t_N)$, measured at times t_N, are corrected for dead time, pulse pileup, and background.

3) A least square polynomial, $N_{LS}(t)$, is determined from the values of $N(t_N)$ by using a least square routine described in the Fortran Manual.[F.3] The program includes options for fitting polynomials to the values of $D(t_D)$, or $D(t_D)$ and $N(t_N)$, but these options are no longer used because a smooth fit to the depleted foil data masks the random variations in the values of F(t) or δ_{28}.

Table D.1. Computer program vocabulary.[a]

External Symbol	Internal Symbol	Classification			Comment
		Input	Internal	Output	
$D(t_D)$	D(I)	*		*	See step 2.
t_D	T(I)	*		*	Input values and values corrected to time after irradiation are given in output.
$N(t_N)$	U(I),ULSQ(I)[b]	*		*	See step 2.
t_N	S(I)	*		*	Input values are given in output.
$N_{LS}(t_D)$	U(I)			*	See step 3.
$\gamma(t_D)$	GAMMA(I)			*	Equation D.1
$F(t_D)$	DDBP(I)			*	Equation D.2
$P(t_D)$	PP(I)	*			See step 6.
$\sigma(F(t_D))$	SDDBP(I)			*	Equation D.4
$\sigma(\gamma(t_D))$	SIGG(I)		*		Equation D.5
$PP(t_N)$			*		Equation D.10
$PP(t_D)$	PPUC(I)		*		Equation D.6
$(N_{LS})RMS$	SIGMAU			*	Equation D.7
$\partial N_{LS}(t_D)/\partial t$	PDRT(I)		*		See step 7.
$\sigma(\delta_{28})$	SDEL(I)			*	See step 8.
$\sigma(P(t))$	PPE(I)	*			See step 8.
$F_{LS}(t_D)$	DLSQ(I)			*	See step 9.
$\delta_{28_{LS}}(t_D)$	DLSQ(I)			*	See step 9.
σ_{RMS}	SIGMA			*	See step 10.
NCASE	NCASE	*			Card 1

(a) Includes quantities mentioned in the discussion.
(b) Values originally stored in U(I) are transferred to ULSQ(I).

Table D.1. Computer program vocabulary (continued).

External Symbol	Internal Symbol	Classification			Comment
		Input	Internal	Output	
M	M	*		*	Card 2
N	N	*		*	Card 2
L	L	*		*	Card 2
a	C	*		*	Card 2
S	E	*		*	Card 2
BD	BD	*		*	Card 2
BU	BU	*		*	Card 2
TAU	TAU	*		*	Card 2
TS	TS	*			Card 3
EC	EC	*		*	Card 3
PPU	PPU	*		*	Card 3
AB	AB	*			Card 3
DLD	DLD	*			Card 3
DELT	DELT	*			Card 3
PD	PD	*			Card 3
PE	PE	*			Card 3
σ_T	SIGT	*		*	Card 3; step 7.
NN	NN	*			Card 4
MN	MN	*			Card 4
MMN	MMN	*			Card 4
MM	MM	*			Card 4
KK	KK	*			Card 4
KL	KL	*			Card 4
σ_P	SIG	*		*	Card 4; step 7.
TD	TD	*		*	Card 4; step 4.
TN	TN	*		*	Card 4; step 4.
TP	TP	*			Card 4
DT	DT	*			Card 4

4) Values of $\gamma(t)$, the ratio of the count rate of the depleted foil to the count rate of the natural foil, are calculated at times t_D, the times of the depleted foil measurements. The equation used to calculate $\gamma(t_D)$ is:

$$\gamma(t_D) = \frac{TN}{TD} \frac{D(t_D)}{N_{LS}(t_D)}, \qquad (D.1)$$

where $N_{LS}(t_D)$ are the least square values of $N_{LS}(t)$ calculated at times t_D, TD is the time interval for the depleted foil counts, and TN is the time interval for the natural foil counts. The quantity, $\gamma(t)$, is discussed in section 3.2.

5) Values of F(t) are calculated at times t_D by using the following equation:

$$F(t_D) = \frac{(EC)\cdot(a)\cdot(\gamma(t_D)) - S}{1 - a\gamma(t_D)} . \qquad (D.2)$$

Equation D.2 is similar to Eq. 3.2.15, with one exception: the correction for differences in foil weights, and for the position at which the foils are counted are included in the quantity, a.

$$a = \frac{1 + R_D}{1 + R_N} \cdot \frac{W_N}{W_D} \cdot (\text{position factor}), \qquad (D.3)$$

where R_D is the ratio of the atom densities of U^{235} and U^{238} in the depleted uranium, R_N is the corresponding ratio for the natural uranium, and the W's are the foil weights. In the MIT cases, the value of $1+R_D/1+R_N$ was 0.992. The "position factor" is the normalization required to correct the foil activities for differences due to irradiations in positions of differing flux. The position factor for most of the MIT measurements was unity because the foils were usually irradiated at adjacent positions within a fuel rod. The change in flux between foils irradiated in adjacent positions was shown in section 4.2.2 to be negligible. The enrichment correction, EC, is defined in Eq. D.9 and is equal to unity for measurements in fuel rods of natural uranium. The factor, S, was defined in section 3.2 as R_D/R_N.

6) Values of δ_{28} are calculated by multiplying values of $F(t_D)$ by appropriate values of $P(t)$, if values of $P(t_D)$, or coefficients of a polynomial equation for $P(t)$ are submitted as input data.

7) The uncertainties in the values of $F(t_D)$ are calculated from the equation:

$$\sigma(F(t_D)) = \left(\frac{a}{1 - a\gamma(t_D)}\right) (EC + F(t_D))\, \sigma(\gamma(t_D)), \qquad (D.4)$$

where $\sigma(X)$ is the uncertainty in X. Equation D.4 was derived by differentiation of Eq. D.2. The values of $\sigma(\gamma(t_D))$ are calculated from the following equation:

$$\left(\frac{\sigma(\gamma(t_D))}{\gamma(t_D)}\right)^2 = \left(\frac{(N_{LS})_{RMS}}{N_{LS}(t_D)}\right)^2 + \frac{1}{D(t_D)} + \left(\frac{\partial N_{LS}(t_D)}{\partial t} \frac{\sigma_T}{N_{LS}(t_D)}\right)^2 + \left(\frac{PP(t_D) \cdot \sigma_P}{N_{LS}(t_D)}\right)^2 . \qquad (D.5)$$

The first term on the right side of Eq. D.5 is the square of the fractional uncertainty in the calculated value of the count rate of the natural foil; the second term is the square of the fractional uncertainty of the count rate of the depleted foil; the third term is the square of the fractional uncertainty in $\gamma(t_D)$ due to σ_T, the uncertainty in the time after irradiation; and the last term is the square of the uncertainty in the natural foil activity owing to σ_P, the fractional uncertainty in $PP(t_D)$, the pulse pileup correction. Equation D.10 is used to calculate values of $PP(t_N)$, and values of $PP(t_D)$, and values of $PP(t_D)$ are calculated from an equation derived from Eq. D.10:

$$PP(t_D) = [N(t_D)]_{\substack{\text{uncorrected} \\ \text{for pileup}}} - [N_{LS}(t_D)]$$

$$= -\frac{TN}{2 \times PPU} + \sqrt{\frac{(TN)^2}{4(PPU)^2} + \frac{TN \times N_{LS}(t_D)}{PPU}} - N_{LS}(t_D), \qquad (D.6)$$

where PPU is the pulse pileup factor which is discussed below. The term $(N_{LS})_{RMS}$, which appears in Eq. D.5, is calculated from the following equation:

$$(N_{LS})_{RMS} = \frac{\sum_{I=1}^{L} (N_{LS}(t_N) - N(t_D))_I^2}{L - (M+1)}, \qquad (D.7)$$

where L is the number of data points for the natural foil, and (M+1) is the number of coefficients of the least square polynomial fitted to the natural foil count rates. The calculation of $\partial N_{LS}(t_D)/\partial t$ is straightforward; the derivative of the least square polynomial is evaluated at times, t_D.

The uncertainties in the values of δ_{28} are calculated if the values of δ_{28} have been calculated, and if values for the uncertainty in P(t) are submitted. The uncertainty in P(t) can also be written in the form of a polynomial equation. The equation used to calculate the uncertainty in the value of δ_{28} is:

$$\left(\frac{\sigma(\delta_{28})}{\delta_{28}}\right)^2 = \left(\frac{\sigma(F(t))}{F(t)}\right)^2 + \left(\frac{\sigma(P(t))}{P(t)}\right)^2 . \qquad (D.8)$$

9) A least square polynomial is fitted to either the calculated values of F(t) or δ_{28}, and values of $F_{LS}(t_D)$ or $\delta_{28_{LS}}(t_D)$ are determined.

10) The quantity, σ_{RMS}, which is the RMS error of the least square polynomial calculated in step 9, is determined.

11) The program prints the output quantities, and either proceeds to the next problem or is terminated.

D.2 INPUT INSTRUCTIONS

Card 1 (Format, I3). NCASE, the number of problems, is included on this card. The maximum number of problems that can be submitted is 999; however, in practice, the largest number ever submitted at one time was 19.

Card 2 (Format, 3I3, 5E11.5). The quantities included on this card, in order, are:

M, the number of coefficients minus one for the least square polynomial that is to be fitted to the natural foil count rates; the maximum

value is 10 or L - 2, whichever is smaller. The limit of L - 2 avoids an overflow from Eq. D.6. The calculation of values of F(t) and δ_{28} is insensitive to values of M, so arbitrary rules were used to select values. For values of L greater than 15, a value of M equal to 4 was used. For L between 8 and 14, M was set equal to 3, and a value of 2 was used for problems in which L was less than 8.

N, the number of data points for the depleted foil; the maximum number is 100.

L, the number of data points for the natural foil; maximum number is 100.

a, the factor defined in procedure 5; the internal symbol for a is C.

S, the factor defined in procedure 5; the internal symbol for S is E, and the value of S used in the calculations was 0.00247.

BD, the depleted foil background in counts per time interval, TD.

BU, the natural foil background in counts per time interval, TN.

TAU, the dead time of the counting system in seconds. A value of 5.0×10^{-6} seconds was measured for TAU and was used in the calculations.

Card 3 (Format 3E10.4, 6E7.1). The quantities included on this card, in order, are:

TS, the time which must be added to the times submitted for the depleted and natural foil counts to correct the data to time after irradiation. In all cases, time values were submitted in minutes, and therefore TS was always submitted in minutes.

EC, the enrichment factor, is defined by the following equation:

$$EC = \frac{N_2^{25}}{N_3^{25}} \frac{1 + R_2}{1 + R_3} \approx \frac{N_2^{25}}{N_3^{25}} . \qquad (D.9)$$

This equation is derived from Eq. 3.2.15, and the symbols are defined in section 3.2. For measurements in natural uranium rods, EC equals unity. The ratio, N_2^{25}/N_3^{25}, is the U^{235} concentration of natural uranium

divided by the U^{235} concentration of the fuel.

PPU, the pulse pileup factor in seconds (see section 4.1.2). This quantity is defined by Eq. 4.1.4. The pulse pileup correction is made as follows:

$$N(t_N) = N(t_N) - PP(t_N) = N(t_N) - \frac{PPU}{TN}[N(t_N)]^2. \qquad (D.10)$$

A similar equation is used to correct the depleted foil data for pulse pileup. To avoid an overflow in the error analysis, a value of PPU greater than zero must be supplied.

AB, an instruction which controls the printout of quantities related to the least square curves; AB is normally greater than zero.

DLD, a print instruction which is normally zero. A positive value of DLD requests values of $D_{LS}(t_D)$, but a LS fit to the depleted foil data is not normally used.

DELT, a control instruction. If DELT is zero, only values of F(t) are calculated. If DELT is positive, δ_{28} is calculated using submitted values of P(t). If DELT is negative, δ_{28} is calculated using submitted coefficients of a polynomial equation used to determine values of P(t) (see flow diagram).

PD, a control instruction which is normally negative. A zero value of PD avoids the least square option for the values of F(t) or δ_{28}; this is useful if the code is only being used to fit a polynomial to data points (see flow diagram).

PE, a control instruction which determines whether the uncertainty in P(t) is to be included in the calculation (see flow diagram). The same convention is used for PE as was used for DELT.

σ_T, the uncertainty in the time after irradiation at which counting began; the internal symbol for σ_T is SIGT. In all cases, time values were submitted in minutes and therefore σ_T was always submitted in minutes. This quantity is discussed in step 7.

Card 4 (Format 6I3, 5E9.3). The quantities included on this card, in order, are:

NN, a control instruction (see flow diagram). If NN is negative, a least square polynomial is determined for the F(t) data, and if

NN is positive, a least square polynomial is determined for the δ_{28} data.

MN, the number of coefficients of the polynomial used to determine values of P(t). Even if P(t) is not used in the calculation, a value for MN must be included on Card 4. The maximum number for MN is 10.

MMN, the number of coefficients of the polynomial used to determine values of the uncertainty in P(t). Even if the uncertainty in P(t) is not used in the calculation, a value for MMN must be included on Card 4. The maximum number for MMN is 10.

MM, the number of coefficients minus one for the least square polynomial of F(t) or δ_{28}. The maximum number is 10 or N - 2, whichever is smaller. A choice of MM equal to 2 was usually used, because the function F(t) is slowly varying and the values of δ_{28} should be essentially constant, making a higher-order polynomial unnecessary.

KK, a control instruction which is always 1 for the first problem (see flow diagram). If it is desired to use the values of $D(t_D)$ and $N(t_N)$, corrected for background, dead time, and pulse pileup in the next problem, a value of 2 is submitted for KK in the next problem.

KL, a control instruction which is normally 2. The value of 2 requires the code to fit a least square polynomial to the natural foil data. If KL is 1, the code will calculate a least square polynomial for the depleted foil data (see flow diagram).

σ_P, the fractional uncertainty in the pulse pileup factor, PPU. A value of 0.1 was used in the calculations (section 4.1.2). The internal symbol for σ_P is SIG.

TD, the counting time for the depleted foil observations in seconds.

TN, the counting time for the natural foil observations in seconds.

TP, the time correction used to normalize the functions, P(t) and $\sigma(P(t))$, to the reference time used in the calculations.

DT, a control instruction which is normally zero (see flow diagram). If DT is unequal to zero, least square polynomials are fitted to the depleted and the natural foil data. If this option is used, KL must equal 1.

Card 5 (Format 6E12.6). The first, third, and fifth numbers are the times of the first three depleted foil observations. The time can be submitted for an arbitrary zero time, and are corrected to times after irradiation in the code by addition of the value TS. The second, fourth, and sixth numbers are the number of counts in the time interval TD for the first three depleted foil observations.

Similar cards are submitted to include all the depleted foil data. A new card is started for the natural foil data. The number of natural foil counts are for the time interval TN. If values of P(t) or coefficients of a polynomial for P(t) are to be included, they follow the natural foil data using the same format. If values or coefficients for the uncertainty in P(t) are to be included, they follow the P(t) data, again using the same format.

Cards for the second problem follow the cards from the first problem. Cards similar to 2, 3, and 4 must be included with each problem. A sample problem is included at the end of the program listing.

D.3 OUTPUT FORMAT

The flow diagram and listing of the program show several output options. The input quantities suggested in the preceding discussion will insure an output format which includes all information of interest; therefore, the discussion will be limited to this format.

The output includes the problem title, the date, and the time at which the calculation begins. The following information is then included for each problem:

1) A table of the input values of the depleted (DEP) and natural (NAT) foil count rates, and times at which the counts were made. The time values in this table have not been corrected to the time after irradiation.

2) The input values of M, N, L, a, S, BD, BU, TAU, PPU, SIG, SIGT, EC, TD, and TN.

3) Values of V(O) through V(M), S(O) through S(2M), and A(O) through A(M). The A's are the least square coefficients of the

polynomial fitted to the natural foil data. The V's and S's are quantities used to calculate the A's. The uncorrected time values are used with these coefficients.

4) A table which includes values of t_D, the times at which the depleted foil was counted, corrected to time after irradiation (TIME); the depleted foil count rates, corrected for background, pileup, and dead time (DEP FOIL); the least square values of the corrected natural foil count rates calculated at times t_D (NAT FOIL); values of $\gamma(t)$ (GAMMA); values of F(t) (DEL/P);[a] the uncertainties of the values of F(t) (SIG D/P); and values of δ_{28} (DELTA) and the uncertainties in the values of δ_{28} (SIG DEL), if these quantities are calculated.

5) The root mean square error of the natural foil least square polynomial (SIG NAT).

6) Value of V's, S's, and A's for the F(t) or δ_{28} least square polynomial. The corrected time values are used with these coefficients.

7) A table which includes the least square values of F(t) (DEL/P(LS)) or δ_{28} (DEL(LS)); the values of the root mean square error of the least square polynomial divided by the least square values of F(t) or δ_{28} (1ST. FRAC. ER.); and the uncertainty values of F(t) or δ_{28} from the previous table divided by values of F(t) or δ_{28} (2ND. FRAC. ER.).

8) The root mean square error of the F(t) or δ_{28} least square polynomial (SIGMA).

---

[a] The notation DEL/P is used because F(t) equals $\delta_{28}/P(t)$.

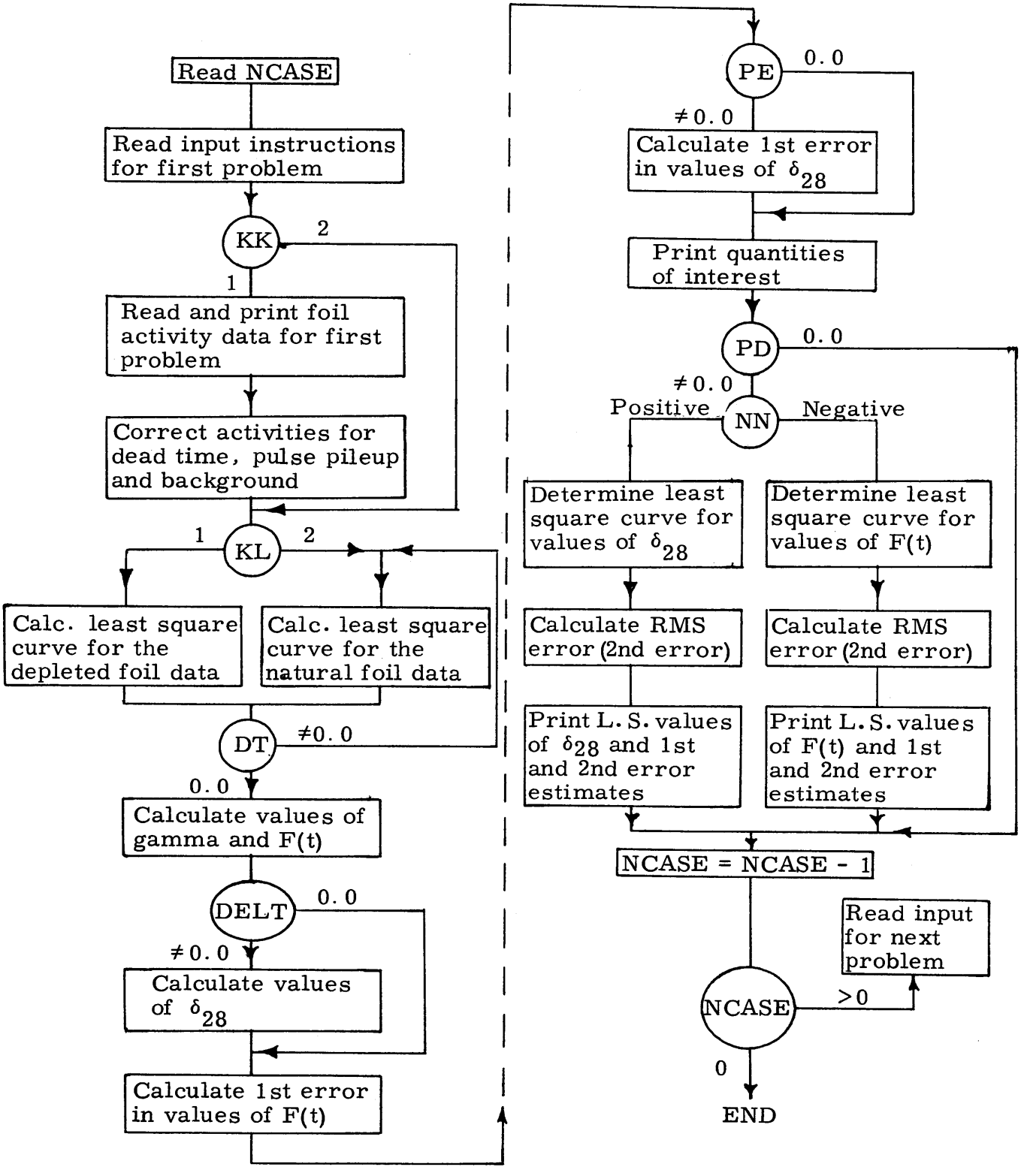

Fig. D.1. Flow Diagram for Computer Program.

TABLE D.2

FORTRAN LISTING OF COMPUTER PROGRAM

```
C          A CODE FOR REDUCING DEPLETED AND NATURAL URANIUM
C          FOIL DATA FROM FAST FISSION EXPERIMENTS
      NIT=4
      NOT=2
      WRITE OUTPUT TAPE NOT,1
    1 FORMAT (30H JOHN R. WOLBERG PROBLEM M1291)
      WRITE OUTPUT TAPE NOT,2
    2 FORMAT (82H REDUCTION OF DEPLETED AND NATURAL
     URANIUM FOIL DATA FROM FAST FISSION EXPERIMENTS)
      WRITE OUTPUT TAPE NOT,4
    4 FORMAT    (32H AT THE BEGINNING OF THE PROBLEM)
      CALL CLOCK (NOT)
      DIMENSION T(100), D(100), SUM(21), V(11), S(100), U(100),PPUC(100)
      DIMENSION DDBP(100), PP(100), SUMRS(100), DEL(100), SDDBP(100)
      DIMENSION PDRT(100), SIGGS(100), A(11), B(11,12), DLSQ(100)
      DIMENSION GAMMA(100),SIGG(100),PPE(100),SDEL(100),AA(11),AAA(11)
      DIMENSION DDT(100), DLLSQ(100), ULSQ(100),AU(11),TDT(100),SDT(100)
      READ INPUT TAPE NIT,5,NCASE
    5 FORMAT (I3)
    8 READINPUTTAPE NIT,9,M,N,L,C,E,BD,BU,TAU
    9 FORMAT  (3I3,5E11.5)
      READ INPUT TAPE NIT,10,TS,EC,PPU,AB,DLD,DELT,PD,PE,SIGT
   10 FORMAT (3E10.4,6E7.1)
      READ INPUT TAPE NIT,11,NN,MN,MMN,MM,KK,KL,SIG,TD,TN,TP,DT
   11 FORMAT (6I3,5E9.3)
      GO TO (12,26,203,270),KK
   12 READ INPUT TAPE NIT,50, (T(I),D(I), I=1,N)
      READ INPUT TAPE NIT, 50, (S(I), U(I), I=1,L)
      WRITE OUTPUT TAPE NOT ,13
   13 FORMAT(49H1    TIME              DEP          TIME          NAT)
      IF (N-L) 14,17,18
   14 WRITE OUTPUT TAPE NOT,15,(T(I),D(I),S(I),U(I),I=1,N)
   15 FORMAT (1H ,1P4E14.5)
      NNN=N+1
      WRITE OUTPUT TAPE NOT,16,(S(I),U(I),I=NNN,L)
   16 FORMAT (29H                                ,1P2E14.5)
      GO TO 20
   17 WRITE OUTPUT TAPE NOT,15,(T(I),D(I),S(I),U(I),I=1,N)
      GO TO 20
   18 WRITE OUTPUT TAPE NOT,15,(T(I),D(I),S(I),U(I),I=1,L)
      NNN=L+1
      WRITE OUTPUT TAPE NOT,19,(T(I),D(I),I=NNN,N)
   19 FORMAT (1H ,1P2E14.5)
```

```
20   PPU=PPU/TD
     DO 21 I=1,N
     D(I)=D(I)/(1.-TAU*(D(I)/TD))
     D(I)=D(I)-(PPU*(D(I)**2))
21   D(I)=D(I)-BD
     PPU=PPU*TD
     PPU=PPU/TN
     DO 22 I=1,L
     U(I)=U(I)/(1.-TAU*(U(I)/TN))
     U(I)=U(I)-(PPU*(U(I)**2))
22   U(I)=U(I)-BU
     PPU=PPU*TN
26   TT=0.0
     TTT=0.0
     LLN=L
     NLL=N
27   LS=2*M+1
     LB=M+2
     LV=M+1
     IF (TT) 29,29,33
29   WRITE OUTPUT TAPE NOT, 30
30   FORMAT(108H1   M   N   L   C                S                DEP BKRD
       NAT BKRD      DEAD TIME      PPU          FRAC ER PPU)
     WRITE OUTPUT TAPE NOT,31,M,N,L,C,E,BD,BU,TAU,PPU,SIG
31   FORMAT (1H ,3I3,1P7E14.5)
     WRITE OUTPUT TAPE NOT,32
32   FORMAT (1H /54H      TIME           ENRICH COR      DEP TIME
       NAT TIME)
     WRITE OUTPUT TAPE NOT,329,SIGT,EC,TD,TN
     GO TO (33,111),KL
33   DO 34 J=2,LS
34   SUM(J)=0.0
     SUM(1)=N
     DO 35 J=1,LV
35   V(J)=0.0
     DO45I=1,N
     P=1.0
     V(1)=V(1)+D(I)
     DO40 J=2,LV
     P=T(I)*P
     SUM(J)=SUM(J)+P
40   V(J)=V(J)+D(I)*P
     DO 45 J=LB,LS
     P=T(I)*P
45   SUM(J)=SUM(J)+P
47   WRITE OUTPUT TAPE NOT, 48
48   FORMAT (1H /40H THE FOLLOWING ARE VALUES V(0) THRU V(M))
     WRITE OUTPUT TAPE NOT, 56,(V(I),I=1,LV)
50   FORMAT (6E12.6)
     WRITE OUTPUT TAPE NOT,55
```

```
 55   FORMAT(1H /41H THE FOLLOWING ARE VALUES S(0) THRU S(2M))
      WRITE OUTPUT TAPE NOT, 56, (SUM(I), I=1, LS)
 56   FORMAT (1H , 1P8E14.4)
 60   DO 65 I=1, LV
      DO 65 K=1, LV
      J=K+I
 65   B(K, I)=SUM(J-1)
      DO 70 K=1, LV
 70   B(K, LB)=V(K)
      DO 85 LL=1, LV
      DIVB=B(LL, LL)
      DO 75 J=LL, LB
 75   B(LL, J)=B(LL, J)/DIVB
      I1=LL+1
      IF (I1-LB) 80, 90, 90
 80   DO 85 I=I1, LV
      FMULTB = B(I, LL)
      DO 85 J=LL, LB
 85   B(I, J)=B(I, J)-B(LL, J)*FMULTB
 90   A(LV)=B(LV, LB)
      I=LV
 95   SIGMA = 0.0
      DO 98 J=I, LV
 98   SIGMA =SIGMA + B(I-1, J)*A(J)
      I=I-1
      A(I)=B(I, LB)-SIGMA
      IF (I-1) 100, 100, 95
100   IF (AB) 113, 113, 105
105   WRITE OUTPUT TAPE NOT, 110
110   FORMAT(1H /40H THE FOLLOWING ARE VALUES A(0) THRU A(M))
      WRITE OUTPUT TAPE NOT, 56, (A(I), I=1, LV)
      GO TO113
111   DO 112 I=1, N
112   DLSQ(I)=D(I)
      GO TO 126
113   GO TO (119, 114), KL
114   IF (TT) 115, 115, 119
115   DO 117 I=1, NNN
      S(I)=TDT(I)
      DLLSQ(I)=DLSQ(I)
      DLSQ(I)=A(1)
      P=1.0
      DO 117 J=1, M
      P=S(I)*P
117   DLSQ(I)=DLSQ(I)+P*A(J+1)
      GO TO 130
119   DO 120 I=1, L
      DLSQ(I)=A(1)
      P=1.0
      DO 120 J=1, M
```

```
      P=S(I)*P
120   DLSQ(I)=DLSQ(I)+P*A(J+1)
      IF (TT) 124,124,122
122   DO 123 I=1,L
123   SUMRS (I)=DLSQ(I)
      GO TO 191
124   IF (DT) 125,139,125
125   IF (TTT) 126,126,130
126   DO 127 I=1,N
      TDT(I)=T(I)
127   DDT(I)=D(I)
      DO 128 I=1,L
      D(I)=U(I)
      SDT(I)=S(I)
      T(I)=S(I)
128   DLLSQ(I)=DLSQ(I)
      NNN=N
      N=L
      TTT=1.0
      DO 129 I=1,LV
129   DEL(I)=A(I)
      GO TO 33
130   DO 131 I=1,L
      ULSQ(I)=U(I)
      U(I)=DLSQ(I)
131   DLSQ(I)=DLLSQ(I)
      N=NNN
      DO 132 I=1,N
      T(I)=TDT(I)
132   D(I)=DDT(I)
      DO 133 I=1,LV
      AU(I)=A(I)
133   A(I)=DEL(I)
      GO TO (139,134),KL
134   IF (N-L) 137,139,135
135   J=L+1
      DO 136 I=J,N
      U(I)=DLSQ(I)
136   DLSQ(I)=DLLSQ(I)
137   L=N
139   P=TN/TD
      DO 140 I=1,L
140   GAMMA(I)=P*DLSQ(I)/U(I)
155   DO 160 I=1,L
160   DDBP(I)=(EC*C*GAMMA(I)-E)/(1.-C*GAMMA(I))
171   GO TO (175,172),KL
172   SIGMAU=0.0
      DO174 I=1,LLN
      P=1.0
      SUMRS(I)=AU(1)
```

```
      DO 173 J=1,M
      P=SDT(I)*P
173   SUMRS(I)=SUMRS(I)+P*AU(J+1)
      SUMRS(I)=(SUMRS(I)-ULSQ(I))**2
174   SIGMAU=SIGMAU+SUMRS(I)
      GO TO 196
175   DO180I=1,N
      P=1.0
      SUMRS(I)=A(1)
      DO 180 J=1,M
      P=T(I)*P
180   SUMRS(I)=SUMRS(I)+P*A(J+1)
      IF (DLD) 191,191,185
185   WRITE OUTPUT TAPE NOT,190
190   FORMAT(1H /79H LEAST SQUARE VALUES OF DEPLETED FOIL
        ACTIVITIES AT TIMES OF DEPL. OBSERVATIONS)
      WRITE OUTPUT TAPE NOT,56,(T(I),SUMRS(I),I=1,N)
191   SIGMA=0.0
      DO 192 I=1,N
      SUMRS(I)=(SUMRS(I)-D(I))**2
192   SIGMA=SIGMA+SUMRS(I)
      Z=FLOATF (N-LV)
      SIGMA = SQRTF(SIGMA/Z)
      IF (TT) 193,193,201
193   IF (DT) 194,203,194
194   SIGMAU=0.0
      DO 195 I=1,L
      SUMRS(I)=(U(I)-ULSQ(I))**2
195   SIGMAU=SIGMAU+SUMRS(I)
196   Z=FLOATF (L-LV)
      SIGMAU=SQRTF(SIGMAU/Z)
      GO TO 203
201   IF (NN) 332,203,325
203   IF (DELT) 204,213,208
204   READ INPUT TAPE NIT,50,(AA(I),I=1,MN)
      DO 205 I=1,L
      PP(I)=AA(1)
      P=1.0
      DO 205 J=1,MN
      P=(S(I)+TP)*P
205   PP(I)=PP(I)+P*AA(J+1)
      GO TO 209
208   READ INPUT TAPE NIT ,50, (PP(I),I=1,L)
209   DO 210 I=1,L
210   DEL(I)=PP(I)*DDBP(I)
213   GO TO (224,214,),KL
214   PPU=PPU/TN
      DO 215 I=1,N
      PPUC(I)=(0.25/(PPU**2))+U(I)/PPU
      PPUC(I)=SQRTF(PPUC(I))
```

```
      PPUC(I)=PPUC(I)-(0.5/PPU)-U(I)
215   SIGGS(I)=((1.0/DLSQ(I))+(SIGMAU/U(I))**2+((PPUC(I)*SIG)/U(I))**2)*
        (GAMMA(I)**2)
      IF (SIGT) 234,234,216
216   DO 218 I=1,N
      PDRT(I)=AU(2)
      P=1.0
      DO 217 K=2,M
      AK=K
      P=T(I)*P
217   PDRT(I)=PDRT(I)+AK*AU(K+1)*P
      SIGGS(I)=SIGGS(I)+(((PDRT(I)*SIGT)/U(I)*GAMMA(I))**2
      SIGG(I)=SQRTF(SIGGS(I))
218   SDDBP(I)=(C/(1.-C*GAMMA(I)))*(EC+DDBP(I))*SIGG(I)
      GO TO 270
224   IF (DT) 225,228,225
225   DO 226 I=1,L
226   SIGGS(I)=((SIGMA/DLSQ(I))**2+(SIGMAU/U(I))**2+SIG)*(GAMMA(I)**2)
      GO TO 233
228   DO 229 I=1,L
229   SIGGS(I)=((SIGMA/DLSQ(I))**2+1.0/U(I)+SIG)*(GAMMA(I)**2)
233   IF(SIGT) 234,234,255
234   DO235 I=1,L
      SIGG(I)=SQRTF(SIGGS(I))
235   SDDBP(I)=(C/(1.-C*GAMMA(I)))*(1.+DDBP(I))*SIGG(I)
      GO TO 270
255   DO 265 I=1,L
      PDRT(I)=A(2)
      P=1.0
      DO 260 K=2,M
      AK=K
      P=S(I)*P
260   PDRT(I)=PDRT(I)+AK*A(K+1)*P
      SIGGS(I)=SIGGS(I)+((PDRT(I)*SIGT)/U(I))**2
      SIGG(I)=SQRTF(SIGGS(I))
265   SDDBP(I)=(C/(1.-C*GAMMA(I)))*(1.+DDBP(I))*SIGG(I)
270   IF(PE) 271,276,273
271   READ INPUT TAPE NIT,50,(AAA(I),I=1,MMN)
      DO 272 I=1,L
      PPE(I)=AAA(1)
      P=1.0
      DO 272J=1,MMN
      P=(S(I)+TP)*P
272   PPE(I)=PPE(I)+P*AAA(J+1)
      GO TO 274
273   READ INPUT TAPE NIT,50, (PPE(I), I=1,L)
274   DO 275 I=1,L
      SDEL(I) =((SDDBP(I)/DDBP(I))**2)+((PPE(I)/PP(I))**2)
      SDEL(I) =(SDEL(I))*((DEL(I))**2)
275   SDEL(I)=SQRTF (SDEL(I))
```

```
276   IF (TS) 280, 280, 277
277   DO 278 I=1, L
278   S(I)=S(I)+TS
      DO 279 I=1, N
279   T(I)=T(I)+TS
      IF (AB) 281, 280, 281
280   WRITE OUTPUT TAPE NOT, 110
      WRITE OUTPUT TAPE NOT, 56, (A(I), I=1, LV)
281   IF (DELT) 284, 299, 284
284   IF (PE) 296, 285, 296
285   WRITE OUTPUT TAPE NOT, 290
290   FORMAT (1H /107H   TIME        DEP FOIL      NAT FOIL      GAMMA
           DEL/P       SIG D/P      P           DELTA)
      WRITE OUTPUT TAPE NOT, 298, (S(I), DLSQ(I), U(I), GAMMA(I),
        DDBP(I), SDDBP(I), PP(I), DEL(I), I=1, L)
295   FORMAT (1H, 1P7E14.5)
      GO TO 306
296   WRITE OUTPUT TAPE NOT, 297
297   FORMAT(1H /109   TIME        DEP FOIL      NAT FOIL      GAMMA
            DEL/P       SIG D/P      DELTA       SIG DEL)
      WRITE OUTPUT TAPE NOT, 298, (S(I), DLSQ(I), U(I), GAMMA(I), DDBP(I),
        SDDBP(I), DEL(I), SDEL(I), I=1, L)
298   FORMAT (1H , 1P8E14.5)
      GO TO 306
299   WRITE OUTPUT TAPE NOT, 300
300   FORMAT(1H /81H   TIME        DEP FOIL      NAT FOIL      GAMMA
            DEL/P       SIG D/P)
      WRITE OUTPUT TAPE NOT, 305, (S(I), DLSQ(I), U(I), GAMMA(I), DDBP(I)
        SDDBP(I), I=1, L)
305   FORMAT (1H , 1P6E14.5)
306   IF (DT) 307, 313, 307
307   WRITE OUTPUT TAPE NOT, 308
308   FORMAT (1H /25H   SIG DEP      SIG NAT)
      WRITE OUTPUT TAPE NOT, 309, SIGMA; SIGMAU
309   FORMAT(1H , 1P2E14.5)
      IF (DT) 319, 319, 310
310   WRITE OUTPUT TAPE NOT, 311
311   FORMAT(1H /93H   TIME        NAT FOIL     NAT FOIL(LS)
           DEP FOIL(LS)  GAMMA        SIG GAMMA    P/DEL)
      DO 312 I=1, L
312   PDRT(I)=1.0/DDBP(I)
      WRITE OUTPUT TAPE NOT, 295, (S(I), ULSQ(I), U(I), DLSQ(I), GAMMA(I),
        SIGG(I), PDRT(I), I=1, L)
      GO TO 319
313   GO TO (314, 317), KL
314   WRITE OUTPUT TAPE NOT, 315
315   FORMAT(1H /11H      SIG DEP)
      WRITE OUTPUT TAPE NOT, 316, SIGMA
316   FORMAT(1H , 1P1E14.5)
      GO TO 319
```

```
317   WRITE OUTPUT TAPE NOT,318
318   FORMAT (1H /11H       SIG NAT)
      WRITE OUTPUT TAPE NOT,316, SIGMAU
319   IF (PD) 322,338,320
320   WRITE OUTPUT TAPE NOT,321
321   FORMAT (1H /36H DEPLETED FOIL AS A FUNCTION OF TIME)
      WRITE OUTPUT TAPE NOT,56, (T(I),D(I),I=1,N)
322   IF (NN) 330,338,323
323   N=L
      M=MM
      TT=1.0
      DO 324 I=1,L
      T(I)=S(I)
324   D(I)=DEL(I)
      GO TO 27
325   DO 326 I=1,L
      T(I)=SDEL(I)/DLSQ(I)
326   U(I)=SIGMA/DLSQ(I)
      WRITE OUTPUT TAPE NOT,328
328   FORMAT(1H /58H   TIME       DELTA(LS)    1ST.FRAC.ER.  2ND.FR
        AC.ER.)
      WRITE OUTPUT TAPE NOT,329,(S(I),DLSQ(I),U(I),T(I),I=1,L)
329   FORMAT (1H ,1P4E14.5)
      WRITE OUTPUT TAPE NOT,110
      WRITE OUTPUT TAPE NOT,56,(A(I),I=1,LV)
      WRITE OUTPUT TAPE NOT,336
      WRITE OUTPUT TAPE NOT,329, SIGMA
      GO TO 338
330   N=L
      M=MM
      TT=1.0
      DO 331 I=1,L
      T(I) = S(I)
331   D(I)=DDBP(I)
      GO TO 27
332   DO 333 I=1,L
      T(I)=SDDBP(I)/DLSQ(I)
333   U(I)=SIGMA/DLSQ(I)
      WRITE OUTPUT TAPE NOT,334
334   FORMAT(1H /58H   TIME       DEL/P(LS)    1ST.FRAC.ER.  2ND.FR
        AC.ER.)
      WRITE OUTPUT TAPE NOT,329,(S(I),DLSQ(I),U(I),T(I),I=1,L)
      WRITE OUTPUT TAPE NOT,110
      WRITE OUTPUT TAPE NOT,56,(A(I),I=1,LV)
      WRITE OUTPUT TAPE NOT,336
336   FORMAT (1H /9H       SIGMA)
      WRITE OUTPUT TAPE NOT,329, SIGMA
338   NCASE=NCASE-1
      IF (PD) 339,344,339
339   DO 340 I=1,LLN
```

```
      U(I)=ULSQ(I)
340   S(I)=SDT(I)
      DO 342 I=1,NLL
      D(I)=DDT(I)
342   T(I)=TDT(I)
      GO TO 345
344   IF (DT) 339,345,339
345   CALL TIME (NOT)
      IF (NCASE) 350,350,8
350   WRITE OUTPUT TAPE NOT,360
360   FORMAT(1H /27H AT THE END OF THE PROBLEMS)
      CALL TIME (NOT)
      CALL EXIT
      END(1,1,0,0,0,0,0,0,0,0,0,0,0,0,0)
```

Note: A Fortran deck and/or a binary deck for this program can be provided on request.

SAMPLE PROBLEM

Input Card

1	1
2	2 4 4+.10290E+01+.24700E-02+.51000E+03+.15600E+04+.50000E-05
3	+.2250E+03+.1000E+01+.3330E+04+.1E+01+.0E+01+.0E+01-.1E+01+.0E+01+.1E+01
4	-10 2 2 2 1 2+.100E+00+.600E+02+.600E+02+.000E+01+.000E+01
5	+.021000E+03+.006908E+06+.064500E+03+.005589E+06+.103000E+03+.004977E+06
6	+.140700E+03+.004167E+06
7	+.009500E+03+.166269E+06 .055000E+03+.124314E+06+.094000E+03+.104093E+06
8	+.129000E+03+.089653E+06

COMPUTER OUTPUT

TIME	DEP	TIME	NAT
2.10000E 01	6.90800E 03	9.50000E 00	1.66269E 05
6.45000E 01	5.58900E 03	5.50000E 01	1.24314E 05
1.03000E 02	4.97700E 03	9.40000E 01	1.04093E 05
1.40700E 02	4.16700E 03	1.29000E 02	8.96530E 04

M N L C	S	DEP BKRD	NAT BKRD	DEAD TIME	PPU	FRAC ER PPU
2 4 4	1.02900E 00	2.47000E-03	5.10000E 02	1.56000E 03	5.00000E-06	3.33000E-05	10.00000E-02

TIME	ENRICH COR	DEP TIME	NAT TIME
1.00000E 00	1.00000E 00	6.00000E 01	6.00000E 01

THE FOLLOWING ARE VALUES V(O) THRU V(M)
4.4813E 05 2.7794E 07 2.6242E 09

THE FOLLOWING ARE VALUES S(O) THRU S(2M)
4.0000E 00 2.8750E 02 2.8592E 04 3.1445E 06 3.6416E 08

THE FOLLOWING ARE VALUES A(O) THRU A(M)
1.5957E 05 -9.3483E 02 2.7501E 00

TIME	DEP FOIL	NAT FOIL	GAMMA	DEL/P	SIG D/P
2.46000E 02	6.37546E 03	1.41147E 05	4.51689E-02	4.61540E-02	1.03624E-03
2.89500E 02	5.06425E 03	1.10710E 05	4.57433E-02	4.68029E-02	1.20296E-03
3.28000E 02	4.45531E 03	9.24536E 04	4.81896E-02	4.95754E-02	1.42009E-03
3.65700E 02	3.64880E 03	8.24767E 04	4.42404E-02	4.51068E-02	1.41973E-03

SIG NAT
1.87302E 03

THE FOLLOWING ARE VALUES V(O) THRU V(M)
1.8764E-01 5.7660E 01 1.8082E 04

THE FOLLOWING ARE VALUES S(O) THRU S(2M)
4.0000E 00 1.2292E 03 3.8565E 05 1.2334E 08 4.0146E 10

THE FOLLOWING ARE VALUES A(O) THRU A(M)
-2.3108E-02 4.6852E-04 -7.6711E-07

TIME	DEL/P(LS)	1ST.FRAC.ER.	2ND.FRAC.ER.
2.46000E 02	4.57255E-02	4.83491E-02	2.26622E-02
2.89500E 02	4.82368E-02	4.58319E-02	2.49387E-02
3.28000E 02	4.80377E-02	4.60219E-02	2.95620E-02
3.65700E 02	4.56391E-02	4.84406E-02	3.11078E-02

THE FOLLOWING ARE VALUES A(O) THRU A(M)
-2.3108E-02 4.6852E-04 -7.6711E-07

SIGMA
2.21079E-03
THE TIME IS 5498.1

AT THE END OF THE PROBLEMS
THE TIME IS 5498.1

APPENDIX E
THE PULSE PILEUP EFFECT

The effect of pulse pileup on the measurements of δ_{28} was discussed in section 4.1.2. A pulse pileup factor, C, was defined by Eq. 4.1.4.

$$N = N_o + CN^2 \qquad (4.1.4)$$

where N is the count rate of a foil corrected for dead time, and N_o is the value that would be measured if coincident (or pileup) pulses were not counted, and CN^2 represents the contribution due to coincident pulses. A value of C equal to 33 μseconds was determined from analysis of the 5-3/4-inch lattice data as explained in section 4.1.2. For comparison with this value, C was estimated:

1) The ratio of the number of counts below 0.72 Mev to the number of counts above 0.72 Mev was determined from a gamma-ray energy spectrum measured with a TMC 256 Channel Analyzer; this ratio was approximately 10. For count rates of 10^5 cpm above 0.72 Mev, the ratio implies that approximately 10^6 cpm are rejected by the discriminator. As indicated below, this ratio was used to estimate the count rate due to pulse pileup.

2) Two types of coincident pulses were considered: regular and overshoot coincidences. The term, "regular," refers to coincidences of the initial phase of two pulses, and "overshoot" refers to coincidences between the initial phase of one pulse and the overshoot phase of another pulse. These terms are graphically defined in Fig. E.1.

3) The resolving time for regular coincidences was determined by using a double pulse generator. The experimental arrangement is shown in Fig. E.2. The value of t, the time between pulses, was varied, and the ratio of the second pulse height to the pulse height of a single pulse was determined as a function of t. One would expect that, for large

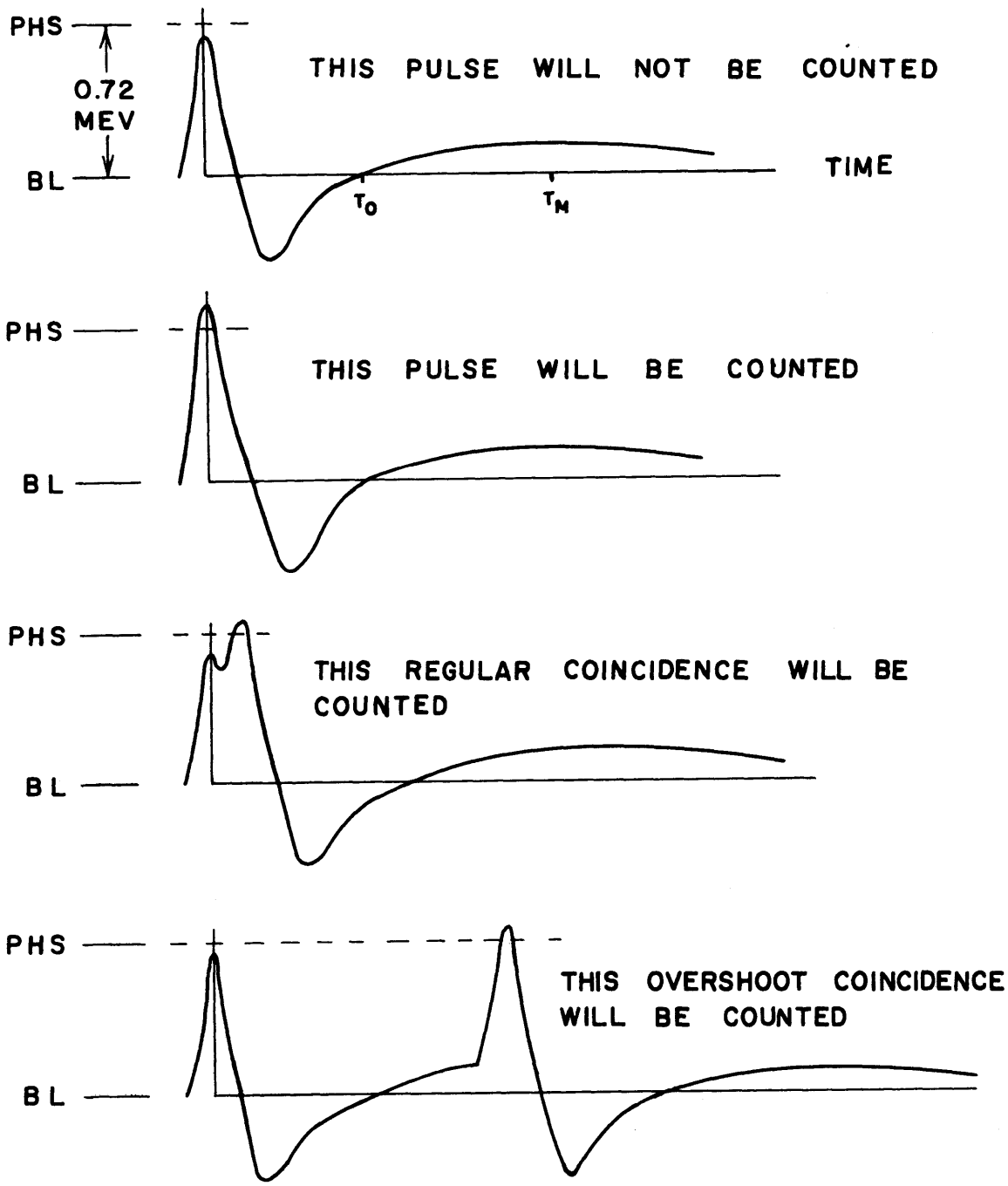

FIG. E-1 SINGLE AND COINCIDENT PULSE SHAPES

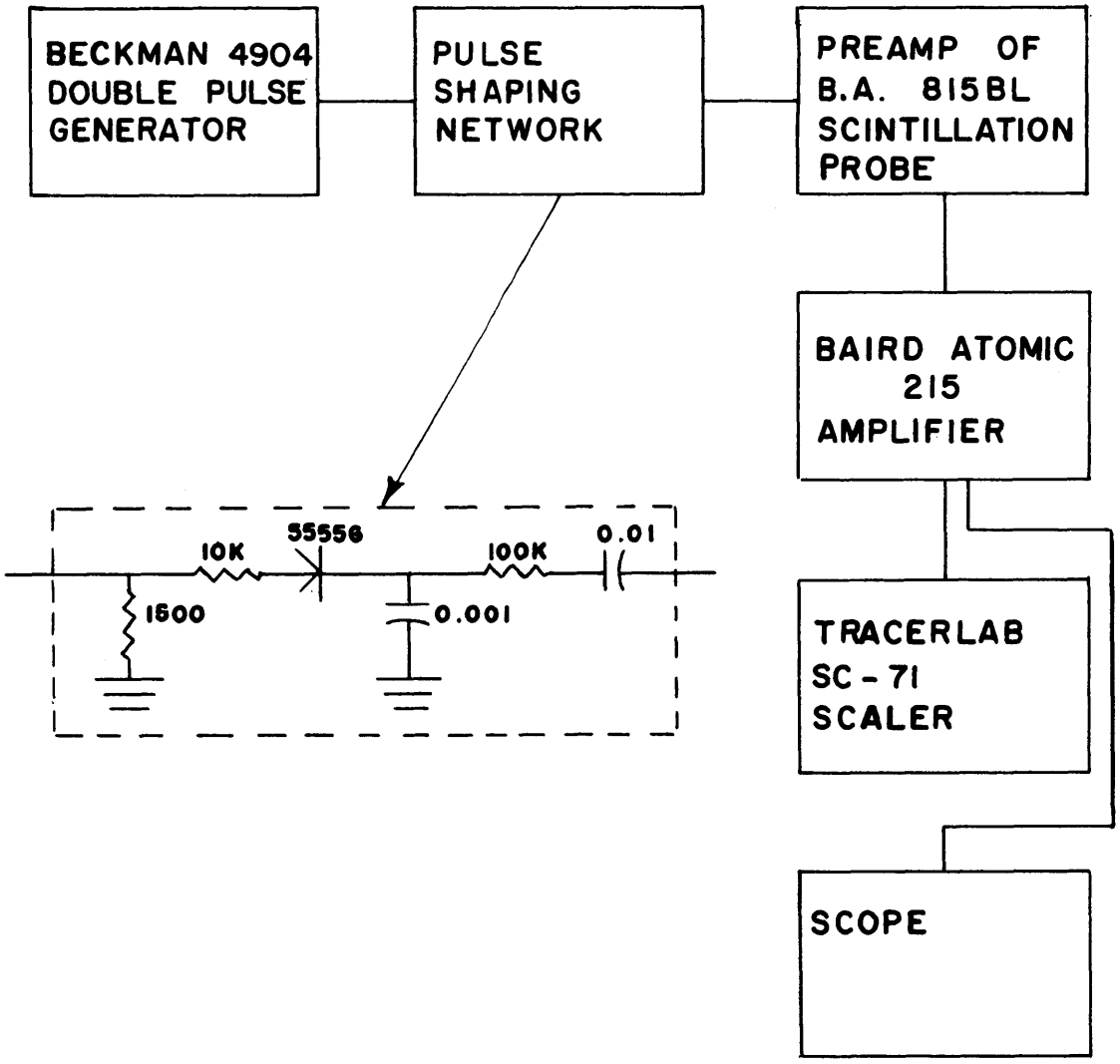

FIG. E-2 EQUIPMENT FOR STUDY OF PULSE PILEUP

values of t, the pulse height of the second pulse would be equal to the value of the first pulse. As t is reduced, the second pulse height will increase by an amount equal to the overshoot of the first pulse. The height will decrease as t becomes smaller than t_m (see Fig. E.1), and then increase as t approaches a value equal to the duration of a single pulse. The measured curve is shown in Fig. E.3. For values of t less than 0.3 μseconds, it is evident that the regular coincidence is nearly complete; that is, the resulting pulse height is approximately twice the height of a single pulse.

The curve was determined by observing the amplifier output on an oscilloscope. The results were checked by determining the PHS settings required to discriminate against the first and second pulses. The curve of pulse height as a function of the PHS setting is linear, and a zero value of PHS corresponds to a pulse of zero height. The ratio of PHS setting of the second pulse to the setting for single pulses is, therefore, equal to the ratio of the pulse heights.

4) The number of regular coincidences which result in pulses of energy greater than 0.72 Mev was estimated. It was assumed that the number of counts as a function of energy was exponential:

$$N(E) = K\, e^{-\lambda E}. \qquad (E.1)$$

This approximation is reasonable, as can be seen from an examination of the gamma-ray spectra of Fig. 4.9. To determine the relationship between K and N_t, the count rate of pulses below the bias setting, Eq. E.1 was integrated between 0 and E_b, the bias setting; the result is

$$N_t = \int_0^{E_b} Ke^{-\lambda E}\, dE = \frac{K}{\lambda}\left[1 - e^{-\lambda E_b}\right], \qquad (E.2)$$

Defining t as the regular coincidence resolving time, the number of regular coincidences with total energy greater than E_b is:

$$N_c(\text{Regular}) = \int_0^{E_b} dE_1 \int_{E_b - E_1}^{E_b} tKe^{-\lambda E_1} Ke^{-\lambda E_2}\, dE_2. \qquad (E.3)$$

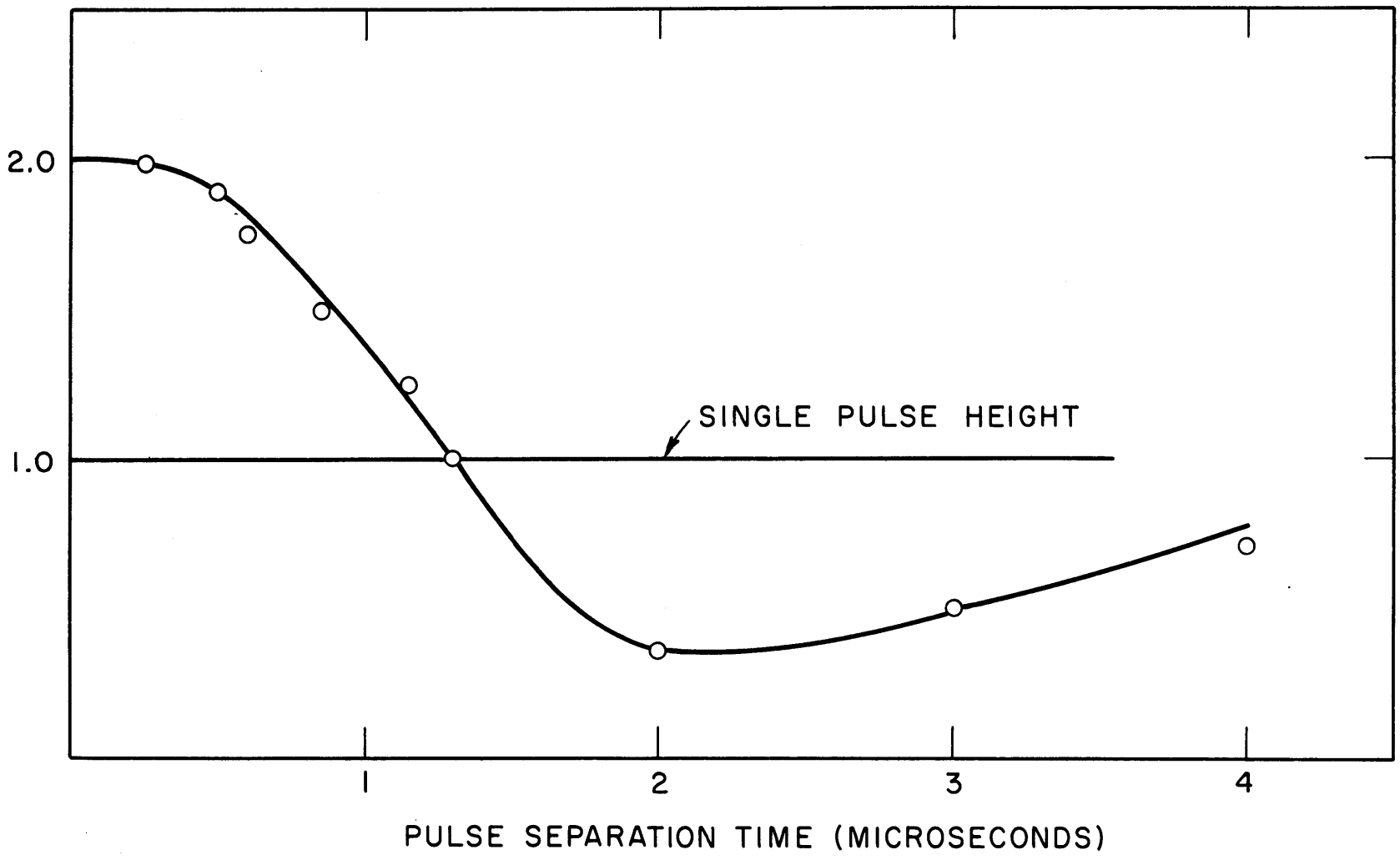

FIG. E-3 SECOND PULSE HEIGHT AS A FUNCTION OF PULSE SEPARATION TIME.

The limits of the first integration imply that only pulses of energy greater than $E_b - E_1$, in coincidence with pulses of energy E_1, result in coincident pulses of energy greater than E_b. The integration yields

$$N_c(\text{Regular}) = \frac{tK^2}{\lambda} e^{-\lambda E_b}\left[E_b - \frac{1}{\lambda}\left(1 - e^{-\lambda E_b}\right)\right] . \qquad (E.4)$$

Substitution of Eq. E.2 into Eq. E.4 gives

$$N_c(\text{Regular}) = \frac{tK^2}{\lambda} e^{-\lambda E_b}\left[E_b - \frac{N_T}{K}\right]. \qquad (E.5)$$

The calculated number of "pileup pulses" from regular coincidences is, therefore, a function of the count rate, the discriminator setting, t, and the value of λ used to represent the gamma-ray energy spectrum. From the spectra, it was estimated that an exponential function in which N(E) is decreased by a factor of 2 in an interval of 0.2 Mev is reasonable. The value of λ was therefore estimated to be $(0.693/0.2)$ Mev^{-1}. The value of E_b was 0.72 Mev. In step 1, it was shown that a count rate of 10^5 cpm implied a value of N_t equal to approximately 10^6 cpm. From Eq. E.2, K was calculated to be 3.78×10^6 cpm. A value of t equal to 0.6 μseconds was estimated from Fig. E.3 and the number of regular coincidence counts was obtained from Eq. E.5; the result was a value of 780 regular coincidence counts per minute for a count rate of 10^5 cpm above 0.72 Mev. The value of C obtained from analysis of the δ_{28} data was 33 μseconds. For a count rate of 10^5 cpm, this value of C implies a pileup rate equal to 5560 cpm. The regular coincidence mechanism therefore represents only about 15 per cent of the total effect.

5) The number of overshoot coincidences was then estimated. An analytic expression which approximates the amplifier output immediately following a pulse is given in the Baird Atomic 215 Non-overloading Amplifier Manual:

$$f(t) = \frac{e^{-t/T_1}}{(T_1/T_2 - 1)} + \frac{e^{-t/T_2}}{(T_2/T_1 - 1)} , \qquad (E.6)$$

where f(t) is the output at time t divided by the height of the pulse. The time constants, T_1 and T_2, are estimated to be 200 μseconds and

1.6 μseconds. The value of 200 μseconds represents the photomultiplier recovery time; the value of 1.6 μseconds is an approximate value of the time constant associated with the amplifier. The average value of the overshoot for a 1-second interval was determined from Eq. E.6. This value was multiplied by the average pulse height and the number of counts per second to estimate the effect of the overshoot on the baseline setting of the amplifier. An increase in the baseline setting has the same effect as a decrease in the discriminator level and will increase the count rate. Using Eq. E.1 and the estimated effect of the overshoot pulses on the baseline, the number of additional counts resulting from overshoot coincidences was estimated.

Assuming that Eq. E.1 is valid from 0.0 Mev to 2.5 Mev, an average value of E equal to about 0.3 Mev was estimated. A value of t_o (see Fig. E.1) equal to 7.7 μseconds was estimated from Eq. E.6. Integration of f(t) from t_o to 1 second, and division by 1 second gave the average value of the overshoot as 1.6×10^{-6}. On multiplying this result by 0.3 Mev, the average height of the overshoot pulse came out to be 0.48×10^{-6} Mev. For a count rate of 10^5 cpm above 0.72 Mev, the total count rate is approximately 1.1×10^6 cpm or 1.83×10^4 cps. The average change in the baseline setting due to overshoot pulses is, therefore, about $1.83 \times 10^4 \times 0.48 \times 10^{-6}$ Mev, or approximately 0.009 Mev. The number of additional counts resulting from a baseline shift of ΔE_b can be estimated from Eq. E.1:

$$N_c(\text{overshoot coincidences}) = \int_{E_b - \Delta E_b}^{E_b} Ke^{-\lambda E}\, dE \approx Ke^{-\lambda E_b} \Delta E_b \,. \tag{E.7}$$

With the estimated value of 0.009 Mev for ΔE_b, the number of overshoot coincidences is estimated to be $3.78 \times 10^6 \times 0.083 \times 0.009$ or 2.8×10^3 cpm. The number of overshoot coincidences is approximately 3.5 times as large as the number of regular coincidences. The question may be asked if Eq. 4.1.4 is valid for overshoot coincidences. The quantities, K and ΔE_b, are proportional to the count rate; thus, from Eq. E.7, it can be concluded that Eq. 4.1.4 adequately describes the pileup effect. The

number of overshoot coincidences is approximately one-half of the number of pileup counts implied from the value of C obtained from analysis of the δ_{28} data. Addition of the calculated values of the regular and overshoot coincidences, the total calculated pileup factor is only 65 per cent of the value obtained from the δ_{28} data. This calculated value of C is actually a high estimate, because the decrease in the count rate owing to the undershoot portion of the pulses was not included in the calculation. It can be concluded that there is a large discrepancy between the two values of C.

6) The value of C was determined by using the two-source method. A value of 9.6 μseconds was determined. This was a factor of 3.5 lower than the value of 33 μseconds obtained from analysis of the δ_{28} data. The measurement was repeated with the same amplifier and a second 1-3/4 × 2-inch scintillation probe. A value in agreement with the lower value of C was obtained. The amplifier was replaced and a value of 14.5 μseconds was determined, indicating that C is sensitive to the condition of the amplifier.

7) Measurements of δ_{28} were made in a single rod at three different heights. The natural foil count rates at 240 minutes after the irradiation were 0.58×10^5, 1.40×10^{-5} and 2.82×10^5 cpm. The count rates were normalized to a value of 1 at 470 minutes and were compared to normalized decay curves determined from irradiations in the 5-3/4-inch lattice. The results are shown in Fig. E.4. The single-rod curves are approximately the same, and are in agreement with a curve from the 5-3/4-inch lattice in which the count rate at 240 minutes was 0.98×10^5 cpm. The curve from the 5-3/4-inch lattice, in which the count rate at 240 minutes was 2.48×10^5 cpm, shows the effect of pileup at higher count rates.

8) The evidence suggests that the pileup effect, which was important in the earlier measurements for the higher-activity foils, had been reduced. Several weak tubes had been replaced in the amplifier after the measurements in the 5-3/4-inch lattice, and it is postulated that the tube changes resulted in changes in the amplifier time constant, T_2. A decrease in T_2 causes a decrease in the overshoot

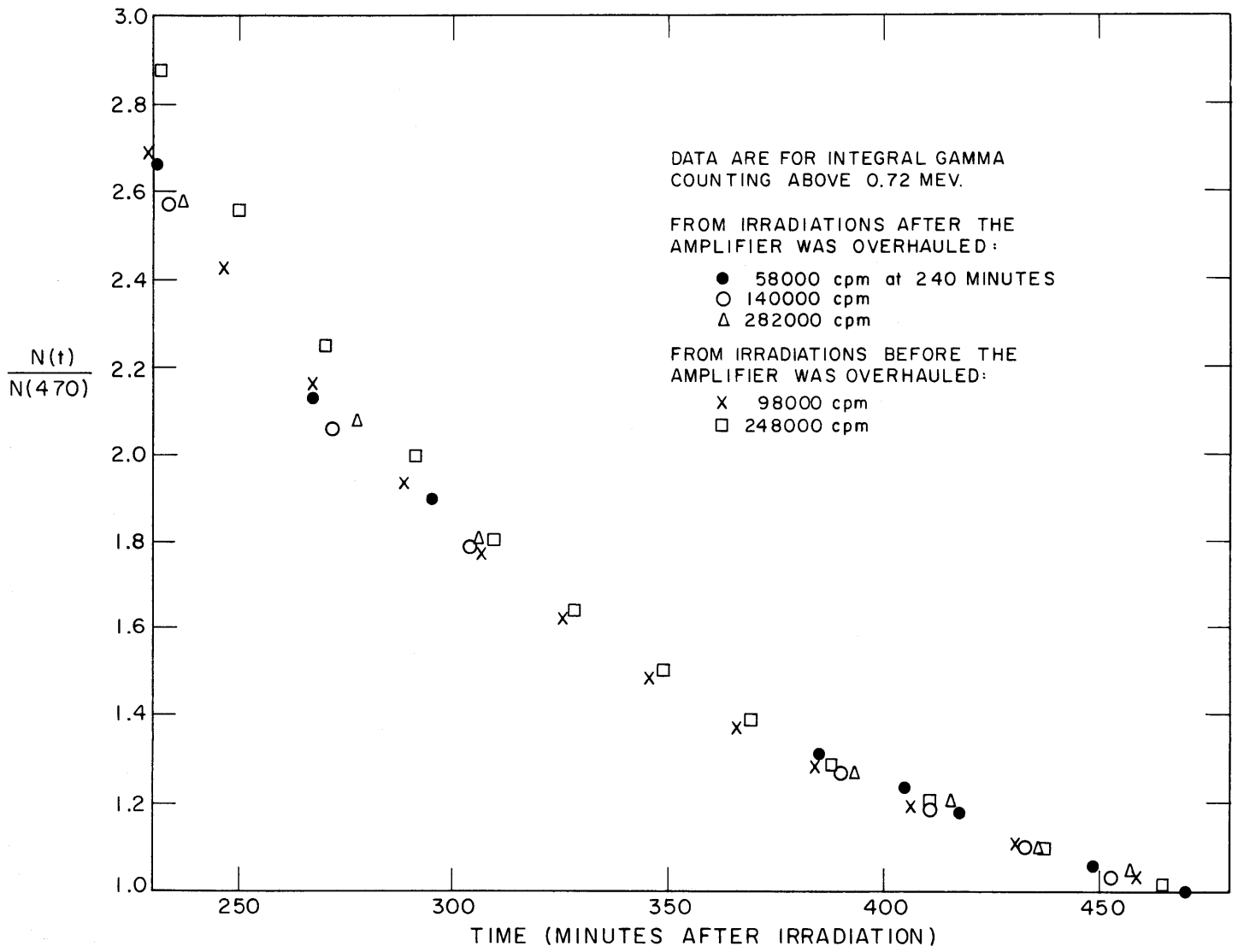

FIG. E-4 NATURAL URANIUM FOIL DECAY CURVES NORMALIZED TO A VALUE OF I AT 470 MINUTES AFTER IRRADIATION.

and therefore a decrease in the overshoot coincidence rate.

It was concluded from this study that pulse pileup can affect the measurements of δ_{28}. It is important to know the pulse pileup factor of the equipment and at what counting rate the pileup correction becomes significant. The problem can be minimized by periodically determining the pileup factor and, if it is too high, finding the source of the trouble. The problem can also be minimized by avoiding high count rates. The next series of measurements in the MIT lattice program will be in 1/4-inch diameter rods. The foil activities will be a factor of about sixteen lower than the activities in the one-inch diameter rods, and therefore pileup should be negligible in these lattices. However, for future measurements in which pileup might be important, the foils can be irradiated in a lower flux, or for a shorter time interval. The problem associated with these procedures is that the depleted foil activity is proportionately reduced. One scheme which permits high depleted foil activities and low natural foil activities is to count the foils at different positions (after irradiating them at the same position). This procedure necessitates an experiment to determine the geometric correction factor required to normalize the activities of the foils.

APPENDIX F
CALCULATIONS OF δ_{28} FOR A SINGLE ROD

Spinrad's method of calculating δ_{28} with the cross sections of Fleishman and Soodak (FS) differs from the Carlvik and Pershagen (CP) method only in notation. The methods differ in their treatments of ϵ, but that problem will not be considered in this discussion in which the notation of Fleishman and Soodak (FS) will be used.

The tabulated FS cross sections include σ_{1f}, σ_{1c}, σ_{11}, σ_{13}, and σ_{1t}. These cross sections are for a group 1 which has a lower energy limit, E_L, equal to 1.40 Mev. This energy is considered to be the U^{238} fission threshold, and the value of σ_{1f} is adjusted to include the effect of fission by neutrons with energies below 1.40 Mev. The CP method utilizes a similar adjustment, but E_L for the CP group 1 is 1.49 Mev. The cross sections σ_{1c} and σ_{1f} refer to capture and fission reactions. The cross section σ_{11} refers to scattering processes in which the neutrons remain in group 1, and σ_{13} refers to processes in which neutrons are scattered out of group 1. The FS value of σ_{11} is corrected for transport effects while the CP value of σ_{11} is not. The cross section σ_{1t} is the sum of the other cross sections:

$$\sigma_{1t} = \sigma_{1c} + \sigma_{1f} + \sigma_{11} + \sigma_{13} . \qquad (F.1)$$

The largest uncertainty in the calculation of δ_{28} results from the uncertainty of σ_{13}, the inelastic scattering cross section.[C.4] This problem is considered by Chernick et al.[C.11] Tabulations of high-energy U^{238} cross sections by Mandeville and Kavanagh,[M.4] Howerton,[H.7] and Yiftah, Okrent, and Moldauer[Y.1] are compared by Chernick and show large differences in the magnitude of the total inelastic cross sections at energies above 1.4 Mev and of the partial cross sections for excitation of the lowest energy levels in U^{238}. Additional comments concerning the cross sections are included in section 2.3 and detailed

discussions are included in references F.2 and C.1.

The expression for δ_{28} is

$$\delta_{28} = \nu_{25} \frac{\sigma_{1f}}{\sigma_{1t}} \frac{f_1 P}{1 - P'\left(\frac{f_1 \nu_1 \sigma_{1f} + \sigma_{11}}{\sigma_{1t}}\right)}, \qquad (F.2)$$

where ν_{25} is the value of ν for U^{235}, f_1 is the fraction of fission neutrons born in group 1, P is the first collision probability, and P′ is the collision probability for subsequent collisions. The collision probabilities P and P′ are approximately equal, and in the FS method, it is assumed that they are equal. The CP method gives a simple equation for calculating P from P′. Values of P′ are tabulated in Case, de Hoffmann and Placzek[C.2] for infinite cylinders as a function of a/ℓ, where a is the cylinder radius, and ℓ is the fast neutron mean free path. The following relationship was used to determine ℓ:

$$\ell = \frac{1}{N\sigma_{1t}} \qquad (F.3)$$

The atomic density, N, was taken to be 0.0473×10^{24} atoms/cm^3 in the calculations of Fleishman and Soodak[F.2] and Carlvik and Pershagen.[C.1] An alternative method of calculating ℓ is to use the expression:

$$\ell = \frac{1}{N\sigma_{tr}} \qquad (F.4)$$

The value of the cross section $(\sigma_{1t})_{FS}$ is obtained by correcting σ_{11} for transport effects, so that Eqs. F.3 and F.4 are equivalent if the FS cross sections are used. The cross section $(\sigma_{1t})_{CP}$ is an actual rather than a transport cross section; hence, Eqs. F.3 and F.4 yield values of $(\ell)_{CP}$ which are different.

Tables of multigroup corss sections are given in ANL-5800, Reactor Physics Constants.[R.1] The fast group cross sections from four ANL-5800 sets are compared with the FS and CP cross sections in Table F.1. The cross sections tabulated in ANL-5800 include values of σ_{tr}, σ_f, σ_c, σ_{er},

Table F. 1. Multigroup U^{238} Cross Sections.

Cross Section Set	Group(i)	f_i	E_L	σ_{it}	ν_i	σ_{if}	σ_{ic}	σ_{i3}	σ_{ii}
1 (10 groups)(a) ANL-5800	1	0.575	1.35	4.86	2.62	0.524b	0.035b	2.04b(b)	2.20b(b)
	2	0.178	0.825	5.0	2.62	0.040	0.125	1.12	3.72
2 (11 groups)(a) ANL-5800	1	0.338	2.25	4.7	2.65	0.59	0.015	2.87	1.23
	2	0.236	1.35	4.5	2.55	0.45	0.062	2.44	1.59
	3	0.178	0.825	5.0	2.47	0.003	0.13	1.20	3.67
3 (6 groups)(a) ANL-5800	1	0.204	3.0	4.00	2.80	0.616	0.02	2.18	1.18
	2	0.344	1.4	4.40	2.50	0.485	0.05	2.04	1.83
	3	0.168	0.9	4.50	2.46	0.044	0.10	1.45	2.91
4 (2 groups) ANL-5800	1	0.575	1.34	4.6	2.6	0.524	0.036	2.03(b)	2.01(b)
	2	0.425	0.0	7.1	2.47	0.005	0.19		
CP	1	0.511	1.49	7.41	2.76	0.545	0.038	2.00	4.83
	2	0.474	0.1	8.01		0.0	0.13	1.30	6.58
FS	1	0.561	1.40	4.541	2.85	0.549	0.032	2.07(b)	1.89(b)
	2	0.439	0.0	6.05		0.0	0.138		5.91

(a) Only the higher energy groups are included in this table.

(b) An amount 0.026b has been added to σ_{11} and subtracted from σ_{13} to account for the extra neutrons from the n, 2n reaction in U-238.

and σ_{in} for each group. Conversion to the FS notation for group i was made on the basis of the following set of equations:

$$\sigma_{tr} = \sigma_{it} \tag{F.5}$$

$$\sigma_c = \sigma_{ic} \tag{F.6}$$

$$\sigma_f = \sigma_{if} \tag{F.7}$$

$$\sigma_{er} + \sigma_{in} = \sigma_{i3} \tag{F.8}$$

$$\sigma_{tr} - \sigma_c - \sigma_f - \sigma_{in} = \sigma_{ii} \tag{F.9}$$

In these equations, σ_{er} is the elastic removal cross section, and σ_{in} is

the inelastic removal cross section.

Values of f_i, E_L, and ν_i are also tabulated for the four sets of data found in ANL-5800 and are included in Table F.1.

The values of ℓ and σ_{tr} which yield the value of 0.051, calculated by Baumann for δ_{28}, and the value of 0.0559 measured at MIT, can be calculated by using the FS cross sections and Eq. F.4.

Table F.2. Values of ℓ and σ_{tr} calculated from FS cross sections, Equations F.1 and F.2.

δ_{28}	Rod Diameter	$P^{(a)}$	$\ell^{(b)}$	$\sigma_{tr}^{(c)}$
0.0530	1.01"	0.265	4.66 cm	4.541b
0.0559	1.01	0.277	4.40	4.80
0.0510	1.00	0.257	4.81	4.39
0.0513	1.01	0.259	4.81	4.39

(a) From Eq. F.2, setting P equal to P′; (b) from Ref. C.2; (c) from Eq. F.4.

A comparison of the calculated transport cross sections from Table F.2 with the tabulated values of $\sigma_{1t}(\sigma_{tr})$ from Table F.1 shows that each value in Table F.2 agrees with at least one value in Table F.1. From the spread in the values of $\sigma_{1t}(\sigma_{tr})$, it can be concluded that the uncertainty in σ_{1t} (or ℓ) is large. If Eq. F.2 is used, with ℓ calculated from Eq. F.3, the calculated value of δ_{28} is insensitive to the value of σ_{1t}. The collision probability P is approximately proportional to $1/\ell$ which is proportional to σ_{1t}; hence, to the first order, σ_{1t} cancels out of the numerator and denominator of Eq. F.2. For this reason, Eq. F.3 was used to calculate ℓ, yielding the calculated values of δ_{28} shown in Table 4.5. The difference between the MIT and SRL calculated values of δ_{28} for one-inch diameter rods need not be explained on the basis of different choices of σ_{tr}. Another possible explanation is a difference in the choice of the value of P. In the MIT calculation, the FS assumption that P equals P′ was used.

Calculated values of δ_{28} based on the cross section sets 1, 4, CP, and FS are included in Table F.3. Sets 2 and 3 are omitted in this comparison because they have two groups above the U^{238} fission threshold.

Table F.3. Comparison of values of δ_{28} calculated with different sets of cross sections.

Cross Section Set	E_L	f	ν_1	σ_{1t}	ℓ(a)	$\delta_{28}^{(b)}$	$\delta_{28}^{(c)}$	$\delta_{28}^{(d)}$	$\delta_{28}^{(e)}$
1	1.35 Mev	0.575	2.62	4.86	4.41 cm	.0501	.0503	.0525	.0492
4	1.35	0.575	2.60	4.6	4.60	.0519	.0521	.0544	.0511
CP	1.49	0.511	2.76	7.41	2.85	.0480	.0481	.0483	.0308
FS	1.40	0.561	2.85	4.541	4.66	.0530	.0530	.0530	.0530

(a) From Eq. F.3. (b) From Eq. F.2, with $\nu_{25} = 2.47$, 1.01" diameter rod, ν_1 given in column 4. (c) Same as (b) except ν_1 is taken as 2.85. (d) Same as (b) except σ_{1f} is 0.549b. (e) Same as (b) except ℓ is 4.66 cm.

An examination of Table F.3 leads to several conclusions:

a) The calculation of δ_{28} is insensitive to σ_{1t} if equations F.2 and F.3 are used. There is only about a 10 per cent spread in the calculated values of $\delta_{28}^{(b)}$, while the values of σ_{1t} vary from 4.54b to 7.4b.

b) The calculation of δ_{28} is insensitive to the value of ν_1 used in Eq. F.2, as is evident from the comparison of $\delta_{28}^{(b)}$ and $\delta_{28}^{(c)}$.

c) The use of a constant value of σ_{1f} for all sets of cross sections decreases the differences among the calculated values of δ_{28}. This can be seen from the comparison of $\delta_{28}^{(b)}$ and $\delta_{28}^{(d)}$. A possible justification for using higher values of cross sections for the calculations with the data of sets 1 and 4 can be seen in Table F.1. In these sets, U^{238} fission is allowed to occur in group 2, but is not considered in the calculations of $\delta_{28}^{(b)}$.

d) Use of a value of ℓ of 4.66 cm together with the CP cross sections leads to a large change in the calculated value of δ_{28}, as is evident from the comparison of $(\delta_{28}^{(b)})_{CP}$ and $(\delta_{28}^{(e)})_{CP}$.

e) The low value of $(\delta_{28}^{(b)})_{CP}$ results from not using a transport cross section for σ_{1t}. The uncertainty of $^{+0.005}_{-0.000}$, listed in Table 4.5 for the CP value, shows the range of values they calculated using different hypotheses for their calculation of σ_{1t}.(C.2)

f) The difference of 0.0029 between the FS calculated value of δ_{28} and the MIT measured value is larger than the uncertainty of 0.0015 estimated for the MIT value. Although a published estimate of the uncertainty in the calculated value is not available, the differences among the calculated values of δ_{28}, using different sets of cross sections as shown in Table F.3, indicate that an error of 0.0029 is not unreasonable. The backscatter effect is not included in the calculation; including this effect in the calculation would reduce the difference.

g) The difference of 0.0029 could be decreased by increasing the value of ν_{25}, f_1, σ_{1f} of U^{238}, or combinations of these parameters. The difference could also be decreased by increasing the ratio $(f_1\nu_1 + \sigma_{11})/\sigma_{1t}$, but a 29 per cent increase in this ratio would be required to increase the calculated value of δ_{28} by only 0.0029.

APPENDIX G
BIBLIOGRAPHY

A.1 Allard, E., "Monte Carlo Study of the Fast Fission Factor," M.S. Thesis, M.I.T. (June 1962).

B.1 Baumann, N.P., Private communication (1961).

B.2 Brolley, J., et al., "Neutron Multiplication in a Mass of Uranium Metal,"CF-1627 (1944).

B.3 Brown, P., "Measurements of the Spatial and Energy Distribution of Neutrons in Heavy Water-Uranium Reactor Lattices," Ph.D. Thesis, Nuclear Engineering Dept., M.I.T., to be completed in June, 1962, and published as an NYO report.

B.4 Bunney L.R., E.M. Scadden, J.O. Abriam and N.E. Ballou, PICG 15, 444 (1958).

C.1 Carlvik, I., and B. Pershagen, "The Fast Fission Effect in a Cylindrical Fuel Element," AEF-70 (1956).

C.2 Case, K.M., F. de Hoffman, and G. Placzek, "Introduction to the Theory of Neutron Diffusion," Vol. 1, (1953).

C.3 Castle, H., H.W. Ibser, G. Sacher, and A.M. Weinberg, "The Effect of Fast Fission on k," Chicago Met. Lab., CP-644(May, 1943).

C.4 Chernick, J., PICG 5, 219 (1955).

C.5 Cranberg, L., et al., Phys. Rev. 103, 662 (1956).

C.6 Critoph, E., CRRP-655, AECL-351 (1956).

C.7 Carter, M.D., A.J. Perks, L.G. Sanders, Atomic Energy Research Establishment, Harwell Report AERE-R3205 (1960).

C.8 Carter, M.D., and A. J. Perks, AERE-M723 (1960).

C.9 Chezem, C.G., Nucl. Sci. Eng. 8, 652 (1960).

C.10 Campan, J.L., P.P. Caluzon, and C.P. Zaleski, IAEA Seminar on the Physics of Fast and Intermediate Reactors, Paper SM-18/29, Vienna, August 3-11, 1961.

C.11 Chernick, J., H.C. Honeck, P. Michael, S.O. Moore, and G. Srikantiah, " The Correlation of Integral Experiments and High Energy Cross Section," Submitted to Nuclear Sci. and Engineering, January 1962.

D.1 Dessauer, G., PICG 12, 320 (1958).

E.1 Erdik, E., J. Nuclear Energy 15, 98 (1961).

E.2 Evans, R.D., "The Atomic Nucleus," McGraw-Hill (1955).

F.1 Feld, B., and L. Szilard, Memo on Criticality Condition for a Fast Neutron Chain Reaction inside a Spherical Shell of Uranium Metal (December 26, 1941).

F.2 Fleishman, M.R., and H. Soodak, Nucl. Sci. Eng. 7, 217-227 (1960).

F.3 Fortran Programmer's Primer, International Business Machines Corporation (1951).

F.4 Futch, A.H., Nucl. Sci. Eng. 5, 61-67 (1959).

G.1 Girard, Y., J.C. Koechlin, J. Moreau, and R. Naudet, PICG 12, 281 (1958).

G.2 Glasstone, S., and M.C. Edlund, "The Elements of Nuclear Reactor Theory," D. von Nostrand, N.Y. (1952).

G.3 Graves, A.C., and D.K. Froman, "Miscellaneous Physical and Chemical Techniques of the Los Alamos Project," McGraw-Hill (1952).

G.4 Grob, V.E., E. Santandrea, and H. Ritz, Nucl. Sci. Eng. 7, 514-524 (1960).

G.5 Grummitt, W.E., and G.M. Milton, J. Inorg. Nucl. Chem. 5, 93 (1957).

H.1 Hawkings, R.C., W.J. Edwards, and Miss E. M. McLeod, AECL-1225, "Tables of Gamma Rays from the Decay of Radionuclides," (1960).

H.2 Heath, R.L., "Scintillation Spectrometry Gamma Ray Spectrum Catalogue," IDO-16408 (1957).

H.3 "Heavy Water Lattice Research Project Annual Report," NYO-9658 (September 30, 1961).

H.4 Hill, D.L., "Fast Effect in Three Lattices," CF-1548 (1944).

H.5 Hone, D.W., E. Critoph, et al., PICG 12, 351 (1958).

H.6 Hughes, D.J., and R.B. Schwartz, "Neutron Cross Sections," 2nd ed., BNL-325 (1958).

H.7 Howerton, R.J., University of California Research Laboratory Report UCRL-5351, Vol. I, Part II (1958).

K.1 Kaplan, I., 22.21 Course Notes, M.I.T.

K.2 Kaplan, I., and J. Chernick, PICG 5, 295 (1955).

K.3 Kinard, F.E., and N.P. Baumann, Trans. ANS 3, 2 (1960).

K.4 Klein, D., A.Z. Kranz, et al., Nucl. Sci. Eng. 3, 403-427 (1958).

K.5 Kouts, H., et al., PICG 12, 446 (1958).

K.6 Kouts, H., G. Price, K. Downes, R. Sher, and V. Walsh, PICG 5, 183 (1955).

K.7 Kouts, H., and R. Sher, BNL-486 (T-111), (1957).

K.8 Kranz, A.Z., WAPD-134 (1955).

K.9 Kranz, A.Z., and G.G. Smith, WAPD-151 (1956).

K.10 Katcoff, S., "Fission Product Yields from Neutron-Induced Fission," Nucleonics 18, (November 1960).

M.1 Madell, J., "Spatial Distribution of the Neutron Flux on the Surfaces of a Graphite-Lined Cavity," Ph.D. Thesis, Nuclear Engineering Dept., M.I.T., NYO-9657 (1962).

M.2 Marshall, H., and L. Szilard, CP-316 (November 1941).

M.3 Meghreblian, R.V., and D.K. Holmes, "Reactor Analysis," McGraw-Hill (1960).

M.4 Mandville, C.E. and D.L. Kavanagh, Curtiss-Wright Report CWR-4028 (1958).

N.1 Nuclear Data Sheets, Nuclear Data Group, National Academy of Science, Washington, D.C.

N.2 Nucleonics, 18, 11, Reference Data Issue (November 1960).

N.3 Nyland, O., "Measurements of the Fast Fission Factor in UO_2-Elements," AE-40 (1961).

P.1 Palmedo, P.F.,"Measurements of the Material Bucklings of Lattices of Natural Uranium Rods in D_2O," Ph.D. Thesis, Nuclear Engineering Dept., M.I.T., published as NYO 9660 (1962).

P.2 Peak, J., Ph.D. Thesis, Nuclear Engineering Dept., M.I.T., to be published as NYO-9662 (1962).

P.3 Pershagen, B., G. Anderson, and I. Carlvik, PICG 12, 341 (1958).

P.4 Price, G.A., et al., "Single Rod Fast Effects and Related Measurements," BNL 616(T-185), (1960).

R.1 Reactor Physics Constants, ANL-5800 (1958).

R.2 Regier, R.B., et al., Phys. Rev. 119, 2017,(1960).

R.3 Rief, H., Nucl. Sci. Eng. 10, 83-89 (1961).

R.4 Rief, H., "An IBM 704 Monte Carlo Code to Calculate Fast Fission Effects in Homogeneous and Heterogeneous Systems," BNL 647(T-206), (1961).

R.5 Roeland, L.W., et al., PICG 15, 440 (1958).

S.1 Shernoff, D.I., B.S. Thesis, M.I.T., (June, 1960).

S.2 Snell, A.H., J. Brolley, J. Levinger, and R. Wilkinson, "Studies on a Five-Ton Metal Pile," Chicago Met. Lab. Report CF-589 (1943).

S.3 Spinrod, B.I., Nucl. Sci. Eng. 1, 455 (1956).

U.1 Untermyer, S., ANL-5070 (1953).

W.1 Weinberg, A.M. and E.P. Wigner, "The Physical Theory of Neutron Chain Reactors," Chicago, the University of Chicago Press, Ch. 20.

W.2 Weitzberg, A., S.M. Thesis, M.I.T. (1958).

W.3 Weitzberg, A., "Measurements of Neutron Capture in U^{238} in Lattices of Uranium Rods in Heavy Water," (doctoral dissertation) M.I.T., NYO 9659 (1962).

W.4 Windsor, H.H., and E. Erdik, Trans. ANS 3, 2 (1960).

Y.1 Yiftah, S., D. Okrent and P.A. Moldauer, "Fast Reactor Cross Sections," International Series of Monographs on Nuclear Energy, Volume 4, Div. II, Pergamon Press (1960).

APPENDIX H
GLOSSARY OF PRINCIPAL SYMBOLS

The page numbers give the location of a more detailed definition or of the first use of a recurring symbol. Symbols used exclusively in the appendices are not included on this list.

δ_{28}	Fission rate in U^{238} to fission rate in U^{235}	Page 1
ϵ	Fast fission factor	1
p	Resonance escape probability	113
f	Thermal utilization	113
η	Neutrons born per neutron absorbed in fuel	113
k_∞	Infinite multiplication factor	113
ν_{25}	Neutrons born per fission of U^{235}	3
ν_{28}	Neutrons born per fission of U^{238}	3
ξ	Average logarithmic energy change per neutron collision	6
σ_s	Neutron scattering cross section	6
$\gamma(t)$	Ratio of the activity of a depleted uranium foil to the activity of a second uranium foil	31
P(t)	Ratio of the number of counts per fission of U^{235} to the number of counts per fission of U^{238}	32
a	Constant involving U^{235} and U^{238} atom densities	33
S	Constant involving U^{235} and U^{238} atom densities	33
R	Ratio of fissions measured in a fission chamber	11
P	First collision probability	22
P′	Second and subsequent collision probabilities	22
N_i^{25}	Atom density of U^{235} in uranium of enrichment, i	31
N_i^{28}	Atom density of U^{238} in uranium of enrichment, i	31
I_{28}/I_{25}	Fissions per atom of U^{238} to U^{235}	32
R_i	N_i^{25}/N_i^{28}	33

F(t)	Counts from U^{238} fission products to counts from U^{235} fission products in a foil of the same composition as the fuel	Page 33
γ	Ratio of 1.60 Mev activity from a depleted foil and a second foil	41
$(\beta^{28})_{La^{140}}$	Fission product yield of La^{140} for fissions of U^{238}	42
$(\beta^{25})_{La^{140}}$	Fission product yield of La^{140} for fissions of U^{235}	42
δ_{28}^{*}	Value of δ_{28} measured by using La^{140} technique	42
δ_{25}	Epicadmium U^{235} fissions to subcadmium U^{235} fissions	62
$\sigma(\delta_{28})$	Estimated error in δ_{28}	81
$\sigma(F(t))$	Estimated error in F(t)	81
$\sigma(P(t))$	Estimated error in P(t)	81